QA: QA

ANL-MGR-GS-000005 REV 00

August 2005

Magma Dynamics at Yucca Mountain, Nevada

Prepared for:
U.S. Department of Energy
Office of Civilian Radioactive Waste Management
Office of Repository Development
1551 Hillshire Drive
Las Vegas, Nevada 89134-6321

Prepared by:
Bechtel SAIC Company, LLC
1180 Town Center Drive
Las Vegas, Nevada 89144

Under Contract Number
DE-AC28-01RW12101

DISCLAIMER

This report was prepared as an account of work sponsored by an agency of the United States Government. Neither the United States Government nor any agency thereof, nor any of their employees, nor any of their contractors, subcontractors or their employees, makes any warranty, express or implied, or assumes any legal liability or responsibility for the accuracy, completeness, or any third party's use or the results of such use of any information, apparatus, product, or process disclosed, or represents that its use would not infringe privately owned rights. Reference herein to any specific commercial product, process, or service by trade name, trademark, manufacturer, or otherwise, does not necessarily constitute or imply its endorsement, recommendation, or favoring by the United States Government or any agency thereof or its contractors or subcontractors. The views and opinions of authors expressed herein do not necessarily state or reflect those of the United States Government or any agency thereof.

QA: QA

Magma Dynamics at Yucca Mountain, Nevada

ANL-MGR-GS-000005 REV 00

August 2005

BSC	SCIENTIFIC ANALYSIS SIGNATURE PAGE/ CHANGE HISTORY *Complete only applicable items.*	Page iii 1. Total Pages: ~~116~~ 114

8/29/05

2. Scientific Analysis Title

Magma Dynamics at Yucca Mountain, Nevada

3. DI (including Rev. No.)

ANL-MGR-GS-000005 REV 00

	Printed Name	Signature	Date
4. Originator	Don Krier	Donathan Krier	8/29/05
5. Checker	Frank Perry	Frank Perry	8/29/05
6. QER	Donna Sinks ROBERT P. KREILTER	Robert P. Kreilter	8/29/05
7. Responsible Manager/ Lead	Greg Valentine	G. Valentine	29 Aug 05
8. Responsible Manager	Mike Cline	Mike Cline	29 Aug 05

9. Remarks

Contributing authors: Ed Gaffney, Gordon Keating, Greg Valentine, Branko Damjanac, and Sebastian Dartevelle

Change History

10. Revision No.	11. Description of Change
00	Initial Issue

CONTENTS

Page

ACRONYMS xi

1. PURPOSE 1-1
   1.1 INTRODUCTION 1-1
   1.2 BACKGROUND 1-2
   1.3 SCOPE 1-3
   1.4 LIMITATIONS 1-5

2. QUALITY ASSURANCE 2-1

3. USE OF SOFTWARE 3-1
   3.1 SOFTWARE TRACKED BY CONFIGURATION MANAGEMENT 3-1
   3.2 EXEMPT SOFTWARE 3-1

4. INPUTS 4-1
   4.1 DIRECT INPUTS 4-1
      4.1.1 Input Parameters 4-1
      4.1.2 Justification of External Sources of Input 4-3
   4.2 CRITERIA 4-6
   4.3 CODES, STANDARDS, AND REGULATIONS 4-7

5. ASSUMPTIONS 5-1
   5.1 ASSUMPTIONS RELATED TO DESCRIPTIONS OF ANALOGUE VOLCANIC SITES 5-1
   5.2 ASSUMPTIONS RELATED TO SIMULATION OF MAGMA DYNAMICS 5-1

6. ANALYSIS 6-1
   6.1 INTRODUCTION 6-1
   6.2 FIELD ANALOGUES 6-2
      6.2.1 East Grants Ridge, New Mexico 6-2
      6.2.2 Paiute Ridge, Nevada 6-5
      6.2.3 Basalt Ridge Area, Nevada 6-9
      6.2.4 Field Analogue Conclusions 6-12
   6.3 BLOCKAGE AND FORMATION OF MAGMA PATHWAYS 6-17
      6.3.1 Blockage by Magma Solidification 6-17
      6.3.2 Secondary Dike Formation in Hot Rock 6-29
   6.4 MULTIPHASE MAGMA FLOW 6-33
      6.4.1 Inputs 6-35
      6.4.2 Initial Interaction with Drifts 6-38
      6.4.3 Discussion 6-40

7. CONCLUSIONS 7-1
   7.1 PRODUCT OUTPUT 7-3

CONTENTS (Continued)

Page

8. INPUTS AND REFERENCES 8-1
8.1 DOCUMENTS CITED 8-1
8.2 CODES, STANDARDS, REGULATIONS, AND PROCEDURES 8-7
8.3 SOURCE DATA, LISTED BY DATA TRACKING NUMBER 8-7
8.4 SOFTWARE CODES 8-8

APPENDIX A - YUCCA MOUNTAIN REVIEW PLAN ACCEPTANCE CRITERIA A-1

APPENDIX B - DATA QUALIFICATION REPORT B-1

FIGURES

Page

6-1. Location Maps and Generalized Geologic Map for Grants Ridge and East Grants Ridge 6-3
6-2. Photograph of the South Side of East Grants Ridge, Showing Rhyolitic Tuffs and Volcaniclastic Host Rocks, Alkali Basalt Plug, and Basaltic Pyroclastic Deposits 6-4
6-3. Geologic Map (Close-Up) of Paiute Ridge–Slanted Buttes, Nevada 6-6
6-4. Geologic Map of the Paiute Ridge Plug, Half Pint Range, Nevada 6-8
6-5. Schematic Cross-Section of Paiute Ridge Plug, Half Pint Range, Nevada 6-9
6-6. Location Map for Basalt Ridge and Basalt Ridge East, Nevada 6-10
6-7. Schematic Drawing of Basaltic Dike Set and Eruptive Equivalents on South Edge of Basalt Ridge East 6-14
6-8. Configuration for Pressure Build-Up Analyses 6-18
6-9. Yielding and Deformation of Scoria Cones Fully Blocked to Various Depths 6-24
6-10. Tangential Stresses Around a Conduit Blocked by Slumping into a Scoria Cone for Different Magma Pressures 6-25
6-11. Tensile Stresses Surrounding Conduit Blocked by Freezing 6-26
6-12. Magma Diversion by a 60° Norma Fault Cutting a Vertical Dike 6-27
6-13. Geometry, Initial and Boundary Conditions of the Secondary Crack Analyzed 6-29
6-14. Location (Relative to the Drift Periphery) of the Magma Front Inside a Joint as a Function of Time: Case 102 6-31
6-15. Results for Magma Temperatures (K) in Secondary Crack 6-32
6-16. Dike Drift Scenarios 6-34
6-17. Color Plot of the Logarithm of Volumetric Solid Concentration at Different Times taken in the Drift for Two Simulations 6-42
6-18. Vertical Profiles of Parameters Calculated at a Distance of 100 m away from the Dike (Blue Curve is Simulation A and Red Curve is Simulation B) 6-43
6-19. Time Sequence at 2 s (Blue Curve) and 5 s (Red Curve) for Simulation A1, 135 m Down the Drift from the Dike 6-44
6-20. Outlet Mass Flux Normalized by the Constant Inlet Mass Flux (182,124 kg/s/m) versus Time 6-45

B-1. Central Portion of Computational Grid for Corroborative Calculations B-3

INTENTIONALLY LEFT BLANK

TABLES

Page

3-1. Computer Software 3-1

4-1. Data Supporting the Development of Input Parameter Values for the Magma Dynamics Analysis 4-2
4-2. Criteria Applicable to this Analysis Report 4-7

6-1. Material Properties 6-19
6-2. Magma Breakout Pressures 6-22
6-3. Inputs for Thermal Simulation with FLAC V4.04 6-31
6-4. Geometry, Wall Boundary Conditions, and Physical Conditions 6-35
6-5. Initial and Flow Boundary Conditions 6-35

B-1. Configurations for Corroboration Calculations B-2
B-2. Data from Evaluations B-4

INTENTIONALLY LEFT BLANK

ACRONYMS

BSC	Bechtel SAIC Company, LLC
DTN	data tracking number
DOE	U.S. Department of Energy
EPRI	Electric Power Research Institute
IA	igneous activity
KTI	key technical issue
NRC	U.S. Nuclear Regulatory Commission
TDMS	technical data management system
TSPA	total system performance assessment
YMP	Yucca Mountain Project
YMRP	Yucca Mountain Review Plan

INTENTIONALLY LEFT BLANK

1. PURPOSE

1.1 INTRODUCTION

Small-volume basaltic volcanic activity at Yucca Mountain has been identified as one of the potential events that could lead to release of radioactive material from the U.S. Department of Energy (DOE) designated nuclear waste repository at Yucca Mountain. Release of material could occur indirectly as a result of magmatic dike intrusion into the repository (with no associated surface eruption) by changing groundwater flow paths, or as a result of an eruption (dike intrusion of the repository drifts, followed by surface eruption of contaminated ash) or volcanic ejection of material onto the Earth's surface and the redistribution of contaminated volcanic tephra. Either release method includes interaction between emplacement drifts and a magmatic dike or conduit, and natural (geologic) processes that might interrupt or halt igneous activity. This analysis provides summary information on two approaches to evaluate effects of disruption at the repository by basaltic igneous activity: (1) descriptions of the physical geometry of ascending basaltic dikes and their interaction with silicic host rocks similar in composition to the repository host rocks; and (2) a summary of calculations developed to quantify the response of emplacement drifts that have been flooded with magma and repressurized following blockage of an eruptive conduit. The purpose of these analyses is to explore the potential consequences that could occur during the full duration of an igneous event.

Specific technical objectives are to:

- Describe analogue dike and conduit configurations to be expected in the unlikely event of a igneous intrusion/eruption at Yucca Mountain. The descriptions will be used as a means of corroboration for data previously presented in *Characterize Eruptive Processes at Yucca Mountain, Nevada* (BSC 2004 [DIRS 169980]).

- Describe the environment to be expected in an emplacement drift if the first intrusion of magma into a drift is pyroclastic.

- Describe the pressures that would be required for magma to break through blockages of dikes and conduits due to scoria avalanches, magma freezing, or faulting.

- Develop quantitative descriptions of magma flow during the formation of secondary dikes emanating from an emplacement drift that has been filled and then further pressurized at times as late as 60 days after initial filling. After 60 days, magma in the drift is sufficiently solid that remobilization is not expected to occur (BSC 2004 [DIRS 170028], Appendix D, Figure D-3).

- Determine the flow field induced in a conduit/drift system by the sudden release of blockage-induced pressures.

- Provide information on uncertainty for parameters related to magma intrusion into the repository and volcanological phenomena examined in previous reports *Dike/Drift Interactions* (BSC 2004 [DIRS 170028]) and *Characterize Eruptive Processes at Yucca Mountain, Nevada* (BSC 2004 [DIRS 169980]).

Toward these ends, (1) field characteristics of relevant geometries from four analogue volcanoes, including some of their subsurface "plumbing", are described; (2) numerical analyses are presented which describe the possible pyroclastic flow of magma from a dike into an empty drift and which investigate the magma pressures needed for magma to break through or to go around a blockage in a dike or conduit above repository level; (3) the pressure calculations provide input to a second series of numerical analyses conducted to estimate the flow-fields of magma that might produce secondary dikes at locations removed from the initial intersection of a drift by a dike, or that might draw magma from an emplacement drift into an erupting conduit, either of which could result in increased volumes of waste being released during an eruption.

1.2 BACKGROUND

This analysis advances aspects of the work reported in *Characterize Eruptive Processes at Yucca Mountain, Nevada* (BSC 2004 [DIRS 169980] and *Dike/Drift Interactions* (BSC 2004 [DIRS 170028]). The descriptions of the physical expressions of basaltic dikes ascendant through silicic tuffs support the numerical calculations, which attempt to define the sequence and properties of interactions resulting from intrusion of an empty repository drift by a magma-filled dike. In particular, *Dike/Drift Interactions* (BSC 2004 [DIRS 170028]) focused on early interaction of dike and drift within seconds to days after intersection. The calculations summarized in the current analysis focus on processes that might occur later in an igneous event. The range for the duration of potential volcanic events within the Yucca Mountain region is based on observations of historical eruptions at volcanoes of similar composition and volume, and is discussed in *Characterize Eruptive Processes at Yucca Mountain, Nevada* (BSC 2004 [DIRS 169980], Section 6.3.3.4). Examining longer durations of the magma-drift interaction focuses some aspects of this analysis on effects of elevated temperatures of the surrounding host rock, which were not addressed in *Dike/Drift Interactions* (BSC 2004 [DIRS 170028]). Analyses presented in *Dike/Drift Interactions* (BSC 2004 [DIRS 170028], Section 6.7.1.2) confirm that after a month the rock surrounding an intruded drift would be heated to temperatures above 300°C to distances of about 2 m from the edge of the drift, resulting in changes to constitutive properties of the host rock.

This analysis also addresses a scenario proposed by Woods et al. (2002 [DIRS 163662]), referred to as the "dog-leg" scenario. In their analysis, basaltic magma might escape the intruded drifts by initiating a new (vertical) fracture at some distance down the drift away from the site of the original intersection by the dike. The analysis is facilitated by use of several simplifying assumptions and boundary conditions, which together tend toward idealized initial conditions, facilitating the instantaneous expansion of volatile gases exsolved from the magma. *Dike/Drift Interactions* (BSC 2004 [DIRS 170028]) provided an assessment and independent analyses of several events and processes related to the "dog-leg" scenario of Woods et al. (2002 [DIRS 163662]). The postulated "dog-leg" scenario also was evaluated by the Igneous Consequences Peer Review Panel in their final report, which found the scenario "improbable" but recommended further investigation (Detournay et al. 2003 [DIRS 169660], Chapter 3.4.8, Chapter 5). The Electric Power Research Institute (EPRI) published an analysis of potential igneous processes at Yucca Mountain, including an analysis of the "dog-leg" scenario (EPRI 2004 [DIRS 171915], Section 4.3).

This report provides additional information to address key technical issue (KTI) agreement igneous activity (IA) 2.18. This KTI agreement relates to providing an evaluation of the effects of magma flow processes on engineered repository structures during the full duration of an igneous event. Agreement IA 2.18 was reached during the U.S. Nuclear Regulatory Commission (NRC)/DOE Technical Exchange and Management Meeting on Igneous Activity, held September 5, 2001, in Las Vegas, Nevada (Reamer 2001 [DIRS 159894], p. 2, Attachment I). A response by the DOE in August 2004 submitted information to address KTI IA 2.18 but, in a subsequent evaluation (Kokajko 2005 [DIRS 174026]), the NRC concluded that the DOE had not extended its analysis of the formation of secondary vents past the analysis of the initial first minutes of a volcanic eruption. The analysis presented in Section 6.3.2 below investigates the effect of higher temperatures in the host rock surrounding a drift, as would result if magma had filled a drift some weeks before a repressurization event that might open a secondary dike path for magma to flow to the surface.

1.3 SCOPE

The analyses documented in this report investigate scientific phenomena or parameters associated with intersection of a repository drift by a magma-filled dike. Aspects of the overall geologic repository are evaluated by documenting near-surface structures of analogue volcanoes for use as corroborative data and by solving mathematical problems by numerical methods that define these scientific phenomena. The analyses rely, in part, on a previously developed and validated mathematical model, specifically that described in *Dike/Drift Interactions* (BSC 2004 [DIRS 170028]), of a low-probability magmatic event intersecting the repository and the numerical manipulations required to calculate impact of the event on repository structures (drifts). No revision of the previous mathematical model was required in order to complete this scientific analysis. The work supporting this scientific analysis report is conducted in accordance with *Technical Work Plan for: Igneous Activity Assessment for Disruptive Events* (BSC 2005 [DIRS 174773], Sections 1.2.1, 2.2.1.1, and 2.2.1.2). The analyses reported here contain only portions of the scope identified for this report in *Technical Work Plan for: Igneous Activity Assessment for Disruptive* Events (BSC 2005 [DIRS 174773], Section 2.2.1). Specifically, the following deviations have been made from the work scope as described in the technical work plan sections:

- This analysis report does not cover gas-flow through drifts due to the need to modify and requalify the appropriate software gas transport through connecting backfilled drifts.

- This analysis report does not discuss the calculation of the “zone of influence” around a dike, which is addressed in *Number of Waste Packages Hit by Igneous Intrusion* (BSC 2005 [DIRS 174066], Appendix G).

- Laboratory analyses of vesicle, crystal, and clast characteristics are not discussed in this report.

The analyses developed in this report address the objectives listed above in Section 1.1 and conclusions are presented in Section 7.

Summaries of field studies at four analogue basaltic intrusive/extrusive sites are given in Section 6.2. The descriptions include characteristics of the feeder dikes (number, thickness, spacing), volcanic conduit geometry, and the width of the feeder-dike zone on approach to the near-surface and surface environment. The sites are East Grants Ridge, New Mexico; and Paiute Ridge, Basalt Ridge, and Basalt Ridge East, Nevada. Assumptions are listed in Section 5. The descriptions of field analogues are used for corroboration of data developed in *Characterize Eruptive Processes at Yucca Mountain, Nevada* (BSC 2004 [DIRS 169980]).

Section 6.3 contains summaries of calculations for repository-level and near-surface level interactions of dike and drift. Sections 6.3.1 and 6.3.2 present analyses of conditions that might result from blockage of a dike or conduit after it has reached the surface. Blockages of dikes and conduits due to scoria avalanches, magma freezing, or faulting are addressed; avalanching and freezing apply to conduits, while freezing and faulting apply to dikes. The analysis uses a two-dimensional thermomechanical code to calculate the response of these geological configurations due to increasing magma pressures at depth to estimate the pressures that would be required for magma to break through the blockages. The software used (FLAC V4.04 (BSC 2004 [DIRS 172432]) or UDEC V3.14 (BSC 2004 [DIRS 172322])) is described in Section 3. Input data and parameters are presented in Section 4.1. Section 5 lists assumptions related to input parameters for the calculation.

Release of pressure in a dike or conduit due to failure of a blockage may result in flow of magma from a flooded emplacement drift into the dike or conduit. This could result in waste packages being drawn into and subsequently erupted through the dike/conduit system that would otherwise have remained in a magma-filled drift. This report presents a two-dimensional analysis of the flow-field induced in a conduit/drift system by the sudden release of built-up magma pressures using a multiphase fluid dynamics code (Section 6.4.2). The software used (GMFIX V1.61 (BSC 2005 [DIRS 174137])) is described in Section 3.1. Input data and parameters are presented in Section 4. Section 5 discusses assumptions related to input parameters for the calculation.

In Section 6.3.2, this report extends the analysis of dike propagation potential in cold host rock presented in *Dike/Drift Interactions* (BSC 2004 [DIRS 170028], Section 6.5.1) to host rock at elevated temperatures (~ 300°C), realized at later times during an intrusive igneous event. The new work includes a thermomechanical analysis of dike extension for effusive magma, in which the propagation into either cold or warm rock is coupled with heat loss into the rock and increase in magma viscosity due to partial crystallization. To simulate the intrusion of pyroclastic magma into pre-existing cracks, the crack openings are used as a boundary condition for calculating multiphase flow with heat loss to the crack walls. The result of these two-dimensional analyses are quantitative descriptions of magma flow during the formation of secondary dikes emanating from an emplacement drift that has been filled and then further pressurized at times as late as 60 days after initial filling. The software used (FLAC V4.04 (BSC 2004 [DIRS 172432]), GMFIX V1.61 (BSC 2005 [DIRS 174137])) is described in Section 3.1. Input data and parameters are presented in Section 4. Section 5 discusses assumptions related to input parameters for the calculation.

Discussion of the analysis of initial pyroclastic flow appears in Section 6.4. This section develops a description of the environment to be expected in an emplacement drift if the first

intrusion of magma into a drift is pyroclastic. This is done by applying a multiphase fluid dynamics code with reasonable initial conditions to simulate the movement of magma up a dike and into an open drift while its water component is expanding or contracting in response to decreasing or increasing pressure. These calculations approximate the three-dimensional nature of the dike/drift combination with a two-dimensional Cartesian geometry. These numerical calculations are not part of the previously developed and validated mathematical model for magma flow into drifts (BSC 2004 [DIRS 170028], Section 6.4), but the two-phase flow approach is standard scientific practice for calculating such processes. The software used (GMFIX V1.61 (BSC 2005 [DIRS 174137])) is described in Section 3.1. Input data and parameters are presented in Section 4.1. Assumptions supporting the calculations are listed in Section 5.

1.4 LIMITATIONS

Limitations of this scientific analysis are listed below:

- The analogue studies of volcanoes are limited by number of volcanoes visited and by availability of accessible exposures to features of interest. For example, the analogue at Basalt Ridge East (Section 6.2.3.3) provides exposures of feeder dikes for 270 m of relief beneath the paleosurface, but the exposures occur at locations that are laterally removed from the area directly beneath the vent (because of the locations of the eroded canyons). Similarly, at East Grants Ridge, a basaltic plug beneath an eruptive sequence is exposed for more than 100 m vertically, but is still not deep enough to observe the magmatic system that fed the volcano. These restrictions limit the breadth of the conclusions and their applicability, but these analogues should provide guidance on real-world structures beneath small-volume basaltic volcanoes.

- Numerical calculations of repressurized magma systems (Section 6.3) require initial and boundary conditions that specify cases within a limited range and are therefore inherently limited in scope. Material properties of basalt, basalt magma, host tuff, and magma-vapor systems are selected to approximate those expected at Yucca Mountain, but cannot define all the variations to be found there or elsewhere. The analyses investigate the most significant and likely uncertainties rather than being fully representative of conditions associated with potential igneous activity at Yucca Mountain.

- Numerical calculations of magma depressurization (Section 6.4) are limited by the same issues stated above. In addition, the drift in the analysis is empty, which will not be the case following closure of the repository, and the material-flow phenomena observed in the analyses would probably not be as simple as shown. Further, the effects of waste packages and drip shields on the flow and their influence on diversion of the gas–particle mixture near an open dike in a drift are not examined. The analyses investigate the most significant and likely uncertainties rather than being narrowly defined scenarios and should not be taken to be fully representative of conditions associated with potential igneous activity at Yucca Mountain.

- Because the scenarios described within this document are focused in scope, no data points or ranges (other than qualified input) or descriptions of analogue subvolcanic structures should be taken or used without stating the purpose and context in which they are used herein.

2. QUALITY ASSURANCE

This Yucca Mountain Project (YMP) analysis report is prepared to LP-SIII.9Q-BSC, *Scientific Analyses*.

Development of this analysis report and the supporting activities have been determined to be subject to the Yucca Mountain Project's quality assurance program (DOE 2004 [DIRS 171539]). Approved quality assurance procedures identified in *Technical Work Plan for: Igneous Activity Assessment for Disruptive Events* (BSC 2005 [DIRS 174773], Section 4) have been used to conduct and document the activities described in this report. The methods that have been used to control the electronic management of data are identified in BSC (2005 [DIRS 174773], Section 8.4). There were no variances from the planned methods.

The report discusses phenomena associated with a potential igneous intrusion into the drift complex of the repository. An igneous intrusion would impact engineered barriers (e.g., waste packages, drip shields) that are classified in *Q-List* (BSC 2005 [DIRS 174269]) as "Safety Category" because they are important to waste isolation, as defined in AP-2.22Q, *Classification Analyses and Maintenance of the Q-List*. The report contributes to the analysis data used to support performance assessment. The conclusions do not directly impact engineered features important to safety, as defined in AP-2.22Q.

INTENTIONALLY LEFT BLANK

3. USE OF SOFTWARE

3.1 SOFTWARE TRACKED BY CONFIGURATION MANAGEMENT

The computer codes used directly in these analyses are summarized in Table 3-1. All software except exempt software (Section 3.2) was fully qualified. All software was obtained from Software Configuration Management and is appropriate for the application. Qualified codes were used only within the range of validation, and have no limitations on their output because of their application.

Table 3-1. Computer Software

Software Title and Version (V)	Software Tracking Number	Code Usage and Limitations	Computer Platform, Operating System
GMFIX V1.61 BSC 2005 [DIRS 174137]	11192-1.61-00	An acquired code to simulate interaction between magma (represented as particles and gas, as would be the case for fragmented magma) rising in a dike and a repository drift, as well as the dynamics associated with decompression of a drift after it has been filled with magma and repressurized due to blockage in the volcanic system; limited to solid particles in vapor.	PC Windows XP
FLAC V4.04 BSC 2004 [DIRS 172432]	10167-4.04-00	This is commercially available software that is used for a very broad range of geomechanical problems including hydraulic, mechanical, and thermal coupling. Used to simulate flow of effusive magma and deformation of blockage to magma flow.	PC Windows 2000
UDEC V3.14 BSC 2004 [DIRS 172322]	10173-3.14-00	Analyzes opening of pre-existing fractures by magma. This is code has been used for hydromechanical behavior of fracture media in related problems in previous reports.	PC Windows 2000

FLAC V4.04 (BSC 2004 [DIRS 172432]) is used in Section 6.3 to analyze mechanical deformation of geologic media in response to applied pressures and to analyze heat loss from a constant viscosity liquid flowing into a secondary dike. UDEC V3.14 (BSC 2004 [DIRS 172322]) is used in Section 6.3 to analyze the intrusion of liquid into a pre-existing crack. GMFIX V1.61 (BSC 2005 [DIRS 174137]), is used in Section 6.4 to analyze the mechanics of partially to fully coupled, two-phase flow with solid or magma fractions of 65 percent or less and temperatures below 1,400 K. Gas compositions range from water vapor to air.

3.2 EXEMPT SOFTWARE

Standard, built-in functions of Microsoft Excel 2000 for the Dell Inspiron 8000 and Dell Optiplex computers or Microsoft Excel 97 for the Compaq V900 computer were used to calculate some parameters. Excel is used to support calculations in Sections 6.3 and 6.4. This software is exempt from the software validation requirements contained in LP-SI.11Q-BSC, *Software Management*. The inputs and outputs of those formulas, and additional information required for an independent technically qualified person to verify the results of analyses using exempt software are provided in Section 6.

INTENTIONALLY LEFT BLANK

4. INPUTS

In this scientific analysis report, input data are derived from two main sources: (1) field measurements of the geometries of intrusive structures, such as feeder dikes, radial dikes, sills, and conduits, at analogue volcanoes (Section 6.2); and (2) YMP data available in the YMP technical data management system (TDMS) for parameters required to perform analyses of (a) blockage of magma pathways (Section 6.3.1) and the potential formation of secondary magma pathways in hot rock at some distance down the drift from the initial dike intersection (Section 6.3.2), and (b) multiphase pyroclastic flow, which may result when a volatile-rich magma-filled dike intersects a repository drift (Section 6.4). In Section 6.2, field data, which typically measure local features, are used to develop overall geometry of the structures present and relate them to processes and to local or regional tectonic structures. The analyses in Sections 6.3 and 6.4 consider scenarios that might occur later in an igneous event, such as blockage of dikes or vents, and changes in rock stress caused by heating of the host rock by magma flooding the drifts and the effect of those changes on secondary dike propagation. Direct inputs to the analyses in Section 6 are described in Section 4.1. Use of several external sources of data is also justified for intended use in Section 4.1.2 per the requirements of LP-SIII.9Q-BSC. Criteria are listed in Section 4.2, and Section 4.3 covers codes, standards, and regulations.

4.1 DIRECT INPUTS

4.1.1 Input Parameters

Data sources used as input to Sections 6.2 through 6.4 are listed in Table 4-1. Only qualified data have been used as input parameters. Data for mechanical properties of tuff from CRWMS M&O (1999 [DIRS 126475], Tables 10 through 13 and Table 15) are qualified for intended use in this report in Appendix B.

The analysis in Section 6.2 uses input from a scientific notebook, *Ash Redistribution, Lava Morphology, and Igneous Processes Studies* (Krier 2005 [DIRS 174079], pp. 93 to 150), which provides the results of field work conducted in late 2004 and early 2005.

The parameter in Table 4-1 called "Fixed hydraulic aperture of secondary crack" is from REV 00 of *Dike/Drift Interactions* (BSC 2003 [DIRS 165923], Section 6.4.10.2.1), which is a superceded YMP document. The results of Case 102, which included a fixed crack opening and average magma velocity, were not carried forward to *Dike/Drift Interactions* (BSC 2004 [DIRS 170028]) when the document was revised, but that case is expected to be characteristic of events that may accompany dike intrusion at Yucca Mountain. There were no software or related issues involving the revision of *Dike/Drift Interactions* (BSC 2003 [DIRS 165923], Section 6.4.10.2.1) that would disqualify it as a source of direct input.

Table 4-1. Data Supporting the Development of Input Parameter Values for the Magma Dynamics Analysis

Data Description	Source	Where Discussed/Used
Field descriptions of analogue sites	Krier 2005 [DIRS 174079], pp. 93 to 150	Section 6.2
Outer diameter of solidified basalt conduit	DTN: LA0407DK831811.001 [DIRS 170768] (first table)	Section 6.3.1
In situ horizontal stress	DTN: SNF37100195002.001 [DIRS 131356], Summary, p. 1	Section 6.3.1
Gravitational acceleration	Incropera and DeWitt 2002 [DIRS 163337], Table A-6	Table 6-1, Section 6.3.1
Loose scoria mechanical properties	Duncan et al. 1980 [DIRS 161776], Table 5 and Equation 3	Table 6-1, Section 6.3.1
Undisturbed mechanical scoria properties	Duncan et al. 1980 [DIRS 161776], Table 5 and Equation 3	Table 6-1, Section 6.3.1
Solidified basalt mechanical properties	Gupta and Sishagiri Rao 2000 [DIRS 174063], Tables 2 and 3	Table 6-1, Section 6.3.1
Solidified basalt friction angle	Hoek and Brown 1997 [DIRS 170501], Figure 8	Table 6-1, Section 6.3.1
Tuff mechanical properties	CRWMS M&O 1999 [DIRS 126475], Tables 10 to 13, and 15	Table 6-1, Section 6.3.1
Fixed hydraulic aperture of secondary crack	BSC 2003 [DIRS 165923], Section 6.4.10.2.1	Section 6.3.2
Host rock thermal conductivity	Detournay et al. 2003 [DIRS 169660], Table 1-2	Table 6-3, Section 6.3.2
Host rock specific heat	Detournay et al. 2003 [DIRS 169660], Table 1-2	Table 6-3, Section 6.3.2
Host rock density	Detournay et al. 2003 [DIRS 169660], Table 1-2	Table 6-3, Section 6.3.2
Magma thermal conductivity	Detournay et al. 2003 [DIRS 169660], Table 1-2	Table 6-3, Section 6.3.2
Magma latent heat	Detournay et al. 2003 [DIRS 169660], Table 1-2	Table 6-3, Section 6.3.2
Initial magma temperature	DTN: LA0407DK831811.001 [DIRS 170768], Table 8	Table 6-3, Section 6.3.2
Magma effective solidification temperature	DTN: MO0508SPAMAGMA.000 [DIRS 175008]	Table 6-3, Section 6.3.2
Width of primary and secondary dikes	DTN: LA0407DK831811.001 [DIRS 170768] (first table)	Table 6-4, Section 6.4
Magmatic particle density	DTN: LA0407DK831811.001 [DIRS 170768] (first table)	Table 6-4, Section 6.4
Magmatic particle diameter	DTN: LA0407DK831811.001 [DIRS 170768] (first table)	Table 6-4, Section 6.4

Table 4-1. Data Supporting the Development of Input Parameter Values for the Magma Dynamics Analysis (Continued)

Data Description	Source	Where Discussed/Used
Horizontal stress at repository level 1,000 years after closure	DTN: MO0411EG831811.000 [DIRS 174959], Disk 1, Figure 6-34	Table 6-4, Section 6.4
Mean ash particle diameter	DTN: LA0407DK831811.001 [DIRS 170768] (first table)	Table 6-4, Section 6.4
Physical properties of pyroclastic flow	Dartevelle 2004 [DIRS 174132], Table A1, A2	Section 6.4
Equations for elastic properties	Timoshenko and Goodier (1970 [DIRS 121096], pp. 10 through 11)	Section 6.3.1

4.1.2 Justification of External Sources of Input

4.1.2.1 Duncan, J.M.; Byrne, P.; Wong, K.S.; and Mabry, P., 1980. *Strength, Stress-Strain and Bulk Modulus Parameters for Finite Element Analyses of Stresses and Movements in Soil Masses.* UCB/GT/80-01. Berkeley, California: University of California, College of Engineering, Office of Research Services. [DIRS 161776]

No data have been found in the literature for the deformational properties of basaltic scoria, either undisturbed or loose. The properties listed are estimated based on tabulated properties for generic gravel (Duncan et al. 1980 [DIRS 161776], Table 5 and Equation 3). The report was released by University of California, Berkeley, which is one of the world's leading institutions in research on constitutive behavior and numerical analysis of soils. The two co-authors, professors J.M. Duncan and P. Byrne, have published a large number of articles on constitutive behavior of soils. The values published in the report are in agreement with the observations of Marachi et al. (1972 [DIRS 157883]).

4.1.2.2 Gupta and Rao. 2000. "Weathering Effects on the Strength and Deformational Behaviour of Crystalline Rocks under Uniaxial Compression State." *Engineering Geology, 56,* pp. 257-274. New York, NY: Elsevier Science B.V. [DIRS 174063]

Gupta and Rao (2000 [DIRS 174063]) was published in Engineering Geology, a peer-reviewed journal. At the time of publication, the authors were at the Department of Civil Engineering, Indian Institute of Technology, Delhi. The properties for basalt are based on measurements on small (centimeter-sized) samples (Gupta and Rao 2000 [DIRS 174063], Tables 2 and 3) and, as discussed in Section 6.3, may overestimate the strength of a larger rock mass. The tensile strength value from this source is considerably higher than from other reports, such as *Fracturing of Etnean and Vesuvian Rocks at High Temperatures and Low Pressures* (Rocchi et al. 2004 [DIRS 173995], Table 3, p. 146); the higher value allows the calculation to reach higher pressures so that a larger region of failure parameter space can be investigated.

4.1.2.3 Hoek, E. and Brown, E.T. 1997. "Practical Estimates of Rock Mass Strength." *International Journal of Rock Mechanics and Mining Science & Geomechanics Abstracts, 34,* (8), 1165-1186. Oxford, England: Pergamon. [DIRS 170501]

Professors E. Hoek and E.T. Brown are leading rock mechanics experts and researchers. The article, *Practical Estimates of Rock Mass Strength* (1997 [DIRS 170501]), was published in the International Journal of Rock Mechanics and Mining Sciences, which is a peer-reviewed journal. This paper incorporated numerous refinements to the original 1980 criterion as discussed in the following paragraphs. In addition, a method for estimating the equivalent Mohr-Coulomb cohesion and friction angle was introduced. In this method, the Hoek-Brown criterion is used to generate a series of values relating uniaxial strength to confining pressure (or shear strength to normal stress) and these are treated as the results of a hypothetical large-scale in situ triaxial or shear test. A linear regression method is used to find the average slope and intercept, and these are then transformed into a cohesive strength *c* and a friction angle f. The most important aspect of this curve-fitting process is to decide upon the stress range over which the hypothetical in situ 'tests' should be carried out. This was determined experimentally by carrying out a large number of comparative theoretical studies in which the results of both surface and underground excavation stability analyses, using both the Hoek-Brown and Mohr-Coulomb parameters, were compared.

The original failure criterion was developed in the early 1980s. The criterion was required in order to provide input information for the design of underground excavations. Since no suitable methods for estimating rock-mass-strength appeared to be available at that time, efforts were focused on developing a dimensionless equation that could be scaled in relation to geological information. The original Hoek-Brown equation was neither new nor unique—an identical equation had been used for describing the failure of concrete as early as 1936. The significant contribution that Hoek and Brown made was to link the equation to geological observations in the form of Rock Mass Rating and later to the Geological Strength Index.

One of the issues that had been problematic throughout the development of the criterion was the relationship between the Hoek-Brown criterion, with the non-linear parameters *m* and *s*, and the Mohr-Coulomb criterion, with the parameters *c* and f. Practically all software for soil and rock mechanics is written in terms of the Mohr-Coulomb criterion and it was necessary to define the relationship between *m* and *s* and *c* and f to allow the criterion to be used to provide input for this software. Addition of this modification of the Hoek-Brown equation in 1983 completed the development of the model.

The Hoek-Brown failure criterion is a basis of standard engineering practice, considered to be the most realistic failure criterion for in situ rock masses. It can be found in many rock mechanics text books published within the last 20 years.

4.1.2.4 Detournay, E.; Mastin, L.G.; Pearson, J.R.A.; Rubin, A.M.; and Spera, F.J., 2003. *Final Report of the Igneous Consequences Peer Review Panel, with Appendices. Las Vegas*, Nevada: Bechtel SAIC Company. [DIRS 169660]

The exact properties of basaltic magma and tuff are variable, even within a single rock unit. The values are, as indicated, selected from ranges used by *Igneous Consequences Peer Review Panel* (Detournay et al. 2003 [DIRS 169660]), a qualified source prepared using AP-2.12Q, *Peer Review*, which has since been superceded by LP-2.12Q-BSC, *Peer Review*. All such data listed in Table 4-1 are the same as used in *Dike/Drift Interactions* (BSC 2004 [DIRS 170028]).

Three properties values of the repository host rock, provided in *Final Report of the Igneous Consequences Peer Review Panel, with Appendices* (Detournay et al. 2003 [DIRS 169660], Table 1-2), were selected over values from DTN: SN0404T0503102.011 (thermal conductivity and density, documented in *Thermal Conductivity of the Potential Repository Horizon* (BSC 2004 [DIRS 169854], Table 6-6) and from DTN: SN0307T0510902.003 (specific heat, documented in *Heat Capacity Analysis Report* (BSC 2004 [DIRS 170003], Table 6-9)). This is because the Detournay et al. data (1) were developed by the Peer Review Panel from YMP-qualified sources as being "typical" values for the repository host rock, (2) the data were previously used in development of analyses in *Dike/Drift Interactions* (BSC 2004 [DIRS 170028]), and (3) consistency across these analyses was desired. The values developed by Detournay et al. (2003 [DIRS 169660]) for these properties are consistent with the values and standard deviations as reported in the respective DTNs.

4.1.2.5 Dartevelle, S., 2004. "Numerical modeling of geophysical granular flows: 1. A comprehensive approach to granular rheologies and geophysical multiphase flows." *Geochemistry Geophysics Geosystems, 5,* (8), 1-28. Washington, D.C.: American Geophysical Union. [DIRS 174132]

This article appeared in the peer-reviewed journal Geochemistry, Geophysics, Geosystems (G^3). The e-journal is published by the American Geophysical Union, which was established in 1919 by the National Research Council. The method reported by Dartevelle (2004 [DIRS 174132]) is derived from Department of Energy multiphase codes of the MFIX family with specific modifications to address complexities of volcanic multiphase flows. Simulations of plinian clouds and base surges in the accompanying paper by Dartevelle et al. (2004 [DIRS 174139], Figures A1, A2, and A3) show many of the features of these phenomena that have not been reliably reproduced by earlier analyses. In addition, the simulations comprise a comparison of calculations with various grid sizes, an essential feature in validating any numerical analysis.

4.1.2.6 Timoshenko, S.P. and Goodier, J.N. 1970. *Theory of Elasticity.* 3rd Edition. New York, New York: McGraw-Hill. [DIRS 121096].

This book is a widely used and cited source for analysis of elastic behavior of materials. It is still used in many colleges and universities as a textbook for study of elasticity by both engineers and scientists, even though it is no longer available except as a reissued paperback. The equations cited, which are unchanged from earlier editions, provide

widely accepted relations for conversion among various elastic constants, as used in Section 6.4.

4.2 CRITERIA

This scientific analysis report provides technical basis for parameters, which will be used by the Total System Performance Assessment (TSPA) to evaluate the effects of an eruption through the repository at Yucca Mountain. The report provides discussion and summaries of uncertainties associated with inputs to the analysis and outputs from the analysis. The information and data in this report are based on field observations of subsurface magmatic dikes and conduits, as well as calculations of basaltic dike interactions with a repository drift and the effects of blockage of the dike or vent, as described in Section 6. The analyses examine specific scenarios that may affect the subsurface environment and engineered barriers by examining phenomena that might occur over the full duration of an igneous event. Appendix A identifies information in this report that addresses *Yucca Mountain Review Plan, Final Report* (NRC 2003 [DIRS 163274]) acceptance criteria and/or review methods related to descriptions of site characterization work (NRC 2003 [DIRS 163274], Section 1.5.3), and the integrated subissues of scenarios analysis and event probability (NRC 2003 [DIRS 163274], Section 2.2.1.2.1.3), mechanical disruption of engineered barriers (NRC 2003 [DIRS 163274], Section 2.2.1.3.2.3), and volcanic disruption of waste packages (NRC 2003 [DIRS 163274], Section 2.2.1.3.10.3).

The regulatory requirements to be satisfied by total system performance assessment are listed in 10 CFR 63.114 [DIRS 173273], *Requirements for Performance Assessment*. The acceptance criteria that will be used by the NRC to determine whether the regulatory requirements have been met are identified in the YMRP (NRC 2003 [DIRS 163274]). The pertinent requirements and YMRP acceptance criteria addressed by this scientific analysis report are listed in Table 4-2, and described in greater detail in the Appendix A. Technical requirements to be satisfied by TSPA are identified in Yucca Mountain *Project Requirements Document* (Canori and Leitner 2003 [DIRS 166275], Section 3).

Table 4-2. Criteria Applicable to this Analysis Report

Requirement Number[a]	Requirement Title[a]	10 CFR 63 Link	YMRP Acceptance Criteria[b]
PRD-002/T-004	Content of Application	10 CFR 63.21(b)(5) [DIRS 173273]	1.5.3, criteria 1 and 2
PRD-002/T-015	Requirements for Performance Assessment	10 CFR 63.114(e) and (f) [DIRS 173273]	2.2.1.2.1.3, criterion 1
PRD-002/T-015	Requirements for Performance Assessment	10 CFR 63.114(a)-(c) and (e)-(g) [DIRS 173273]	2.2.1.3.2.3, criteria 1 to 4
PRD-002/T-015	Requirements for Performance Assessment	10 CFR 63.114(a)-(c) and (e)-(g) [DIRS 173273]	2.2.1.3.10.3, criteria 1 to 3

Sources: [a] Canori and Leitner 2003 [DIRS 166275]
[b] NRC 2003 [DIRS 163274]

4.3 CODES, STANDARDS, AND REGULATIONS

No specific formally established code or standards have been identified as applying to this analysis. The applicable regulation is 10 CFR Part 63 [DIRS 173273], as specified in Section 4.2 and Table 4-2.

INTENTIONALLY LEFT BLANK

5. ASSUMPTIONS

This section describes the assumptions applicable to the use of the magma dynamics analysis. Each assumption listed is followed by a rationale for use, and a disposition in this report.

5.1 ASSUMPTIONS RELATED TO DESCRIPTIONS OF ANALOGUE VOLCANIC SITES

Assumption 5.1.1–The subvolcanic structures (basaltic dikes, sills, conduits, etc.) of volcanic units described in Section 6.2 are analogous to potential basaltic intrusive events at Yucca Mountain.

Rationale–Basaltic dikes and conduits that feed relatively small-volume basaltic volcanoes express the same general subvolcanic magma supply and delivery characteristics in a given geologic setting and with wallrock of similar chemical and mechanical characteristics.

Where Used–This assumption is used in Section 6.2.

5.2 ASSUMPTIONS RELATED TO SIMULATION OF MAGMA DYNAMICS

Assumption 5.2.1–The Lathrop Wells volcano is considered to be an appropriate analogue for future volcanic activity at Yucca Mountain.

Rationale–Lathrop Wells volcano is the most recent volcano within 50 km of Yucca Mountain.

Where Used–This assumption is used in Section 6.3.

Assumption 5.2.2–The tectonic features, such as normal faulting, that are characteristic of the region surrounding Yucca Mountain, are appropriate analogues for potential tectonic events at Yucca Mountain.

Rationale–The current tectonic setting of Yucca Mountain is not likely to change substantially during the expected period for postclosure performance because this is a short time on the scale of the tectonic history of the region.

Where Used–This assumption is used in Section 6.3.

INTENTIONALLY LEFT BLANK

6. ANALYSIS

6.1 INTRODUCTION

This analysis report focuses on dynamics of magmatic processes that might occur during the full duration of a volcanic event at Yucca Mountain, should one occur. Such processes include the development of blockages and their effects on the development of single or multiple conduits or magma pathways to the surface, pressure and magma flux variations within a magma-repository system due to temporary blockages at or above the repository, or to variations (e.g., magma pressure or magma flux) at the magma source. To understand how such geometrically complex and time-dependent processes might influence conditions within the repository, it is necessary to combine two approaches. The first of these involves the study of field analogues that provide insight into how natural magmatic systems of the appropriate size and composition behave (compared to likely future events in the Yucca Mountain area). The second approach is to use numerical analysis to constrain the specific interactions between the natural magmatic system and repository structures such as emplacement drifts. Both analogue studies and numerical analyses are reported in this section. The analogue studies expand upon and corroborate field data on conduit and dike dimensions that are reported in *Characterize Eruptive Processes at Yucca Mountain, Nevada* (BSC 2004 [DIRS 169980]). The numerical studies expand upon work reported in *Dike/Drift Interactions* (BSC 2004 [DIRS 170028], Sections 6.2, 6.4, and 6.5), which focused on the initial interactions between rising magma and repository structures. The analyses reported here focus instead on processes that might occur later during an igneous event.

Field analogue analyses are reported in Section 6.2. These include relatively small volume, alkali basalt centers that have been deeply eroded such that part of the "feeder" system (dikes and conduits) is exposed. This sometimes allows direct measurement of conduit size and shape, description of features indicative of the interaction between wall rocks and rising magma, and the interaction between rising magma and pre-existing structural weaknesses such as faults and joints.

The effects of blockages or plugs in the intrusive system and eruptive conduits are described in Section 6.3. Mechanisms for development of blockages might include: (1) collapse or avalanching of material from the inner cone slopes of a volcano into a vent; (2) solidification of magma in a dike or conduit to form a plug; (3) down-dropping of small fault blocks into a vent or dike; and (4) blockage of repository drifts due to collapsed drift walls/crown and "bulldozing" of waste packages and drip shields by flowing magma. The first three of these mechanisms are addressed in this report. Blockage may cause a build-up of pressure in the magma–repository system until the blockage fails, which then could result in a sudden decompression of the system. Two numerical codes used to study some of these processes associated with the formation and disruption of blockages, as described in Section 6.3.1, are FLAC V4.04 (BSC 2004 [DIRS 172432]) and UDEC V3.14 (BSC 2004 [DIRS 172322]). Resulting flow of multiphase magma is analyzed using the code GMFIX V1.61 (BSC 2005 [DIRS 174137]) and is described in Section 6.4.2.

Secondary magma pathways or breakouts might increase the number of waste packages that could be involved in an eruptive event. The dike propagation aspects of this work are herein conducted with the software code FLAC V4.04 (BSC 2004 [DIRS 172432]) and discussed in

Section 6.3.2, whereas the details of magma flow are addressed with GMFIX V1.61 (BSC 2005 [DIRS 174137]), as described in Section 6.4. A hypothetical example has been previously analyzed by Woods et al. (2002 [DIRS 163662]).

Because the scenarios described within this document are focused in scope, no data points or ranges (other than qualified input) or descriptions of analogue subvolcanic structures should be used without stating the purpose and context in which it is used herein.

6.2 FIELD ANALOGUES

This section describes analogue subvolcanic features at four sites in Nevada and New Mexico.

6.2.1 East Grants Ridge, New Mexico

East Grants Ridge is an erosional remnant of an alkali basaltic volcano, approximately 2.6 Ma in age (Laughlin et al. 1993 [DIRS 174240], Table 3), that is part of the Mount Taylor volcanic field in New Mexico (Perry et al. 1990 [DIRS 173994], Figure 1; Keating and Valentine 1998 [DIRS 111236]; WoldeGabriel et al. 1999 [DIRS 110071]). Erosion and faulting has resulted in "inverse topography," whereby the Grants Ridge lava flows, which originally flowed west-southwest along the axis of a paleovalley, are now preserved as a high-standing mesa due to the erosional resistance of the lavas relative to the underlying tuffs and sedimentary rocks. Lavas of Grants Ridge (East Grants Ridge on Figure 6-1) erupted from an approximately north-10°-west-trending chain of vents and flowed mainly westward (with minor lava flowing eastward). The vent locations are indicated by inward-dipping beds of welded scoria and spatter, the remnants of pyroclastic cones that formed around the vents; these features indicate that there were from 2 to 4 vents, and that the chain of vents was between 1 km and 1.5 km long.

The south side of East Grants Ridge exposes a plug-like body of vertically jointed, massive alkali basalt that intrudes older rhyolitic tuffs and volcaniclastic deposits (Figure 6-2) (Keating and Valentine 1998 [DIRS 111236]; WoldeGabriel et al. 1999 [DIRS 110071]). These deposits are capped by beds of scoria and spatter, variably welded, that dip radially away from the ~125-m-wide plug, giving the appearance of a dissected scoria cone and feeder conduit. Based upon this appearance, Crumpler (2003 [DIRS 174074], pp. 161 and 163) interpreted the southern face of East Grants Ridge to be a dissected remnant of a simple scoria cone that was originally circular in map view. He interpreted the alkali basalt plug to be a solidified lava lake that originally filled the crater of the cone and extended downward into the underlying deposits to a depth of about 100 m, below which the plug narrows rapidly into a 2-m-wide dike. However, further examination of the outcrops (Krier 2005 [DIRS 174079], pp. 93 to 97, 116 to 117, and 146) show that the plug is relatively constant in width (~125 m) as it extends downward into underlying deposits to the lowest depth of exposure (~40 m beneath the pre-alkali basalt paleosurface). Also, the exposed plug appears to be the southern end of a vent chain or fissure, not the feeder for a simple circular cone. The geometry of the plug as it extends laterally beneath East Grants Ridge is not known, but could be similar to elongated plugs or wide dikes exposed elsewhere around the Mount Taylor volcanic field, which has experienced deeper levels of erosion since the period of active basaltic volcanism.

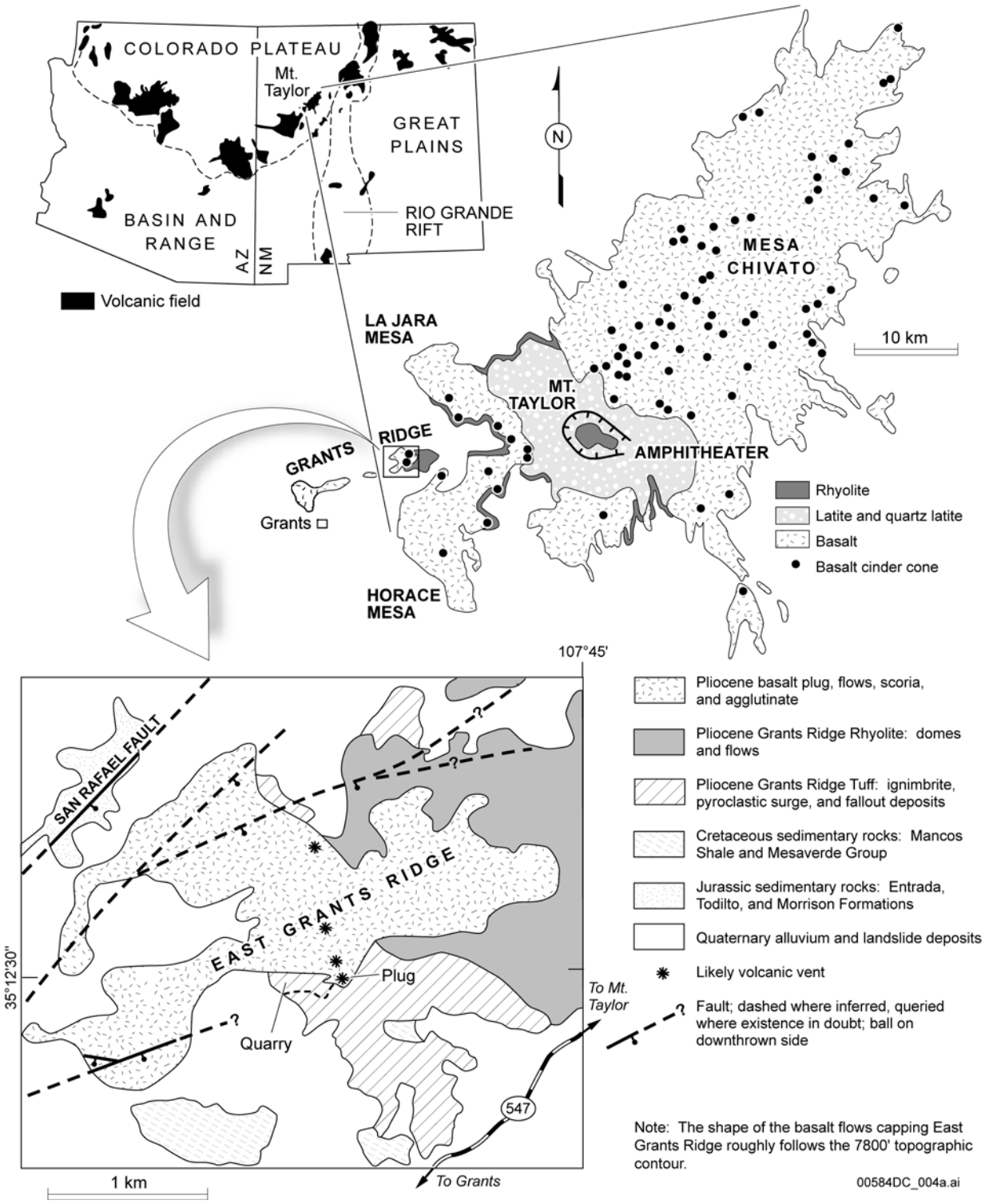

Source: Modified from Keating and Valentine 1998 [DIRS 111236], Figure 1.

Figure 6-1. Location Maps and Generalized Geologic Map for Grants Ridge and East Grants Ridge

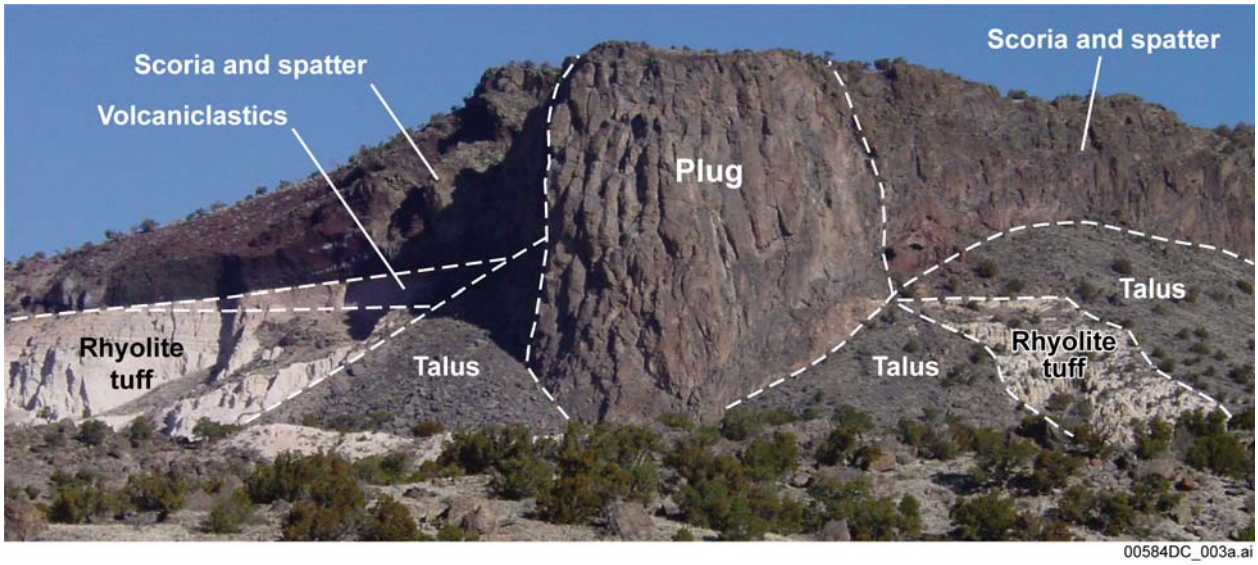

NOTE: For illustration purposes only.

Figure 6-2. Photograph of the South Side of East Grants Ridge, Showing Rhyolitic Tuffs and Volcaniclastic Host Rocks, Alkali Basalt Plug, and Basaltic Pyroclastic Deposits

In detail, the contact between the host tuff and the basaltic lava plug undulates on scales of meters such that local contact orientations are quite variable but the overall orientation is near-vertical. Undulations range from gentle low-amplitude (~1-m) scallops into the tuff, to angular blocks (protrusions) of tuff surrounded on three sides by basalt, to short spur-like dikes (most of these extend less than 2 m into the tuff, although one vertical dike, exposed in a quarry wall, extends about 50 m into the tuff; this dike is up to ~1-m thick near the plug). There are also short sill-like protrusions into the tuff; these are on the order of a 1-m thick and their original lateral extent is unknown due to erosion of the cliff walls. The tuff/basalt contact is exposed and accessible over about 100 vertical meters on the west, east, and south sides. Orientations of the contact vary locally, with dips ranging from as low as 12° (basalt over tuff) to as much as 80° to 90°, but a vast majority of visible contacts are near-vertical. Small blocky protrusions of tuff into the basalt mass produce local occurrences of rhyolitic tuff over basalt. Local peperitic textures indicate some mechanical mixing of alkali basalt and tuff host rock within distances of several decimeters from the contact between the two rock types, and the fused nature of the host tuff within ~1 m of the contact provides evidence of thermal interaction between the two (WoldeGabriel et al. 1999 [DIRS 110071]).

Location of vents associated with the 2.6-Ma East Grants Ridge eruption episode are aligned approximately 90° to regional fissures associated with the Mount Taylor volcanic field, as described by Crumpler (1980 [DIRS 173900], p. 254). A fault-bounded graben, with limited exposures in Jurassic sedimentary rocks, is located ~1,400 m north of the ridge and projects into the aligned vents (Thaden et al. 1967 [DIRS 174076], Plate 1); however, the relation to vent alignment is equivocal. Similarly, 5 km south of the ridge, the position of two Pliocene(?) basaltic vents in alignment with East Grants Ridge vents suggests possible structural control, but any direct evidence is buried beneath lavas and younger talus. Mapped faults shown in Figure 6-1 are nearly orthogonal to the vent chain. Stratigraphic displacement between the top of

the pre-alkali basalt volcaniclastics on the west side, relative to the east side, of the plug indicate that the plug might correspond with a fault scarp, but it is not possible to determine the orientation of this potential fault due to burial by basaltic deposits.

There are up to four possible vent locations on East Grants Ridge, including the exposed basalt neck described above. They are low-relief features marked by inward dipping scoria beds and topographic lows, some of which are breached by erosion. Vent spacing between these locations are 125 m, 325 m, and 800 m, respectively (Figure 6-1).

6.2.2 Paiute Ridge, Nevada

Magma of alkali basaltic composition was intruded into Paleozoic carbonates and shales and middle Miocene silicic tuffs at Paiute Ridge, located immediately east of the Nevada Test Site (Byers and Barnes 1967 [DIRS 101859]) (Figure 6-3). The $^{40}Ar/^{39}Ar$ age of the basalt is 8.58 ± 0.07 Ma (Ratcliff et al. 1994 [DIRS 106634], p. 416). The volcanic complex is composed of dikes, sills, scoria cone remnants, and lava flows that are well exposed within uplifted and eroded structural blocks. Petrologic, paleomagnetic, and field relations are consistent with a single, brief magmatic pulse of alkali basalt (Perry et al. 1998 [DIRS 144335], p. 5-29; Ratcliff et al. 1994 [DIRS 106634], p. 415; Carter Krogh and Valentine 1996 [DIRS 160928], p. 3). Although highly eroded, the complex is thought to have had a total volume of a few tenths of a cubic kilometer (volume < 1 km^3, Carter Krogh and Valentine 1996 [DIRS 160928], p. 3). The dikes and sills were intruded into a small, north-northwest-trending horst and graben system; topographic reconstruction shows that the current exposures are at a depth of 100 m to 250 m beneath the paleosurface at the time of intrusion (Crowe et al. 1983 [DIRS 100972], p. 266; Carter Krogh and Valentine 1996 [DIRS 160928], p. 10). These exposures, then, represent a subsurface level that is in the range of 50 m to 200 m above the average elevation of the planned Yucca Mountain repository.

Graben-forming faults may have formed pathways for magma ascent, as several of the dikes are coincident with normal faults in the area (Valentine et al. 1998 [DIRS 119132], p. 5-43; Crowe et al. 1983 [DIRS 100972], p. 265). The subvertical dikes range from 3 m to 20 m in width and have produced contact metamorphic vitrophyre and mineralogic alteration in the surrounding tuff up to 3 m from the contact (Keating et al. 2002 [DIRS 174077], p. 432).

One feature within the Paiute Ridge intrusive complex that may represent a subvolcanic conduit is a plug located in the south-central part of the complex (Figure 6-3). The top of the plug is approximately 27 m lower than the base of the mapped subaerial basalt flows (1,597 m) (Keating 2005 [DIRS 174988], p. 45; Byers and Barnes 1967 [DIRS 101859]). Approximately 38 vertical meters of plug are exposed, from approximately 30 m to 70 m in depth below the paleosurface. The elongate morphology of the plug reflects a complex coalescence of about eight mapped dikes (Figure 6-4). Four prominent dikes (1-m to 3-m wide) join at the northern end of the plug and, together with the intervening baked rhyolite tuff country rock, form a rough ridgeline. The largest of these dikes (dike #1 in Figure 6-4) is continuous with the main, dense basalt mass of the plug. Three additional dikes (1-m to 2-m wide) adjoin the plug on the east side, and one merges tangentially with the plug on the southwest edge.

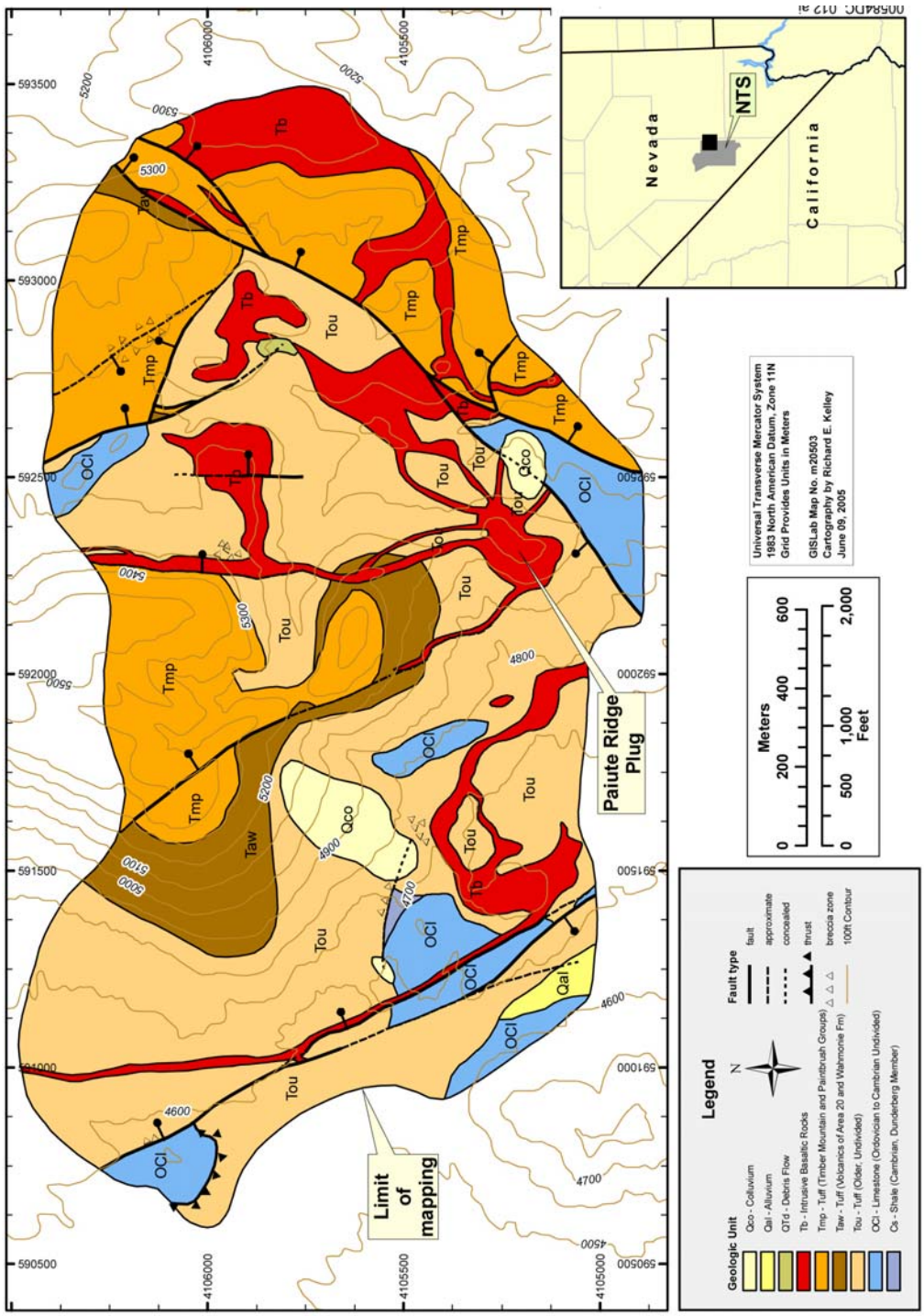

Source: Modified from map by Goff et al. (in Perry et al. 1998 [DIRS 144335], p. 5-45).

Figure 6-3. Geologic Map (Close-Up) of Paiute Ridge–Slanted Buttes, Nevada

The plug is interpreted as a zone of intersection of several dikes that formed a central conduit and a surrounding zone of disturbed host rock. The convergence of the dikes was at least partially controlled by local structures, as indicated by the co-location of dikes and faults and the orientation of intrusions parallel to the trend of the local graben (Valentine et al. 1998 [DIRS 119132], p. 5-45; Carter Krogh and Valentine 1996 [DIRS 160928], p. 4). The central, dense basalt conduit is irregular in shape, approximately 100 m north-south by 50 m to 70 m east-west. It contains zones of basalt-dominated breccia and rhyolite-dominated breccia near its center (summit) (Figure 6-4). In some areas (western flank) the contact between the dense basalt (or basalt breccia) and the rhyolite tuff country rock is sharp, formed by a near-vertical zone of vitrophyre in the tuff about 1-m thick, beyond which is undeformed, subhorizontally bedded host tuff. On the southwestern flank of the plug, the contact zone extends several tens of meters from the contact with the dense basalt. In this area, the transition from basalt to host tuff is gradual, beginning with 1-m to 2-m-wide stringers of remobilized (fluidal) tuff within the basalt and grading outward into tuff-hosted breccia containing angular basalt clasts and blocks. The mixed breccia contains a flow-banded, frothy tuff matrix with angular and rounded basalt clasts with quenched rinds. Ledges of basalt (1-m to 2-m thick) occur throughout this zone, which are interpreted as discontinuous, roughly concentric dikes related to the central dense basalt of the conduit (Figures 6-4 and 6-5). Radial dikes were also observed on the southwestern and eastern flanks. The overall dimensions of the contact mixing zone including the dense basalt are approximately 220 m north-south by 110 m east-west (Figure 6-4), or about twice the size of the body of dense basalt (Keating 2005 [DIRS 174988], pp. 35-45).

In this type of basaltic conduit, the convergence of several major dikes creates a wide zone of brecciation, melting, and remobilization of the country rock (Figure 6-5). While the size of the actual conduit for magma flow to the surface (50 m × 100 m) (Keating 2005 [DIRS 174988], p. 41) is similar to those measured at other analogue sites, the large zone of host rock brecciation, melting, and dike intrusion has not been observed in other analogue volcanic sites (e.g., East Grants Ridge, Section 6.2.1). A large zone of brecciation is observed near the vent area at Basalt Ridge, but only very high in the section (Section 6.2.3).

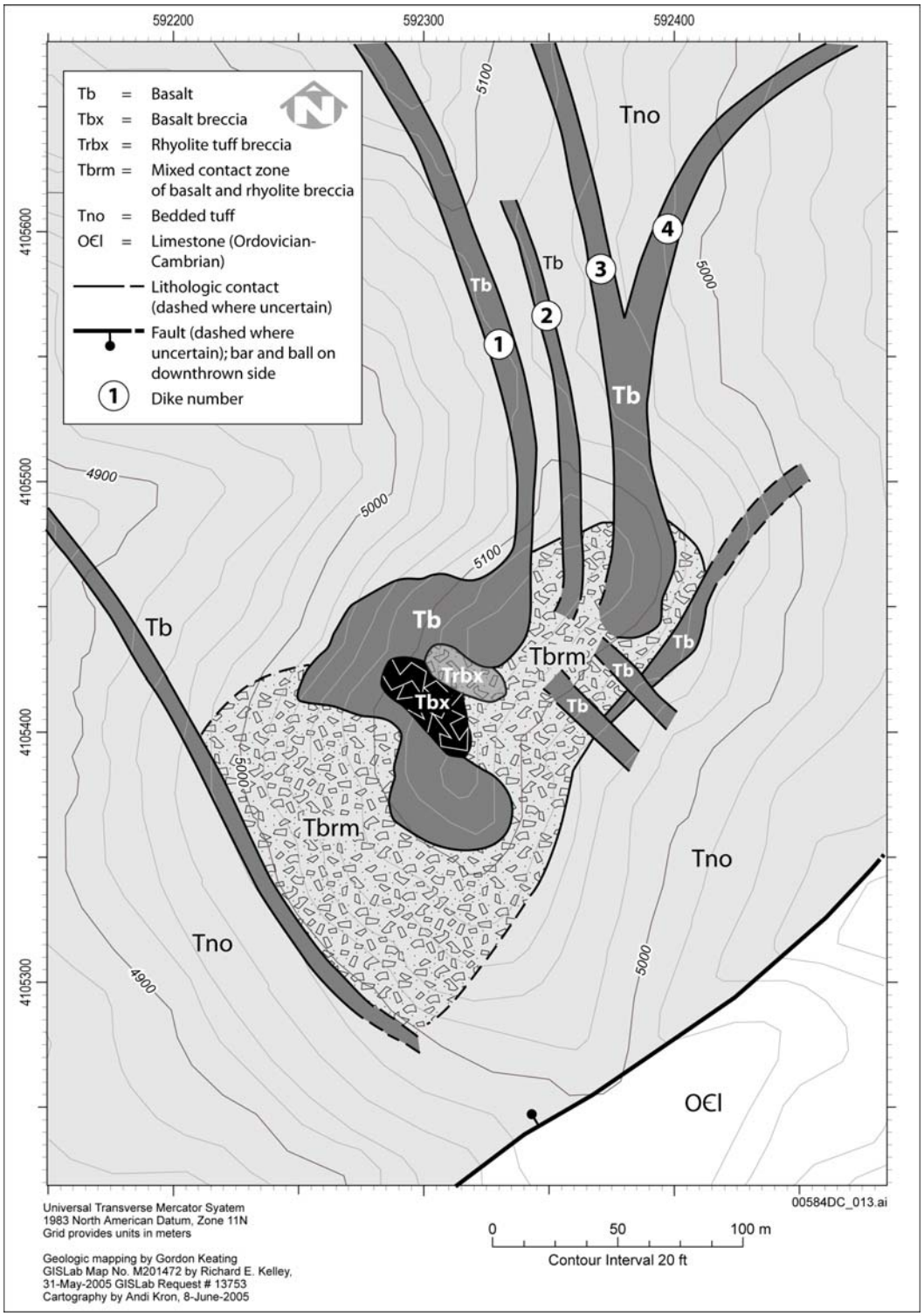

NOTE: See Figure 6-3 for location. For illustration purposes only.

Figure 6-4. Geologic Map of the Paiute Ridge Plug, Half Pint Range, Nevada

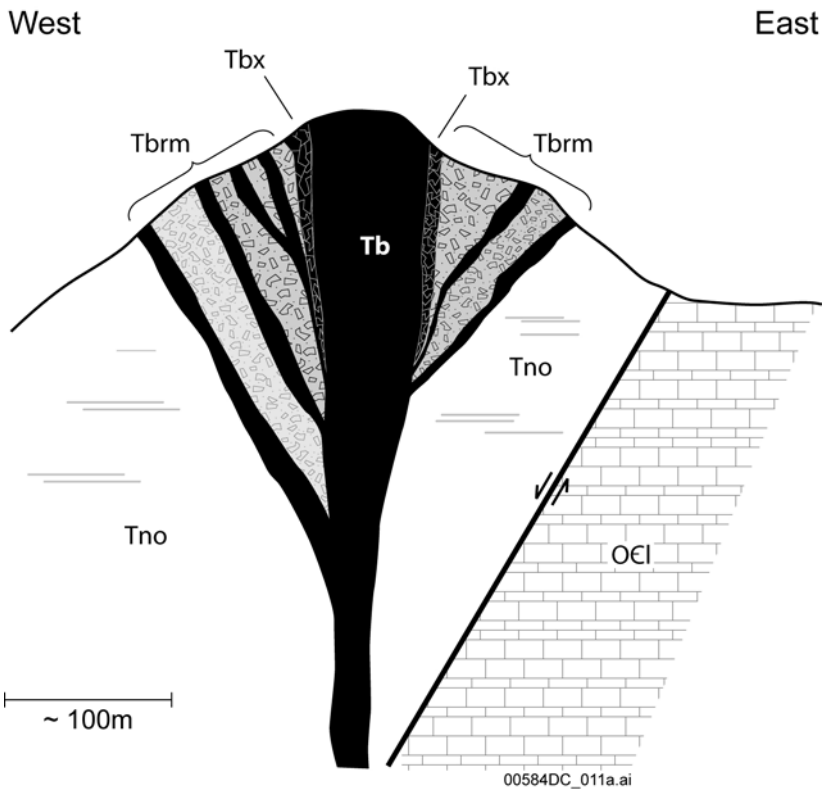

NOTES: See Figure 6-4 for explanation of geologic units. Cross-section depicts inferred geologic relations near the southern end of the plug. Not to scale. For illustration purposes only.

Figure 6-5. Schematic Cross-Section of Paiute Ridge Plug, Half Pint Range, Nevada

6.2.3 Basalt Ridge Area, Nevada

6.2.3.1 Overview

Basaltic volcanic rocks of Miocene age were erupted during silicic volcanic activity associated with the Black Mountain caldera complex of the southern Nevada volcanic field (Byers et al. 1976 [DIRS 104639]; Christiansen et al. 1977 [DIRS 157236], pp. 953 to 954; Crowe et al. 1983 [DIRS 100972]; Slate et al. 1999 [DIRS 150228]). These basalts postdate Timber Mountain—Oasis Valley volcanism by ~2 million years. Basalt Ridge and a nearby ridge (informally called Basalt Ridge East), sites of basalt eruptions, are located on northern Pahute Mesa at the northern boundary of the Nevada Test Site (Orkild et al. 1969 [DIRS 106460], Figure 1). The units capping the ridges were informally called Basalts of Pahute Mesa, and radiometric ages of 9.1 ± 0.7 Ma (Basalt Ridge) and 8.8 ± 0.1 Ma (Basalt Ridge East) are provided by Perry et al. (1998 [DIRS 144335], p. 2-18). Perry et al. (1998 [DIRS 144335], p. 2-18) also refer to a third, easternmost remnant basalt outcrop, which is not discussed here. The two ridges are underlain by linear dike sets, welded agglutinates and scoria, and alkali-basalt flow remnants; they represent eroded subvolcanic and surface deposits associated with ascending basalt dikes and eruptive equivalents, with paleosurfaces and host rocks exposed in adjacent canyons. The analogue sites provide detail of the interaction of pre-existing structure (stratigraphic layering and vertical cooling joints within silicic ignimbrites of the host rocks) and

rising dikes, including dike thicknesses, branching, and sill formation within host rock. Field analogue sites reported here are documented by Krier (2005 [DIRS 174079], pp. 93 to 150).

6.2.3.2 Basalt Ridge, Nevada

Basalt Ridge is an eroded remnant of a volcanic center. It is 2,500-m long and 300-m to 1,000-m wide; feeder dikes extend outward from beneath the eruptive units and are exposed to 300 m southwest and 700 m northwest, respectively (Figure 6-6). Based on the outcrop area of ~1.25 km^2, the minimum volume of these eroded basalt deposits is 0.07 km^3. The feeder system is oriented in a N30°E-S30°W direction. The basalt exposures are described from the deepest outcrops of the feeder dikes, the shallow subsurface, and the surficial deposits.

Deep Exposures–The deepest exposures of the feeder dike are on the northeast wall of the incised canyon southwest of Basalt Ridge. The dike is well exposed over about 150 m of vertical relief and a map distance of 300 m. At its deepest level, the dike is a single, vertical, 1-m to 2 m-thick tabular mass. Locally, the dike follows the trend of cooling joints where they are developed in the welded portions of host ignimbrites; occasionally the dike "wanders" over short (2-4 m) distances regardless of joint continuity. The dike can bifurcate into two or three closely spaced and subparallel branches, enclosing blocks of host ignimbrite with minor widening of the overall dike zone. Vesicle development is poor at this depth beneath the paleosurface (≤ 150 m), but breccia development occasionally marks the dike margins.

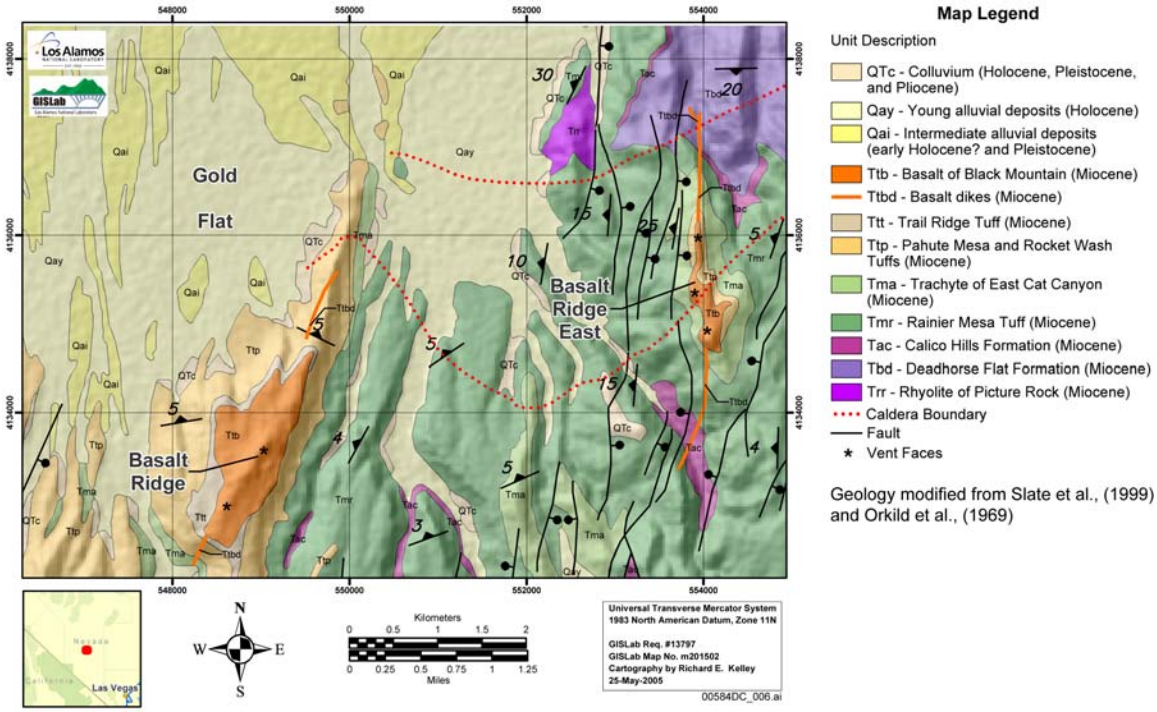

Source: Modified from Slate et al. (1999 [DIRS 150228], Plate 1) and Orkild et al. (1969 [DIRS 106460], Figure 1).

Figure 6-6. Location Map for Basalt Ridge and Basalt Ridge East, Nevada

Shallow Exposures–At 30 m to 35 m below the paleosurface, the dike(s) gradually widens to 8.5-m to 10-m up-section upon approach to a contact between a weak, plinian pumice and ash fall and overlying welded ignimbrite of the Thirsty Canyon Group (Orkild et al. 1969 [DIRS 106460], Figure 1). The basalt mass also includes altered blocks of rhyolite tuff ripped from levels below this exposure. A basalt sill is developed at this level and protrudes ~30 m in a NW direction, resulting from intrusion into the weaker and more porous plinian-ash fall horizon. Sill thickness varies from ~3 m to a blunt, rounded terminus of basalt ≤ 1-m wide at its NW extent. No sill is present on the opposite (SE) side of the exposure. Within the sill, trains of fine vesicles are folded on a sub-meter scale and interrupted by similar crosscutting trains, indicating multiple intrusions of stringers of basalt. Nearby, remarkable commingling of basalt and re-melted host tuff and are visible on centimeter- to meter-scales, including swirled masses, black and stretched vitrophyric clasts of rhyolitic tuff enclosed in basalt, basalt stringers enclosed in vitrophyre, stretched bubbles in intruded tuff, rare drip textures, and smooth, rippled surfaces of fluidal contacts between melted tuff and basaltic magma. Several short, bulbous masses of basalt, up to 25-cm wide and with pillow-lava morphology, are present within the commingled zone, illustrating a local, highly fluid environment and contrasting strengths and viscosities of materials during sill formation. The heat of the basaltic magma and compression during intrusion into the weak, porous plinian fall material produced an aureole of dense, black vitrophyre that extends 2.0 m to 3.5 m beyond the last basalt outcrop, and about 1 m from the top and bottom of the sill margin. Two thin (< 1-m) fingers of basalt extend from the sill vertically into the overlying welded tuff and occupy pre-existing joints; over this exposure, they terminate with blunt dike tips before reaching the paleosurface.

Surface-Level Exposures–Basalt Ridge is capped by Miocene basaltic vent facies lithologies including massive welded agglutinate, lapilli, blocks and aerodynamically shaped bombs, all overlying alternating layers of agglutinate and densely welded agglutinate, limited bedded scoria, and lava flows. Nearly all loose scoria lapilli and ash has been removed by erosion and no cone constructs remain. The feeder dike(s) described above can be traced to within several meters of the contact with the eruptive facies; one or more feeder dikes are exposed along much of the length of the ridge apex. Bedding along the ridge flanks consistently dips in toward the ridge axis and indicates that linear fissure eruptions up to 2,500 m in length were the initial eruptive mechanism of dike intersection with the surface. The present volcanic pile represents 55 m to 70 m of initial Hawaiian-type fissure-eruption deposits upon a northward sloping paleosurface of 4 vol %. Individual vents (isolated necks suggesting a focused eruption location developing from fissure eruptions) are difficult to identify in the eroded fissure deposits, but may be marked by higher accumulations of vent facies rocks. The spacing between two such accumulations at Basalt Ridge is approximately 750 m.

6.2.3.3 Basalt Ridge "East", Nevada

Basalt Ridge East is located 5 km NE from Basalt Ridge on northern Pahute Mesa (Figure 6-6). Basalt breccias, welded agglutinates, and lava flows cap the linear ridge for ~1,600 m, whereas outcrops of the feeder dike extend for 1,500 m south and 800 m north of the eruptive cap, respectively (Orkild et al. 1969 [DIRS 106460], Figure 1). The dike system is oriented in a N5°W-S5°E direction and is exposed in steep canyons on the south and north edges of the ridge.

Exposures at the southern edge of Basalt Ridge East provide an estimate of the elevation of the paleosurface upon which basalts were erupted from ascending dikes. That elevation, ~ 2,068 m at the southern exposure, is at the intersection of the dike system and flat-lying scoria beds immediately above rhyolite tuff at the vent. The scoria beds are the remnants of cone material formed during initial eruption of the dike. The paleosurface slopes ~ 4% toward the north, based on field observations and measurements on the geologic map of Orkild et al. (1969 [DIRS 106460], Figure 1).

Figure 6-7 is a composite sketch drawn from field observations and shows relations described below. It is important to note that Figure 6-7 represents laterally continuous outcrops exposed over a 1,200-m distance, which are projected onto the plane of the page; therefore, field relations vertically beneath the vent deeper than ~50 m are not observed. The feeder dike obtains its lowest exposure in the canyon bottom to the south at an elevation ~ 270 m below the paleosurface of 2,068-m in elevation (denoted with a minus sign; e.g., –270 m). At its deepest level, the feeder dike appears as one or two dikes in a ~ 4-m-wide zone. It ascends with nearly vertical, westerly dip. Two poorly developed, 1-m to 3-m long, sills are present about –140 m below the paleosurface. At approximately –90 m below the paleosurface, the dike is 11-m wide, composed of massive basalt with a central 2-m-wide breccia zone. Above this level (from –90 m to –52 m below the paleosurface), the dike branches to form five to six dikes over a 25-m zone, with the largest (main) dike being 2.8-m wide and the thinnest being < 50-cm wide. Continuing up-section to –48 m below the paleosurface, the dike zone comprises three to four dikes (fewer than below) separated by lenses of rhyolitic tuff, and has widened to 28 m to 30 m. Above this elevation, the dike zone can be followed about 300 m north to the remaining overlying exposures. At –35 m below the paleosurface, the dike zone is some 40-m wide, mostly massive but including poorly welded zones of angular breccia, particularly at the contact with tuff. At this point, an expanse of light gray tuff about 15-m across is present within the dike material and might be intact host rock separating branching dikes and breccias, or may be "floating" in the dike material. Finally, just 20 m to 25 m below the eruptive surface, the dike boundaries flare outward at roughly 45° from horizontal. The elevation of the flaring on the east side is 10-m to 12-m higher than on the west. At the paleosurface, the vent has grown from 80-m to 100-m wide. Above this level, inward dipping, alternating agglutinates merging upward into densely welded spatter and lavas create a resistant pile of dense basalt vent facies for most of the linear ridge northward.

Black vitrophyric rhyolite tuff marks the contact zone with the host rhyolite ignimbrites through which the basaltic dikes intruded. At lower elevations in the section where the dike zone is thinner, the vitrophyric rind is tens of centimeters thick. High in the section, 12 m below the flaring of the dike, the vitrophyre is about 3-m thick. The contact grades from intensely commingled basalt and remelted chunks of tuff breccia with well-developed vitrophyric textures in the first meter, to nonbrecciated black vitrophyre, and to the original unaltered tuff. The unaltered parent tuff (vitric, highly pumiceous, nonwelded tuff) is exposed within 10 m of the dike material.

Possible focused (single) vent locations on Basalt Ridge East are obscured by erosion, which has removed the overlying deposits down to predominantly fissure eruption deposits. Three

locations of possible vents are noted on Figure 6-6, with spacings of 500 m and 600 m, respectively.

6.2.4 Field Analogue Conclusions

The dikes or plugs observed at the Paiute Ridge, Basalt Ridge, and Basalt Ridge East, Nevada; and East Grants Ridge, New Mexico, provide illustrations of basalt magma emplacement within ignimbrite or silicic ash host rocks. While this limited set of analogues cannot capture the total range of subvolcanic geometries, it is instructive when considering near-surface dike propagation and structure and is relevant to the Yucca Mountain disruptive events scenario. Conclusions from the field analogue studies are summarized here.

A. The Basalt Ridge and Basalt Ridge East, Nevada, areas provide evidence for magma feeder systems narrowing with depth. At the 270-m depth at Basalt Ridge East, nearly equivalent to repository depth, the dike system is 2-m to 4-m wide yet fed 2-km-long fissure eruptions with abundant Hawaiian-style eruptions that had a surface-vent width of approximately 100 m. However, the exposures at the 270-m depth are not directly beneath the vents.

B. As feeder systems ascend toward the surface, their complexity may increase due to the influence of the free surface. In deep exposures at Basalt Ridge, Nevada, a narrow system of dikes branches, incorporates host rock, and re-forms as it ascends. Closer to the surface (within 50-m to 150-m in depth), the splaying of dikes occupies a continually wider zone, which eventually flares into the overlying eruptive vent; multiple dikes are found nearer the paleosurface. This may also be the case at Paiute Ridge, where the exposed sills and a remnant of the volcanic neck (conduit) may represent depths of from approximately 130 m to 30 m beneath the eruptive surface, respectively, if reconstruction of the paleotopographic relief is correct.

C. No conduit is exposed at Basalt Ridge East, but the observed dike swarm narrows with depth (there are no exposures *vertically* beneath the vent: Section 6.2.3). Below about the 150-m depth, a more-or-less constant dike zone width of 2 m to 4 m is maintained. The neck at Paiute Ridge may represent the near-surface portion of an irregularly shaped 110-m-wide massive basalt conduit, perhaps as shallow as about 30-m in depth below the eruptive surface (Keating 2005 [DIRS 174988], p. 45). If the disturbed zone around the neck is included, the irregular conduit is ~210 m in diameter. The change in diameter with depth of the Paiute Ridge neck is not known.

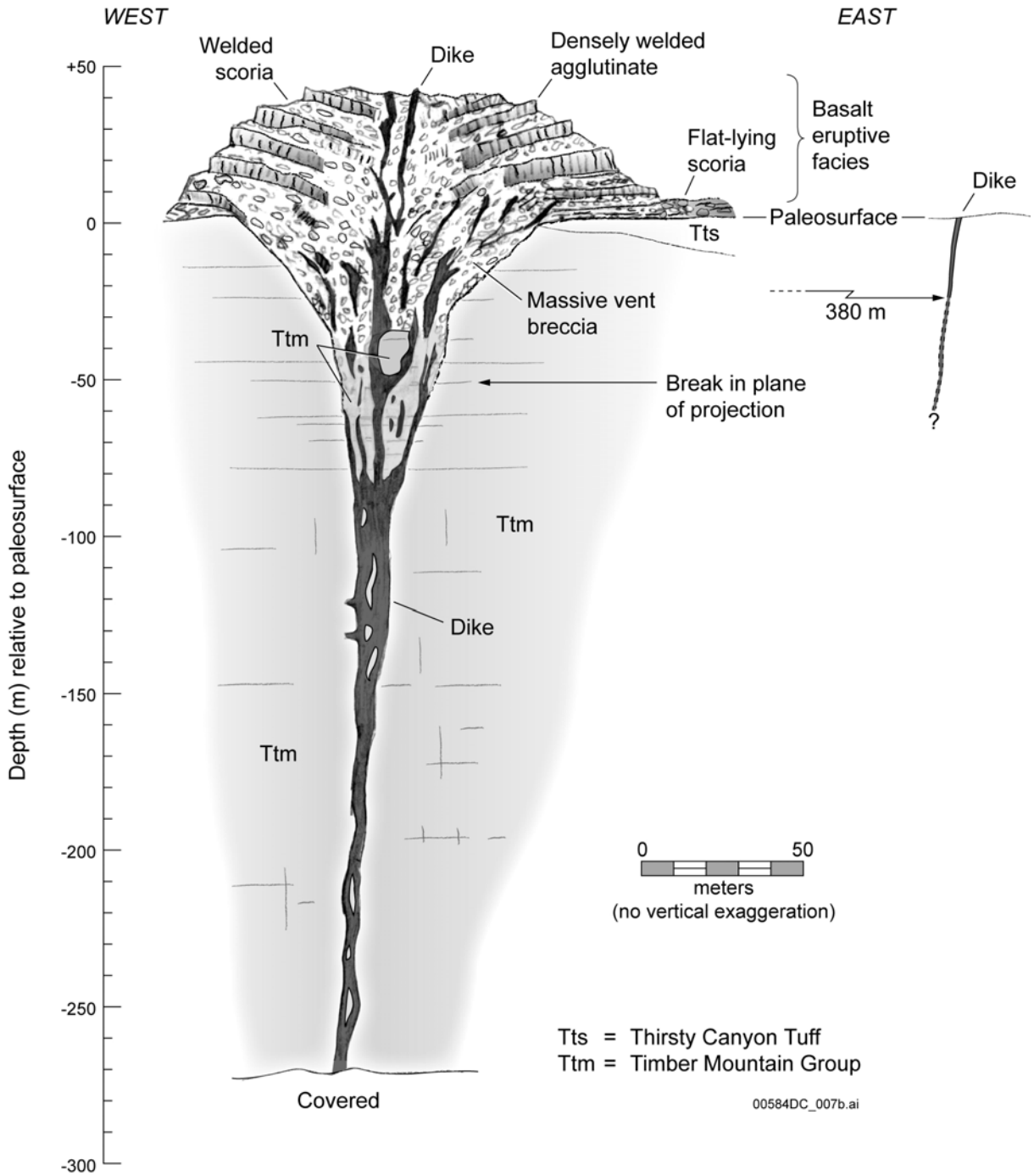

NOTE: The view is along the plane of the dike set. The eruptive pile shows welded scoria and densely welded agglutinates dipping inward toward the fissure eruption marked by the location of the dikes. All loose scoria material has been removed by erosion. The upper one-third of the figure is displaced from the lower two-thirds by about 100 m because of canyon geometry, so that the subsurface part of the system is juxtaposed with the surface features. The arrow labeled 380 m on the right of the figure shows the approximate distance to the nearest dike. The vertical extent of the dike is unknown, as indicated by the question mark. For illustration purposes only.

Figure 6-7. Schematic Drawing of Basaltic Dike Set and Eruptive Equivalents on South Edge of Basalt Ridge East

D. The depth of intrusion of Paiute Ridge sills (and the deepest exposures of multiple-dike sets) is estimated to be between 100 m to 250 m (Crowe et al. 1983 [DIRS 100972], p. 266; Carter Krogh and Valentine 1996 [DIRS 160928], p. 10), whereas, at Basalt Ridge East, the transition depth from a one- or two-dike set to multiple parallel dikes is considerably shallower at 50 m to 80 m. Basalt Ridge East does not appear to achieve the structural complexity of Paiute Ridge with multiple sills and dikes, and long dikes that are radial to a central volcanic neck. Both intrusion complexes are hosted by ignimbrite flows with variable properties, although Paiute Ridge sills are restricted to within tens of meters of the underlying Paleozoic sedimentary rocks. Based on these small-volume basaltic analogues in similar host tuff, development from an ascending one- or two-dike set toward a complex network of multiple-dike injections is more characteristic of shallow levels of intrusion (<250 m).

E. Given the height and diameter of the basalt plug at East Grant Ridge, New Mexico, the neck is notable for a relative lack of accompanying parallel or radial dikes (alignment of vents suggest at least one dike (Thaden et al. 1967 [DIRS 174076], Plate 1)). The subsurface extent of the ~125-m-diameter neck is unknown, but the plug maintains this diameter at the current exposure with no indication of tapering to a smaller diameter (in contrast to Crumpler 2003 [DIRS 174074], pp. 161 and 163). This is the only evidence of a vertically cylindrical conduit within this set of analogues.

F. The Basalt Ridge and Paiute Ridge dikes were emplaced parallel to NNE- and NNW-trending normal faults, respectively. Paiute Ridge dikes parallel north-south-trending fault structure but converge to the south; their intersection coincides with the conduit and the broader disturbed zone around the exposed neck. The longest dike (> 4,000 m) in the set was emplaced directly within a fault plane, although most of the other dikes and dike segments do not visibly occupy faults. In map view, the dikes pinch and swell in thickness over distances of tens of meters. At one location, a 2-m to 4-m-thick dike increases in thickness to ~20 m where it supplied magma to one of the larger sills, suggesting the increase in dike thickness was related to sill formation.

G. Trends of pre-existing structural elements are a guide but not a predictor of dike trends and vent and conduit locations. Structural control at the analogue sites underscores the role of pre-existing structures on the formation of dikes and conduits. Paiute Ridge dikes are parallel to or occupy NNW- and NNE-trending faults, but curve from both directions to intersect at the conduit to the surface. The East Grants Ridge vents are in-line with a small structural graben north of the site and with aligned centers to the south, but this trend is orthogonal to the majority of fissures in the Mt. Taylor volcanic field of which it is a part.

H. The analogue sites can be interpreted to show a general trend of decreasing complexity of dike swarm geometry with depth. At Basalt Ridge East, the eruptive pile of inward-dipping, welded agglutinate is immediately underlain by ~100-m-wide vent area, but the vent narrows to ~40 m at a shallow 35-m depth. The zone continues to narrow to a 2-m to 4-m-wide zone at a depth of 150 m and maintains this width to at

least 270 m below paleosurface. No massive plug is observed at the Basalt Ridge vent. In contrast, East Grants Ridge plug is one of about four vents which fed a voluminous lava field, yet the one exposed plug maintains (at current exposures) a relatively straightforward vertical geometry; the variation on the contact is on the order of 3 m to 5 m over about 100 m of vertical exposure. There is no exposure of the deeper feeder system that delivers magma to this plug.

I. Parameter distributions for a potential basaltic igneous event at Yucca Mountain provided ranges for dike width, dike spacing, and conduit diameters. Uncertainty related to those distributions was related to a limited amount of published data or poor exposures in the region. The field analogue work reported here corroborates these distributions in the following ways.

Dike Width–Widths of dikes observed at the analogue sites fall within the probability distribution given in *Characterize Eruptive Processes at Yucca Mountain, Nevada* (BSC 2004 [DIRS 169980], Table 7-1). That distribution is described as having a minimum of 0.5 m, mean of 1.5 m, and a 95th percentile value of 4.5 m. The maximum width observed at Paiute Ridge of ~20 m is associated with feeding a horizontal sill and is captured by the log-normal distribution.

Dike Spacing–Dike spacing observed at the analogue sites falls within the probability distribution given in *Characterize Eruptive Processes at Yucca Mountain, Nevada* (BSC 2004 [DIRS 169980], Table 7-1). That distribution is described as uniform from 0 m to 1,500 m.

Number of Dikes Associated with Formation of a New Volcano–In *Characterize Eruptive Processes at Yucca Mountain, Nevada* (BSC 2004 [DIRS 169980], Table 7-1), this parameter is described as a log-normal distribution with a minimum of 1, a mode of 3, and a 95th percentile of 6. Analogues described in the present report range from ≥ 1 at East Grants Ridge to ≤ 10 at Paiute Ridge. Note that Paiute Ridge was used to capture the "maximum" for this parameter in BSC (2004 [DIRS 169980], Table 7-1).

Conduit Diameter–Conduit diameters at depths equivalent to repository depth are not directly observed at the analogue sites. The probability distribution given in *Characterize Eruptive Processes at Yucca Mountain, Nevada* (BSC 2004 [DIRS 169980], Table 7-1) is described as triangular with a minimum equal to dike width, mode diameter equal to 50 m, and maximum value of 150 m. The maximum value was based on early work at East Grants Ridge, which was re-evaluated with a value of ~125 m in an east-west direction. The total north-south diameter is obscured by overlying eruptive products and has an unknown, perhaps larger, length. Paiute Ridge basalt intrusion includes a complex volcanic neck exposed above the equivalent repository depth. The diameter of the massive neck interior is a ~100-m irregular shape, but if the intruded, disturbed zone surrounding the basalt is included, it increases to 220 m × 110 m. The map area with the included disturbed area is 15 to 20 percent larger than the maximum area represented in (BSC 2004 [DIRS 169980], Table 7-1). Based on other exposures at Basalt Ridge East, the Paiute

Ridge conduit probably decreases in effective diameter with depth. The Basalt Ridge East feeder dike flares upward from a few meters to ~100-m wide at the vent, but is only 2 m to 4-m wide near repository depth.

6.3 BLOCKAGE AND FORMATION OF MAGMA PATHWAYS

This section presents analyses addressing various aspects of the movement or blockage of magma during a potential intrusion into drifts at Yucca Mountain. These situations are representative of some geometries that potentially could develop during the course of an igneous event. Three cases in which the primary path for magma to reach the surface is blocked are analyzed in Section 6.3.1, which addresses blockage by slumping of scoria, solidification during a pause in eruption, or blockage by faulting. The potential for magma breakout is evaluated in these cases. A new analysis of the loss of heat from a secondary dike into cold or preheated rock is presented in Section 6.3.2. These analyses apply numerical codes to simulate the specific conditions. Direct input parameters, simplifications and idealizations are discussed in each subsection.

6.3.1 Blockage by Magma Solidification

Three different scenarios or configurations for blockage of magma in a conduit or dike were considered as shown in Figure 6-8. The first (Figure 6-8a) considers magma flow through a conduit feeding a scoria cone and involves the blockage of magma by loose scoria slumping inward, blocking the vent with solidification of underlying magma, resulting in a solid plug at the top of the conduit. Whether the slumping prevents magma flow long enough to permit the solidification, or a temporary halt in magma flow allows the scoria to slump inward, this scenario is intended to examine the phenomena that would be expected following a pause in building of a scoria cone such as the one at Lathrop Wells volcano. The second configuration (Figure 6-8b) arises from a temporary interruption of magma supply to a lava flow leading to formation of a plug of solidified magma blocking a conduit. This scenario investigates the effect of intermittency of magma supply to an effusive eruption that has produced a lava flow. A third scenario (Figure 6-8c) may arise if a syn-eruptive displacement on a fault cuts a feeder dike at depth. This case addresses one potential effect of earthquakes that frequently accompany volcanic activity including dike injection. All three analyses provide information on the limits of pressure that might build up in a conduit or dike if flow were halted; this can be related to analysis of growth of secondary dikes out of a magma-filled drift (BSC 2004 [DIRS 170028], Section 6.5.1.2) and to estimates of how closely a dike can approach a drift before it will break through the intervening rock (BSC 2004 [DIRS 174066], Appendix G). The third scenario also provides insight into the potential for magma to be diverted from its original path to a different path along a newly formed fault.

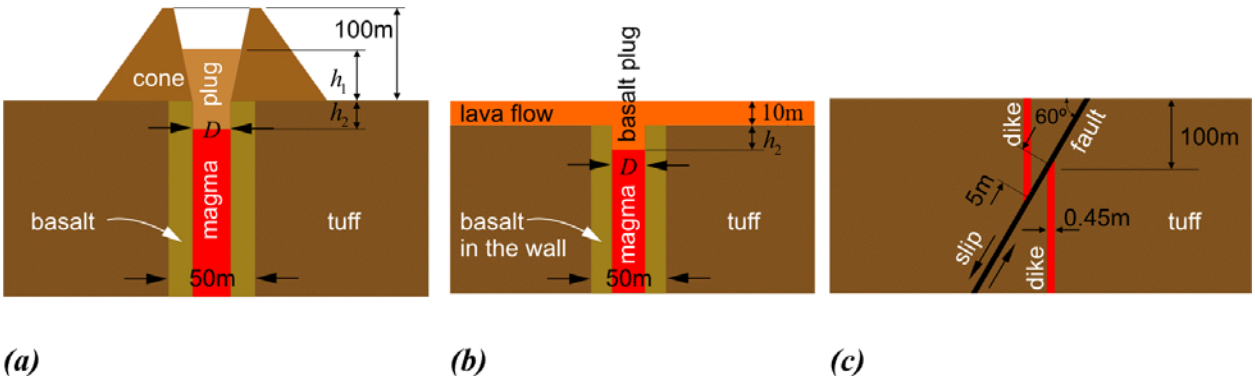

NOTE: (a) and (b) are axially symmetric about the center of the conduit. For illustration purposes only.

Figure 6-8. Configuration for Pressure Build-Up Analyses

6.3.1.1 Inputs

Roller boundary conditions (fixed displacement normal to the boundary, free in the tangential direction) were applied at the bottom of the calculation (150 m below the original ground surface for the conduits, 500 m for the dike) and the vertical far-field boundaries (240 m from the axis of the conduit or 500 m on either side of the dike). Gravitational acceleration of 9.81 m/s^2 (rounded from Incropera and DeWitt 2002 [DIRS 163337], Table A-6) acted vertically downward throughout. All materials were represented as elastic, perfectly plastic, Mohr-Coulomb materials having the properties listed in Table 6-1.

Values for bulk and shear moduli in this table, if not directly presented in the cited source documents, were developed from the inputs cited using the relations $K=E/(3(1-2\nu))$, and $G=E/(2(1+\nu))$, where K = bulk modulus, G = shear modulus, E = Young's modulus, and ν = Poisson's ratio (Timoshenko and Goodier 1970 [DIRS 121096], pp. 10 and 11). The zone of solid basalt surrounding the conduit is set to have an outer diameter of 50 m, which is the mode of the distribution presented in DTN: LA0407DK831811.001 [DIRS 170768] (first table). The cross-sectional area of the conduit actively transporting magma is assumed to be either 5 m or 15 m in diameter. The smaller value is rounded from the 95th percentile value of 4.5 m given in DTN: LA0407DK831811.001 [DIRS 170768] (first table). The higher value is consistent with the mode value diameter of 50 m and with the statement in *Characterize Eruptive Processes at Yucca Mountain, Nevada* (BSC 2004 [DIRS 169980], Section 6.3.1.1) that the whole cross-sectional area of a conduit may not be active at the same time. A low value will result in large values for magma pressure required to break through a blockage, and is in that sense conservative. The larger value is expected to be representative of conduits which are likely to form in a potential Yucca Mountain eruptive volcanic event. The three scenarios that are considered (see Figure 6-8) each take place in the uppermost 100 m of Yucca Mountain, which is composed of Tiva Canyon welded tuff (TCw). Thus, the appropriate rock (tuff) properties are those of the TCw.

Table 6-1. Material Properties

Material	Density (kg/m3)	Bulk Modulus (GPa)	Shear Modulus (GPa)	Cohesion (MPa)	Friction Angle (º)	Tensile Strength (MPa)	Source
Loose scoria	1,300	16.7	10	0	40	0	Assumed equivalent to generic gravel-like material, and estimated based on Duncan et al. 1980 [DIRS 161776], Table 5 and Equation 3. Cohesion of 0.1 MPa is for undisturbed scoria. Stiffness (shear modulus) of loose scoria is assumed to be 50% of stiffness of undisturbed scoria.
Undisturbed scoria	1,500	33.3	20	0.1	40	0	
Basalt	2,960	25.0	19.5	32.7	50	27	Gupta and Rao 2000 [DIRS 174063], Tables 2 and 3, except friction angle from Hoek and Brown 1997 [DIRS 170501], Figure 8, with GSI ~90 and m_i = 25. GSI (Geologic Strength Index) is index for rock mass characterization. m_i is parameter in Hoek-Brown failure criteria (Hoek and Brown 1997 [DIRS 170501]).
Tuff	2,310	16.8	12.1	3.9	57	2.35	Properties of TCw unit, Category 5 (CRWMS M&O 1999 [DIRS 126475], Tables 10 through 13, and 15, including Young's modulus (29.39) and Poisson's ratio (0.21).

Inputs: Blockage by Slumping–For this analysis, the scoria cone is set to have a height of 100 m, an outer slope of 50° and a summit crater diameter twice the diameter of the conduit at the base of the cone (i.e., 30 m for a 15-m conduit diameter, and 10 m for a 5-m conduit diameter). The height is on the order of the Lathrop Wells volcano (~140 m) (BSC 2004 [DIRS 169980], Appendix C, Section C2). The angle of the outer slope of the cone has negligible effect on the results of the calculations in that the effect of the angle on the stresses beneath the cone and breakout pressure is small. The summit crater diameter is selected to result in relatively steep slopes inside the crater. A steeper slope of the crater wall will lead to a larger breakout pressure. The assumed geometry of the crater inside the cone is possible, because the calculations showed that the wall of the crater inside the cone was stable under static conditions for the selected properties of the undisturbed scoria. Because it is expected that an average slope of the crater wall will be smaller than the assumed slope, the selected geometry yields an overestimate of the breakout pressure. Higher breakout pressures will increase the potential for formation of a secondary dike out of a drift of the sort analyzed in BSC (2004 [DIRS 170028], Section 6.5.1.2).

Inputs: Blockage by Solidification–For the analysis initial conditions, the solidified lava flow is selected to be 10-m thick, and the solidification into the conduit extends 30 m below the base of

the flow (h_2 in Figure 6-8). The lava thickness is in accord with the finding presented in *Characterize Eruptive Processes at Yucca Mountain, Nevada* (BSC 2004 [DIRS 169980], Section C4).

Inputs: Blockage by Faulting–For problem formulation, the analyzed fault is selected to be a normal (dip-slip) fault with a dip of 60°, with a strike parallel to the dike, and a throw of 5 m. The fault intersects the dike at a depth of 100 m. This fault geometry is typical of observed faults in the Yucca Mountain region, as described in *Yucca Mountain Site Description* (BSC 2004 [DIRS 169734], Section 4.3.2.2, Table 4-9). The parallel strike is selected so as to make the problem two-dimensional. The fault throw is very large for a volcanic-related earthquake, but is only a factor of about two larger than the maximum-measured, per-event slippage measured in the Yucca Mountain region (BSC 2004 [DIRS 169734], Table 4-9). The depth of intersection is arbitrary, but the discussion in Section 6.3.2 provides an approach to project the results for other depths of intersection.

The in situ horizontal stress for the analyses in this section are selected to be 0.5 times the vertical component of the overburden stress. This is consistent with field measurements of in situ stresses at Yucca Mountain (DTN: SNF37100195002.001 [DIRS 131356], Summary, p. 1). The fault and the original dike above the fault are assumed to have initial hydraulic apertures of 5 mm. Calculation of dike propagation after displacement by a normal fault requires an initial fracture of some width (aperture) for any potential magma flow path (dike). A 5-mm value was selected as the initial aperture of the fault and of the potential vertical continuation to represent slightly open pathways but to minimize any bias as to which pathway the magma will follow in the calculations.

6.3.1.2 Calculational Approach

Approach: Blockage by Slumping–This analysis of blockage by scoria slumping into an eruptive cone used the FLAC code, V4.04 (BSC 2004 [DIRS 172432]) with an axisymmetric mesh. Undisturbed scoria properties (Table 6-1) were used to represent the volcanic cone; the plug was treated as loose scoria (Table 6-1). The interface between the loose and undisturbed scoria was assumed to have a friction angle of 30°, except for three calculations where the interface friction angle was 40°. The mechanical properties of solidified basalt used in this analysis, as listed in Table 6-1, were for room temperature. Rocchi et al. (2004 [DIRS 173995], p. 149, Figures 13 to 15) found that the mechanical properties of basalt are not affected by temperatures below 600°C, so the effect of temperature on mechanical properties was not included in the calculations. Calculations considered various heights of the plug, both above (scoria, h_1 in Figure 6-8) and below (solid basalt, h_2 in Figure 6-8) the original ground surface, two different conduit diameters, and two different values for the friction angle between the plug and the conduit wall.

The calculation proceeded in three steps: (1) stresses due to cone construction and convergence around the conduit after the magma overpressure in the conduit returned to zero were calculated; (2) the plug was generated inside the conduit and the calculation was run to equilibrium, generating horizontal stresses at the contact between the plug and the conduit wall due to lateral deformation of the plug under gravity; and (3) uniform magma overpressure was applied on the conduit walls and the bottom of the plug. Magma overpressures were increased in increments of

0.25 MPa and stresses were allowed to equilibrate before the next pressure increment. Breakout was manifested by the inability of the simulation to achieve equilibrium.

Approach: Blockage by Solidification–This analysis considered a case where magma supply pauses so that a surface basalt flow stops, with the solidification extending 30-m deep into the underlying conduit (h_2 in Figure 6-8b). The solidified lava flow on the top of the conduit was taken to be 10-m thick. The sequence used for analysis of breakout of the solidified basalt plug was the same as for the scoria plug. These calculations were done with FLAC V4.04 (BSC 2004 [DIRS 172432]) with an axisymmetric mesh using the input parameters listed in Table 6-1.

Approach: Blockage by Faulting–This analysis addressed cutting of a dike by a fault as shown in Figure 6-8c. A plane-strain, two-dimensional, coupled hydromechanical problem was analyzed using the numerical code UDEC V3.14 (BSC 2004 [DIRS 172322]). The input parameters for the calculations were the same as those used in the wide-aperture case discussed in Section 6.4.4.1 of *Dike/Drift Interactions* (BSC 2004 [DIRS 170028]). The initial magma pressure in the segment of the dike below the intersection was in equilibrium with the horizontal stresses. Magma was injected at the bottom of the analysis at the rate of 0.45 m^2/s per unit strike length, corresponding to a magma velocity of 1 m/s, and the calculation was run until it reached steady state.

6.3.1.3 Results

Blockage by Slumping–A summary of the breakout pressures calculated assuming different dimensions of the scoria plug is presented in Table 6-2.

There are two possible mechanisms for magma breakout from the plugged conduit. A first mechanism is that the entire scoria plug may move upward, in most cases dragging adjacent portions of the previously undisturbed volcanic cone. The second involves development of hydrofractures in the conduit wall. When the hydrofracture mechanism is expected to result from magma pressures lower than would be needed to move the scoria plug, the breakout pressure is indicated in Table 6-2 in parentheses along with the pressure needed to move the plug.

Sensitivity of breakout pressure prediction to the diameter of the conduit and the friction angle was investigated in the calculations by varying those two parameters. Increase in friction angle resulted in increase of the breakout pressure (cases 10 and 12 relative to cases 4 and 6, respectively) as did a smaller conduit diameter (cases 13 and 15 relative to cases 1 and 3, respectively). When the breakout was a result of a shearing mechanism (highlighted rows in Table 6-2), upper-bound plug accelerations were calculated and are listed in the last column of Table 6-2. These accelerations are taken to be the magma pressure times the base area of the plug divided by the mass of the entire plug (i.e., friction, tensile and shear strength of scoria in both the plug of slumped scoria and in the "undisturbed" cone are ignored). Accelerations are tabulated only for cases where the pressure required to push the entire scoria plug upward is less than the hydrofracture pressure.

Based on the stress field around the pressurized conduit, hydrofractures would initially be vertical; however, upon propagating into the rock mass, they may intersect fractures of other

orientation before reaching the surface. Propagation of hydrofractures was not analyzed directly, only the conditions (tensile stress in the basalt adjacent to the conduit) required for fracture initiation. The pressures listed in Table 6-2 are calculated using the tensile strength of basalt measured by Gupta and Rao (2000 [DIRS 174063], Table 3), which was determined on intact samples of relatively small size, for which pre-existing fractures and defects in the tested specimens were small compared to the size of the tested sample. Actual in situ tensile strengths may be either higher or lower. On the one hand, thermal cycles may cause fracturing of the basalt in the conduit, resulting in significant reduction of the tensile strength compared to values determined on the intact samples. Rocchi et al. (2004 [DIRS 173995], Table 3) measured the tensile strength of small basalt samples and reported a value of 6.4 MPa. Pressures needed to initiate hydrofractures listed in Table 6-2 are based on this value. If the tensile strength of the basalt rock (in the immediate wall of the conduit) is 6.4 MPa and if the scoria plug fills a portion of the conduit below the ground surface (h_2>0), then hydrofracture of the conduit wall is expected at magma pressures near 10 MPa (cases 6, 8, 9, 11 and 12).

Table 6-2. Magma Breakout Pressures

Case No.	h_1 (m)	h_2 (m)	D (m)	Friction Angle (°)	Breakout Pressure (MPa)	Acceleration (m/s^2)
1	20	0	15	30	0.5*	16
2	60	0	15	30	2.7*	19
3	100	0	15	30	*7.0 (5.8)	
4	20	25	15	30	1.8*	28
5	60	25	15	30	8.8*	51
6	100	25	15	30	*19.6 (9.6)	
7	20	50	15	30	6.9*	71
8	60	50	15	30	*21.0 (10.1)	
9	100	50	15	30	*32.7 (10.2)	
10	20	25	15	40	5.6*	87
11	60	25	15	40	*24.3 (9.7)	
12	100	25	15	40	*27.8 (9.7)	
13	20	0	5	30	0.8*	25
14	60	0	5	30	*9.5 (7.5)	
15	100	0	5	30	*10.0 (7.5)	

NOTES: * Critical breakout pressures required to move the entire scoria plug. The values in the parentheses are the pressure that causes hydrofracture of the conduit wall. The expected breakout pressure is the smaller of the two.

Highlighted rows are explained in text.

For illustration purposes only.

On the other hand, if a layer of basalt, plastically deformable due to near-solidus temperatures, but contained by surrounding elastic basalt and tuff, were to block hydrofractures, much higher magma pressures could build up. So the high tensile strength reported by Gupta and Rao (2000 [DIRS 174063], Table 3) was used in order to reach high enough magma pressures to investigate the second mechanism, that is to determine deformations of the plug and cone. Figure 6-9 shows the deformation of the scoria plug (arrows or "vectors") and plasticity conditions in the cone for (a) case 3 and (b) case 1, illustrating the failure mechanism when the critical pressure is

achieved. The plasticity condition is illustrated for each computational zone in the scoria cone and scoria plug as follows:

- No symbol (only along base of cone in Figure 6-9) indicates the cell has never yielded
- Green indicates a cell that has yielded previously, but is now elastic
- Purpose indicates cells that are currently at yield in tension
- Orange indicates cells that are currently at yield in shear.

The deformation is indicated by brown arrows with a tail at the current location of a node and extending in the direction of its total displacement with a length determined from the scale bar. In both cases, deformation shortens the scoria plug and moves it upward.

Figure 6-10 illustrates tangential stress profiles in the solidified basalt near the conduit wall (i.e., 1.25 m from the wall) for several magma pressures for a scoria plug filling the entire 100-m depth of the scoria cone and extending beneath the original ground surface to a depth of 25 m (case 6, Figure 6-10(a)) or 50 m (case 9, Figure 6-10(b)). Depths in Figure 6-10 are relative to the original (pre-cone) ground surface. The hydrofracture pressure is the smallest magma pressure that generates the tensile stress in the wall equal to the tensile strength of the basalt. The tensile strength of Rocchi et al. (2004 [DIRS 173995], Table 3) is indicated by the dashed vertical line. For case 3 where h_2=0 (Table 6-2), the hydrofracture pressure is only 6.5 MPa, almost equal to the 7 MPa required to displace the entire scoria plug.

Blockage by Solidification–Results for breakout after blockage by solidification (Figure 6-8b) are illustrated in Figure 6-11, which shows tangential stresses adjacent to the conduit for a magma pressure of 10.26 MPa. Stresses at the wall would be sufficient to generate radial hydrofractures in basalt with a tensile strength of 6.4 MPa as determined by Rocchi et al. (2004 [DIRS 173995], Table 3). Such hydrofractures would result in radially propagating dikes that might look similar to the dikes around the central conduit at Paiute Ridge (Section 6.2.2) if exposed by later erosion.

Blockage by Faulting–Figure 6-12 shows the dike aperture distribution at the end of the faulted simulation (i.e., at steady state) (Figure 6-8c). The fault offset has forced the magma to turn and continue along the fault toward the surface, albeit with a reduced aperture of only ~0.15 m. The pressure increased from its pre-faulting equilibrium pressure of 1.2 MPa to a maximum of 1.42 MPa, before decaying over the next 200 s to a new equilibrium value near 1.3 MPa. All of these pressures are less than the 1.5 MPa component of confining stress normal to the fault at this depth. The difference, which is not large, results from a moment (force times distance), or leverage effect, such that the higher pressure in the source dike, acting at the dike-fault intersection, causes the upper fault block to incrementally rotate clockwise, thus opening the fault aperture.

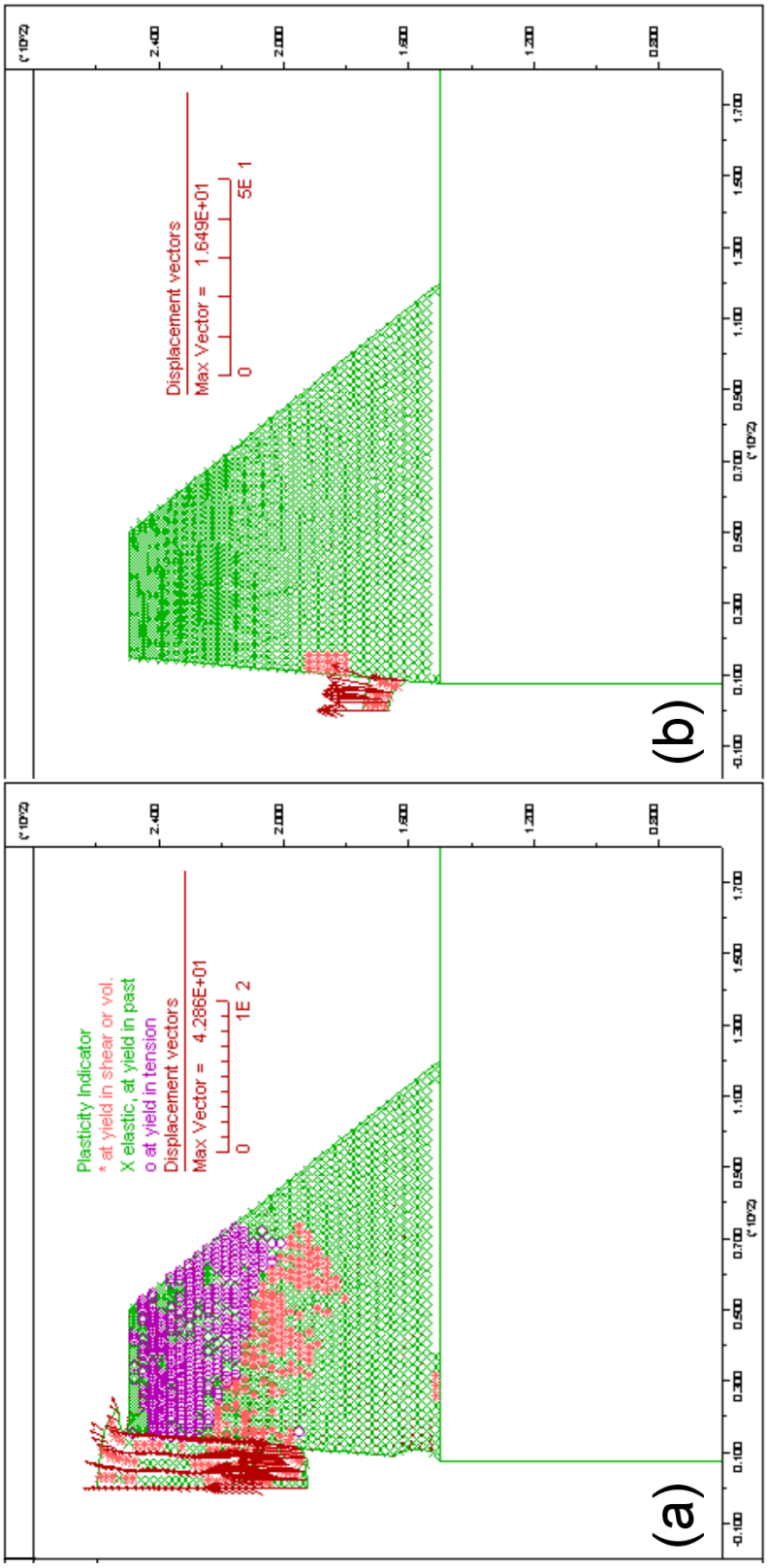

NOTE: All dimensions and vector lengths are in meters. For illustration purposes only. (a) Case 3; (b) Case 1.

Figure 6-9. Yielding and Deformation of Scoria Cones Fully Blocked to Various Depths

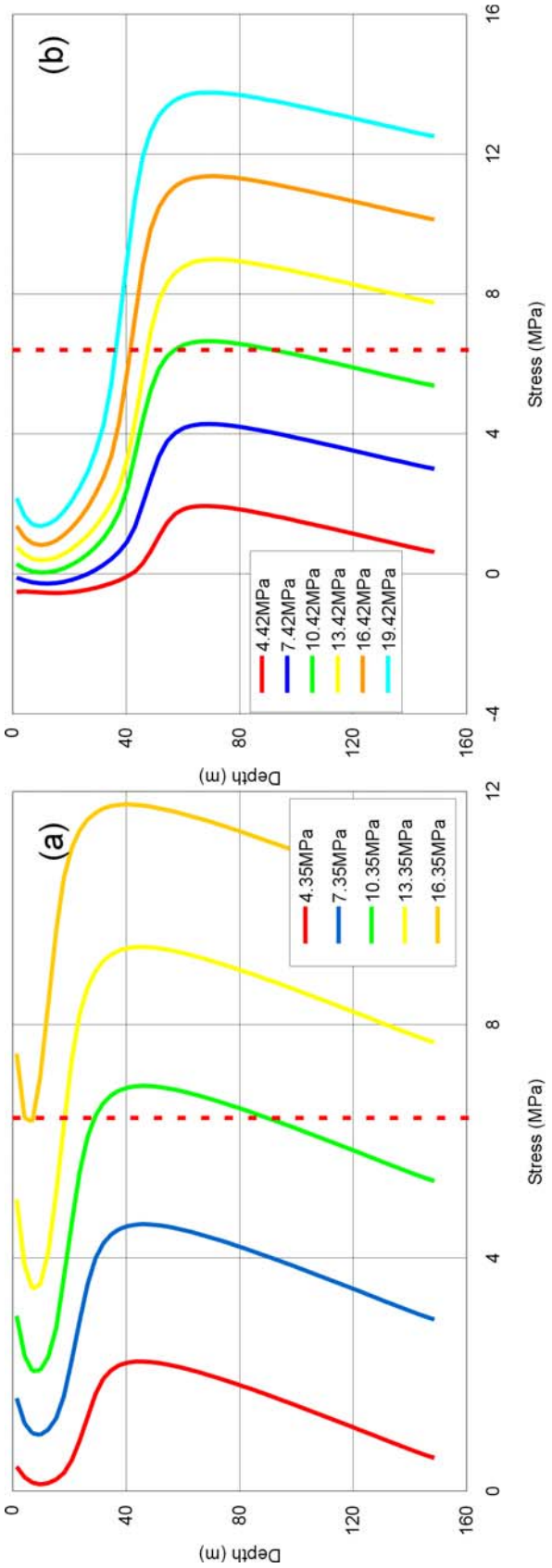

NOTE: The vertical dashed line is tensile strength reported by Rocchi et al. 2004 [DIRS 173995], Table 3, and is used for interpretation. For illustration purposes only. (a) Case 6; (b) Case 9.

Figure 6-10. Tangential Stresses Around a Conduit Blocked by Slumping into a Scoria Cone for Different Magma Pressures

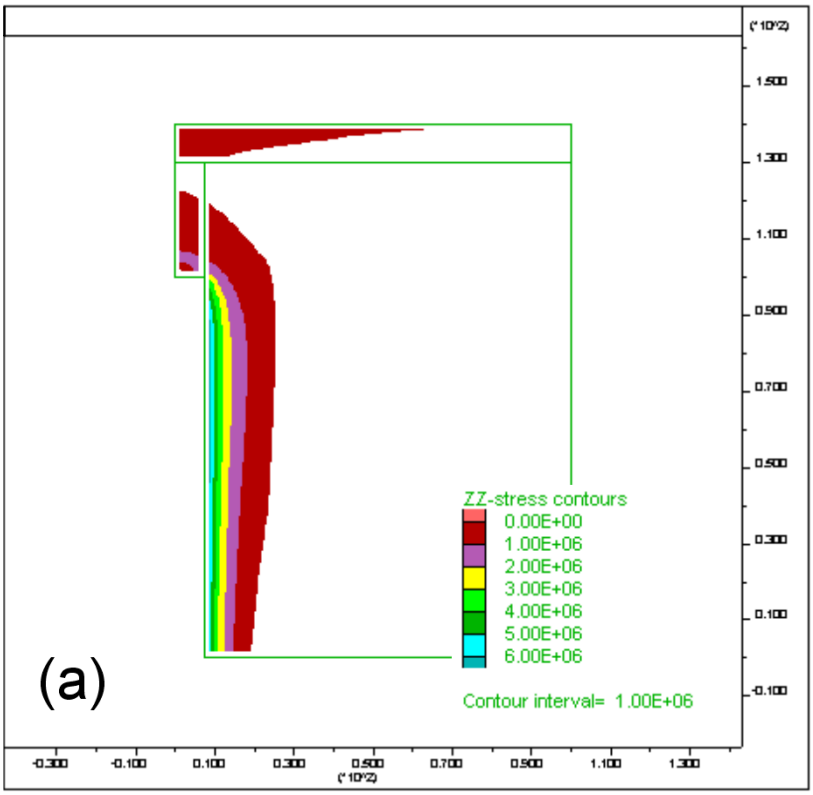

NOTE: Dimensions are in meters (m).
Stresses are in pascals (Pa).
For illustration purposes only.

Figure 6-11. Tensile Stresses Surrounding Conduit Blocked by Freezing

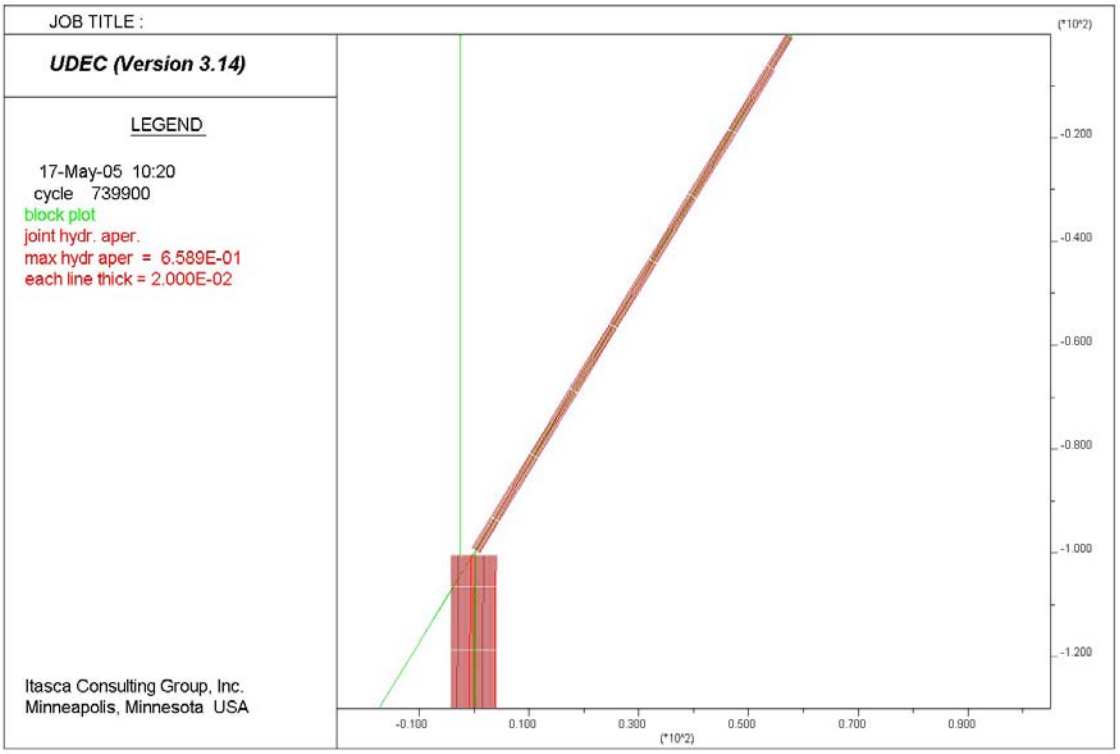

NOTE: X and Y dimensions are in meters (m).
The width of the red pattern is proportional to dike aperture (m).
For illustration purposes only.

Figure 6-12. Magma Diversion by a 60° Norma Fault Cutting a Vertical Dike

6.3.1.4 Interpretation

Blockage by Slumping or Solidification–In the case of hydrofracture, the magma pressure will decay relatively gradually after the breakout at the conduit boundary wall due to viscous drag limiting magma velocities in the newly opening crack. Indeed, the analysis of Section 6.3.2 suggests that such radial dikes may be of limited extent. Such cases are indicated in Table 6-2 as unshaded. The hydrofracture pressure is virtually independent of plug height (h_1) as can be seen by comparing Case 8 with Case 9 or Case 11 with Case 12. On the other hand, comparison of Case 6 with Case 9 indicates that h_2 does affect the pressure needed for breakout by hydrofracture; this is because the breakout will occur at greater depth (as is indicated by the depths of the maxima in Figure 6-10). A simple extrapolation of hydrofracture pressure based on a linearly elastic stress analysis can be made to estimate behavior of deeper plugs if it is assumed that the rock mass is homogeneous and isotropic. With this approach, the hydrofracture pressure for blockage by slumping or lava solidification will increase by about 0.23 MPa for every 10-m increase in the depth, h_2. This may be compared with the 0.6-MPa difference between breakout magma pressures with $h_2 = 25$ m (case 6) and $h_2 = 50$ m (case 9). By analogy, the same relationship between change of h_2 and change of breakout pressure will also apply to blocked

conduits under lava flows. Hydrofracture pressures calculated in this analysis are similar to those used in analysis of secondary breakout pressures presented in BSC (2004 [DIRS 170028], Section 6.5.1), so no deviations from the response predicted in that report are found.

The magma pressures listed in Table 6-2 for magma in a conduit to break out of a blockage by hydrofracture provide limits on the magma pressures that might lead to formation of a secondary dike from a drift. The calculated pressures are within or below the range of pressures for which secondary dike formation was analyzed in BSC (2004 [DIRS 170028], Section 6.5.1.2). But when additional hydrostatic pressure due to up to 300 m of basaltic magma (several more MPa) is added to the near-surface breakout pressures, the present analysis shows that higher pressures could occur in the repository drift than were analyzed in BSC (2004 [DIRS 170028]). Because the higher potential magma pressures in the drift were not explored in BSC (2004 [DIRS 170028]), the possibility of opening a secondary dike from the drift under these conditions cannot be definitively ruled out.

For small cones (i.e., similar to the cases highlighted in Table 6-2), magma pressures great enough to cause shearing failure within the cone can be reached before hydrofracture will occur. Such pressures are still within the limits analyzed in BSC (2005 [DIRS 170028], Section 6.5.1.2), but, as with hydrofracture, conclusions regarding secondary dike formation in BSC (2005 [DIRS 170028], Section 8.1.2) may not adequately bound secondary dike formation in those situations as well except for very thin blockages.

Hydrofracture from a conduit may be inhibited by plastic deformation of warm basalt rock surrounding a molten core with resulting further increase in magma pressure. This could lead to a rapid breakout from longer cones as a result of a shearing mechanism, which involves deformation of the entire scoria plug. The main reason for rapid breakout is a sudden decrease in shear resistance (strain softening and/or reduction of friction as a function of relative velocity) on the interface between the disturbed and undisturbed scoria and within the undisturbed scoria as a result of plug movement and deformation. Such a breakout could occur as a rapid, perhaps explosive, event resulting in acceleration of material to several times normal gravitational accelerations. This analysis does not allow proper estimates of velocities of ejecta that could result, but indicates the potential for the violent ejection of projectiles from a collapsing cone. Because the magma pressures needed to generate this type of failure are greater than the range considered in the analysis of BSC (2004 [DIRS 170028], Section 6.5.1.2), the conclusions regarding secondary dike formation cited in BSC (2004 [DIRS 170028], Section 8.1.2) may not apply if hydrofracture from a conduit is inhibited by plastic deformation of warm basalt rock surrounding a molten core.

Blockage by Faulting–This analysis demonstrates that magma may follow an active fault to the surface if it cuts an active dike, but it does not require such behavior. The results indicate that a magma pressure of about 1.4 MPa would be needed to open a fault cutting a dike 100 m below the surface. The pressure required to inject magma into a fault that has just cut a dike should vary with depth in a manner similar to hydrofracture pressure, as described in the first paragraph of this section. If a fault were to block a dike just above the repository (at a nominal 300-m depth) the expected magma pressure might rise as high as 6 MPa before magma moved to follow the new fault. This is near the lower end of magma pressures analyzed with respect to secondary dike formation in BSC (2004 [DIRS 170028], Section 6.5.1.2), so the results of BSC (2004

[DIRS 170028], Section 8.1.2) that secondary dike formation is not expected can be applied to blockage of a dike by faulting.

6.3.2 Secondary Dike Formation in Hot Rock

Dike/Drift Interactions (BSC 2004 [DIRS 170028], Section 6.5.1.4.2) concluded that the "dog-leg" scenario due to secondary dike opening by magma injection into pre-existing joints intersecting the emplacement drift is not possible, because the magma would freeze before the secondary dike propagated far beyond the drift. The original analysis relied upon simplifying assumptions including: (1) the magma injection occurred under ambient thermal conditions (25°C) without any preheating of the wall rock either by radioactive thermal energy or by magma in the drift; and (2) magma injection and heat conduction were completely uncoupled in separate calculations. The analyses reported here investigate the effects of heat conduction from the magma into the surrounding rock mass which may become important late in the full duration of an igneous event, and the effect of the temperature of the rock mass on the time necessary for magma to freeze.

6.3.2.1 Approach

Heat conduction from the magma injected into the pre-existing crack from an emplacement drift was analyzed using the numerical code FLAC V4.04 (BSC 2004 [DIRS 172432]). A schematic drawing of the problem is shown in Figure 6-13. Magma is injected into a crack with a constant aperture, a, at the constant temperature, T_{liq}, such that the magma front is moving at a constant velocity, v. The initial temperature of the surrounding rock mass, T_0, is assumed to be uniform.

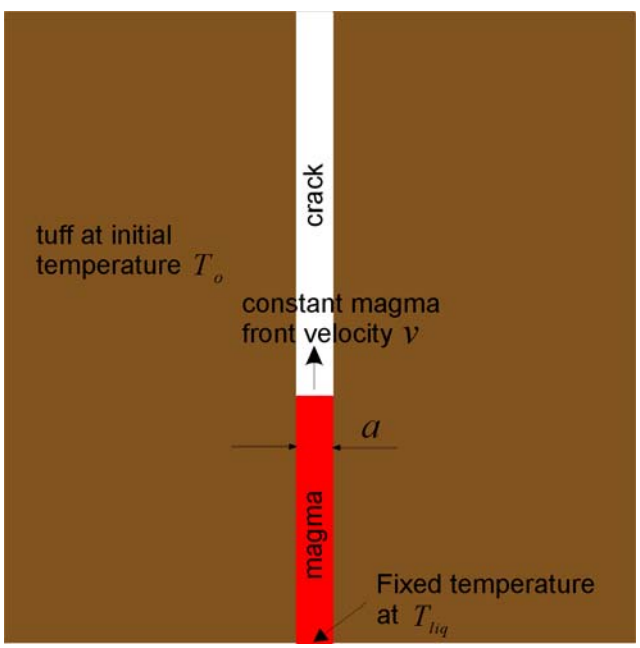

NOTE: For illustration purposes only.

Figure 6-13. Geometry, Initial and Boundary Conditions of the Secondary Crack Analyzed

There was no coupling between thermal and mechanical processes. Instead, a fixed crack opening and average magma velocity were derived from a coupled hydromechanical calculation reported in *Dike/Drift Interactions* (BSC 2003 [DIRS 165923], Case 102, Section 6.4.10.2.1). The results of case 102 were not carried forward to *Dike/Drift Interactions* (BSC 2004 [DIRS 170028]) when the document was revised, but there were no software or related issues involving the revision of *Dike/Drift Interactions* (BSC 2003 [DIRS 165923], Section 6.4.10.2.1) that would disqualify this dimension as direct input. The thermal calculation in the present analysis was not coupled with the hydromechanical simulation; the effects of any temperature change in the magma due to heat conduction on changes in viscosity or of pressurized magma flow possibly widening the crack were not included in the analysis. Other input parameters for the analysis are listed in Table 6-3. The liquidus temperature reflects a water content of 2 wt % for effusive flow.

Latent heat of the phase change or in this case the latent heat of crystallization can be accounted for in an analysis by increasing the specific heat. The specific heat of magma was increased from the tabulated value of 1,100 J/kg-K (Detournay et al. 2003 [DIRS 169660], Table 1-2) to 1,945 J/kg-K to include the effect of one half of the latent heat (350 kJ/kg) (Detournay et al. 2003 [DIRS 169660], Table 1-2) being released as the magma cools to the point where 50 percent of its volume is crystallized. The increase is calculated by averaging the latent heat of phase change over the temperature range across which the phase change occurs. The temperature of the intruding magma is 1,379 K (DTN: LA0407DK831811.001 [DIRS 170768], Table 8). The temperature at which 50 percent of magma is solidified is 1,172 K (DTN: MO0508SPAMAGMA.000. [DIRS 175008]). Averaging 50 percent of the latent heat of melting over the temperature change of 207 K (i.e., [(350,000 J/kg)/2]/207 K = 845 J/kg-K), the equivalent increase in specific heat is 845 J/kg-K. As a result, the total specific heat is equal to 1,100 + 845=1,945 J/kg-K.

Crack aperture histories presented in BSC (2003 [DIRS 165923], Section 6.4.10.2.1, Case 102) show that the crack is 11.8 mm wide and still widening at the drift wall by 0.05 mm/s after 104 s and is only 5 mm wide at a range of 16 m from the drift wall. In the present analysis, the constant crack aperture was 11.8 mm. The position of the magma front as a function of time calculated in *Dike/Drift Interactions* (BSC 2003 [DIRS 165923], Section 6.4.10.2.1, Case 102) is reproduced in Figure 6-14. The magma-front velocity is nearly constant and compares well with the constant value 0.172 m/s used in this analysis, as indicated by the red line in Figure 6-14.

In order to demonstrate the effect of preheating of country rock by magma that has filled a drift for a few months, calculations were conducted for homogeneous initial host rock temperatures of 20°C (293 K) and 300°C (573 K). The latter value represents temperatures a few months after initial intrusion of a drift as approximated from the results presented in *Dike/Drift Interactions* (BSC 2004 [DIRS 170028], Section 6.7).

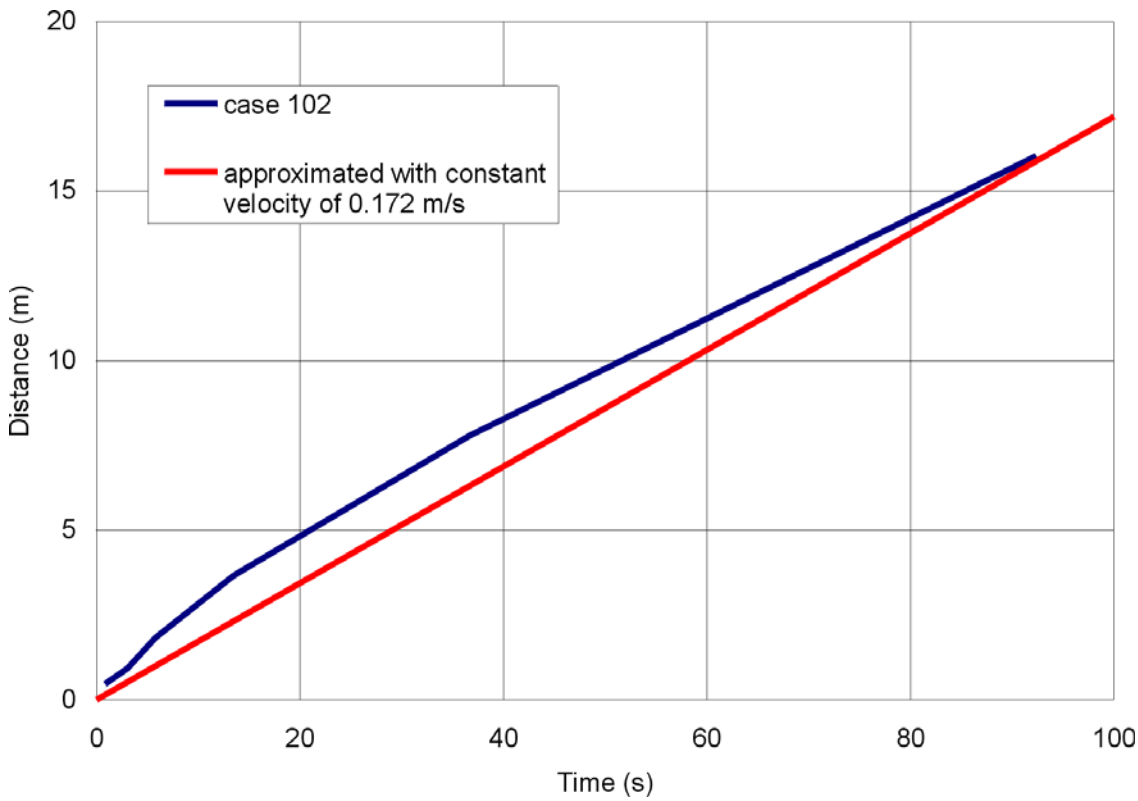

Source: Modified from BSC 2003 [DIRS 165923], Figure 57.

Figure 6-14. Location (Relative to the Drift Periphery) of the Magma Front Inside a Joint as a Function of Time: Case 102

Table 6-3. Inputs for Thermal Simulation with FLAC V4.04

	Property	Value	Source
Host Rock	Thermal Conductivity (W m^{-1} K^{-1})	0.75	Detournay et al. 2003 [DIRS 169660], Table 1-2. (Selected from the range 0.5 W m^{-1} K^{-1} to 1.0 W m^{-1} K^{-1})
	Specific Heat (kJ kg^{-1} K^{-1})	1.0	Detournay et al. 2003 [DIRS 169660], Table 1-2
	Density, ρ (kg m^{-3})	2,000	Detournay et al. 2003 [DIRS 169660], Table 1-2
Magma	Thermal Conductivity (W m^{-1} K^{-1})	0.60	Detournay et al. 2003 [DIRS 169660], Table 1-2 (Selected from the range 0.2 W m^{-1} K^{-1} to 1.0 W m^{-1} K^{-1})
	Latent Heat or Crystallization Enthalpy (kJ kg^{-1})	350	Detournay et al. 2003 [DIRS 169660], Table 1-2 (Selected from the range 250 kJ kg^{-1} to 550 kJ kg^{-1})
	Specific Heat with 50% Crystals per Volume (kJ kg^{-1} K^{-1})	1.945	The specific heat of magma has been increased from 1.100 kJ kg^{-1} K^{-1} to 1.945 kJ kg^{-1} K^{-1} (from Detournay et al. 2003 [DIRS 169660], Table 1-2 to include the effect of half of the latent heat (350 kJ/kg) being released as magma cools to a temperature where half of its volume has crystallized.
	Intrusion or Liquidus Temperature, T_{liq} (K)	1,379	DTN: LA0407DK831811.001 [DIRS 170768], Table 8 Water Weight Content = 2%
	Effective Solidification Temperature, T_s (K)	1,172	DTN: MO0508SPAMAGMA.000 [DIRS 175008]

6.3.2.2 Results

Results are presented in Figure 6-15. Temperature profiles along the centerline of the crack at several times and temperature histories at several locations relative to the magma front are shown for both initial temperatures. The temperatures reported are the maximum values, at the center of the crack, because heat flow is from the magma into the rock. The effective solidification temperature, T_s, is indicated as a horizontal black line. When the temperature falls below the solidification temperature, the magma will be so viscous that further flow along the crack will be negligible on the scale of the calculations. The results indicate that, in both cases, the magma effectively will freeze in the crack in less than 100 s, precluding further propagation. Solidification occurs sooner in the case of the cold surrounding rock (~60 s) than in the case of the hot rock (> 70 s to 75 s).

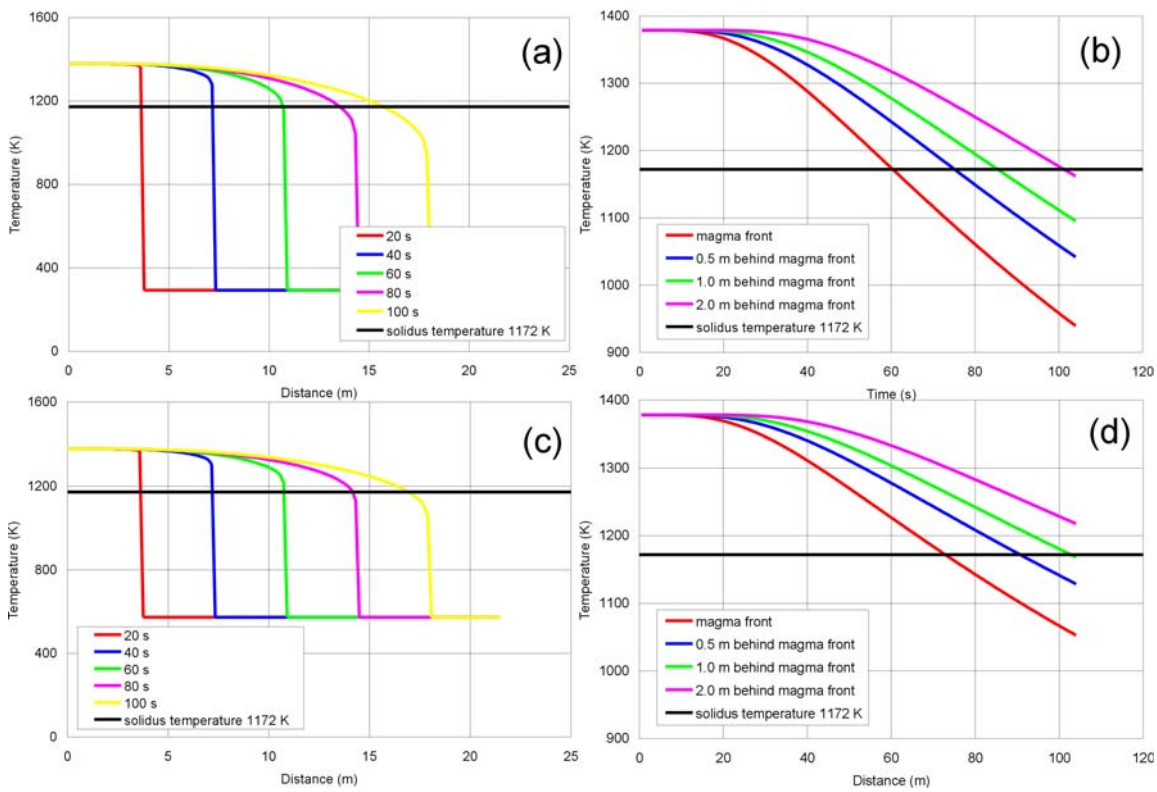

NOTES: (a) Maximum temperature in secondary dike vs. distance from drift wall: initial rock temperature of 298 K (25°C).

(b) Temperature at center of secondary dike vs. time (s) with initial wall rock temperature of 298 K (25°C).

(c) Maximum temperature in secondary dike vs. distance from drift wall: initial rock temperature of 573 K (300°C).

(d) Temperature at center of secondary dike vs. time (s) with initial wall rock temperature of 573 K (300°C).

For illustration purposes only.

Figure 6-15. Results for Magma Temperatures (K) in Secondary Crack

6.3.2.3 Conclusions

Dike/Drift Interactions (BSC 2003 [DIRS 165923], Section 6.4.10.2.1, Case 102) finds that the crack would have been narrower earlier in its history, so the postulate of fixed crack width will underestimate cooling of any magma flowing therein. Furthermore, from the same source, the crack width at a range of 7.8 m from the drift edge after 60 s is expected to be under 6 mm, so that the present calculation with a crack of fixed width of 11.8 mm will also underestimate magma cooling. These two arguments combined demonstrate that magma will cool quickly before propagating far into a secondary crack, whether the country rock is at ambient or elevated temperature. Furthermore, *Dike/Drift Interactions* (BSC 2004 [DIRS 170028], Figure 6-98) shows that temperatures are not expected to rise above ~130°C after an intrusion as close as 7 m from the centerline of a drift.

The results of this analysis reinforce the conclusion of *Dike/Drift Interactions* (BSC 2004 [DIRS 170028], Section 6.5.1.4.2) that magma attempting to open a secondary dike by intruding a pre-existing crack will solidify before the crack can grow to an appreciable width. Solidification will occur both early in the intrusive event, when the wall rock is near ambient temperature, as stated in *Dike/Drift Interactions* (BSC 2004 [DIRS 170028], Section 6.5.1.4.2), and later if the wall rock temperature is as high as 300°C. According to *Dike/Drift Interactions* (BSC 2004 [DIRS 170028], Section 6.7.1.2), such temperatures are expected at a distance of 2.25 m from the edge of the drift for as long as a few months after intrusion of magma into a drift but are not expected to extend as far as 4.25 m. Thus the conclusion of *Dike/Drift Interactions* (BSC 2004 [DIRS 170028], Section 6.5.1.4.2) that newly forming secondary dikes will solidify before escaping the immediate vicinity of a drift can be extended to later times during an igneous event. This conclusion should not be applied to the propagation of dikes from depth. The model described in *Dike/Drift Interactions* (BSC 2004 [DIRS 170028], Section 6.3.3 through Section 6.3.7) considers that condition, where propagation is facilitated by the long lever arm between the crack tip and magma pressurizing the crack over a range of depths greater than a kilometer.

6.4 MULTIPHASE MAGMA FLOW

In order to calculate the conditions within a repository drift that is intersected by magma rising in a dike, it is important to account for the two-phase nature of the magma. This two-phase nature is caused by the presence of both vapor and incompressible droplets or particles (pyroclasts) of silicate melt. The two phases may flow with different velocities but are coupled to each other by drag and heat exchange. Also, the process of filling a drift with multiphase magma is time-dependent, and simulation of this process must account for two or three dimensions. This section reports two-dimensional, time-dependent calculations conducted using the two-phase code GMFIX V1.61 (BSC 2005 [DIRS 174137]), which is well suited to address the drift-filling process. GMFIX V1.61 solves partial differential equations describing the conservation of mass, momentum, and energy for gas with dispersed droplets or particles, accounting for coupling between the phases.

As discussed in *Characterize Eruptive Processes at Yucca Mountain, Nevada* (BSC 2004 [DIRS 169980]), as well by Nicholis and Rutherford (2004 [DIRS 173945], p. 491), a future volcanic event at Yucca Mountain is likely to be driven by a relatively volatile-rich (on the order

of 4% H_2O) magma. At shallow depths that pertain to the repository horizon, rising magma is likely to be a two-phase mixture of melt (basaltic in composition) and gas. The gas phase will be dominated by exsolved water. Two sets of stylized calculations are presented.

1. Calculation of the flow dynamics associated with initial interaction between rising magma, under a relatively high (e.g., lithostatic) pressure, and a repository drift at an initial low (atmospheric) pressure. For these calculations, two dike-drift intersection configurations are used. For the first configuration (Simulation A, Figure 6-16a), the vapor-filled crack at the top of the propagating dike extends along its original trajectory above the repository. This represents a situation where the magma front follows behind the newly opened dike-tip cavity (BSC 2004 [DIRS 170028], Section 6.3.7). Calculations with this configuration allow both lateral flow into the intersected drift and upward flow into the dike-tip cavity. A second configuration (Simulation B, Figure 6-16b) is similar to the first but is assumed to have a secondary opening at some distance down-drift from the primary dike. This opening is assumed to extend upward to the surface from the crown of the drift and allows for an analysis of the partitioning of flow between the main dike and the hypothetical open pathway.

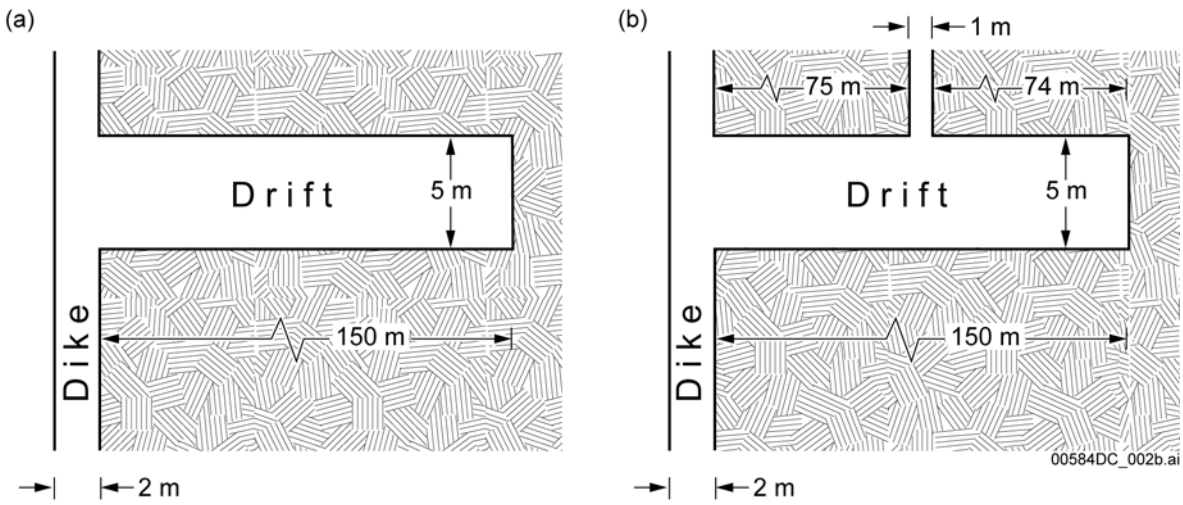

NOTE: For illustration purposes only. Simulation A and A1 are represented by (a); Simulation B is represented by (b).

Figure 6-16. Dike Drift Scenarios

2. *Calculation of flow at a later time during the course of an igneous event (BSC 2004 [DIRS 169980], Section 6.3.3.4, event duration information) after an intersected drift has been flooded with pyroclasts and pressurized.* The specific scenario (Simulation A1) address situations where there is a rapid decompression of the magmatic system due to failure of a blockage feature in the volcanic vent above the repository; the blockage feature might be pyroclastic debris that has clogged the vent, or solidified magma (Section 6.3.1). The scenario uses the same geometry as shown in Figure 6-16a, but the initial condition is that the entire dike-drift system is filled with pyroclasts and gas at a pressure determined by the stresses in the country rock, and then the mixture is allowed to decompress and flow out the top of the dike.

6.4.1 Inputs

Table 6-4 lists the values of the computational mesh and material properties used for the calculations, and Table 6-5 lists the initial and boundary conditions for each of the three calculations (Simulations A, B, and A1). All of the calculations are two-dimensional and in Cartesian coordinates.

Table 6-4. Geometry, Wall Boundary Conditions, and Physical Conditions

Geometry	Cartesian
Horizontal Length X [m])	150
Horizontal Resolution ΔX [m]	0.5
Number of Grid-Points in the X-Direction	305
Vertical Length Y [m]	19
Vertical Resolution ΔY [m]	0.5
Number of Grid-Points in the Y-Direction	39
Dike Width [m]	2
Grain Diameter [mm]	0.5
Grain/Magma Density [kg/m^3]	2,500
Wall	No-slip wall (all phases)

Source: See Table 4-1.

Table 6-5. Initial and Flow Boundary Conditions

	Simulations	A	B	A1
Drift	Pressure [Pa]	10^5	10^5	125 x 10^5
	Temperature [K]	298	298	1,373
	Calculated Gas Density [kg/m^3]	1.169	1.169	19.73
	Mass Fraction of Water in Vapor Phase	0	0	1.0
	Volumetric Solid Concentration [vol %]	0	0	40
	Calculated Mixture Density [kg/m^3]	1.169	1.169	1,011.8
Inlet	Mixture Temperature [K]	1,373	1,373	N/A
	Gas Pressure [Pa]	125×10^5	125×10^5	N/A
	Calculated Gas Density [kg/m^3]	19.73	19.73	N/A
	Mass Fraction of Water in Vapor Phase	1.0	1.0	N/A
	Calculated Mixture Density [kg/m^3]	1,011.8	1,011.8	N/A
	Mixture Vertical Speed [m/s]	90	90	N/A
	Volumetric Solid Concentration [vol %]	40	40	N/A
	Mass flux [kg/s/m]	182,124	182,124	N/A
Main Outlet	Gas Pressure [Pa]	10^5	10^5	10^5
	Gas Temperature [K]	298	298	298
Secondary Outlet	Gas Pressure [Pa]	N/A	10^5	N/A
	Gas Temperature [K]	N/A	298	N/A

The drift in the two-dimensional analyses assumes the third dimension is made of one cell 5-m wide (hence there is no finite-volume discretization along the third dimension). This is a requirement for application of the two-dimensional GMFIX V1.61 software (BSC 2005 [DIRS 174137]). This will underestimate drag between the flow and drift walls relative to a cylindrical drift, but those will be negligible during the short duration simulated. Because the outlets at the upper edge of the computation are not longer (in the third dimension) than the drift itself, the strength of depressurization waves will be underestimated during the duration of the analyses relative to the true three-dimensional configuration of a long dike intersecting individual 5-m-diameter drifts. The two-dimensional analyses are intended to provide insight into flow phenomena and preliminary values of such key parameters as dynamic pressure, pyroclast (particle) concentration, and temperature for a limited set of scenarios and as such should not be treated as a comprehensive analysis.

All walls (denoted by solid lines on Figure 6-16) are no-slip boundaries for both vapor and particle phases in the calculations. The feeder (primary) dike is assumed to be 2-m wide, which is within the probability distribution function for dike width that is presented in *Characterize Eruptive Processes at Yucca Mountain, Nevada* (BSC 2004 [DIRS 169980], Table 7-1).

The drift is selected to have a length of 150 m (including the intersection with the dike) and a height of 5 m. This length, which is shorter than planned drifts, represents a dike intersection 150 m from the end of a drift and as such is only one of many possible combinations of drift length beyond a dike intersection. The end of the drift is treated as a closed vertical boundary, a simplification of the more complex geometry that backfill in the access drifts and turnouts and magma bulkheads will present to the flow. The height is an approximation of the design value taking into account the discretization of the computational mesh.

The primary dike is assumed to be limited to a total vertical extent of 19 m. This length is selected in order to limit the computational time needed for the analyses. It is much smaller than any expected length of a dike, but the small value is compensated by employing an adaptive inflow/outflow boundary to minimize reflections from the end of the computational mesh.

For computational purposes the secondary opening (Simulation B) is set to a width of 1 m. This large opening is much greater than the range of secondary dike openings of a pre-existing fracture calculated in *Dike/Drift Interactions* (BSC 2004 [DIRS 170028]), which did not exceed 27-mm width at distances from the drift of several meters when analyzed under unexpected hydrovolcanic conditions (BSC 2004 [DIRS 170028]), Section 6.5.2.3). The hypothetical 1-m width is selected to provide a minimum of two zones in the computational mesh selected for this analysis. This opening is an unrealistic representation of the repository host rock conditions but allows for the analysis of partitioning of flow between the main dike and a presumed opening further down the intersected drift, and evolution of multiphase flow as it moves down the drift.

The diameter of magma particles is assumed to be 0.5 mm. This represents a compromise between the requirement of the GMFIX V1.61 code (BSC 2005 [DIRS 174137]) to have a single grain size and the natural situation where grain size can vary from fine ash to boulder size. It may be considered a rough geometric mean diameter. It is within the distribution of mean particle sizes recommended in *Characterize Eruptive Processes at Yucca Mountain, Nevada* (BSC 2004 [DIRS 169980], Table 7-1).

The density of magma particles is assumed to be 2,500 kg/m^3. This is an approximation based on a silicate liquid density calculated in *Characterize Eruptive Processes at Yucca Mountain, Nevada* (BSC 2004 [DIRS 169980], Table 6-4) and assumes that the 0.5 mm particles are not vesiculated.

The initial temperature of magma in the dike in all analyses and in the drift for the decompression analyses is 1,373 K (1,100°C). This value is within the range of liquidus temperatures in *Characterize Eruptive Processes at Yucca Mountain, Nevada* (BSC 2004 [DIRS 169980], Table 7-1).

Vapor in the magma is assumed to be pure water (molecular weight 18.0152 kg/kmol). The assumption of pure water is for computational convenience, but *Characterize Eruptive Processes at Yucca Mountain, Nevada* (BSC 2004 [DIRS 169980], Table 6-3) indicates that water is expected to be the most abundant gas species (averaging 73 mol %) for basaltic volcanism in the Yucca Mountain region. CO_2 (14 percent) is second in expected abundance, followed by SO_2 (9 percent) and other less abundant species.

The magma is assumed to have initial volume fractions of 40 percent condensed silicate and 60 percent vapor. The value for condensed silicate melt is higher than the equilibrium decompression value for a pressure of 12.5 MPa (BSC 2004 [DIRS 169980], Figure 6-3) water contents above approximately one weight percent. For the analyses of magma intrusion into the drift, this value is justified by the fact that much of the vapor in the leading edge of the magma is expected to have already separated from the condensed phase by the time the magma front arrives at the drift. This value will quickly modify to a steady state to be consistent with the initial temperature, pressure, and velocity of the magma. For the decompression analyses, it is expected that pyroclasts and gas have filled the drift and pressurized as would happen if the volcanic system were temporarily blocked.

The magma in the intrusion analyses (Simulations A and B) is assumed to be at an initial pressure of 12.5 MPa and both the vapor and silicate fractions are assumed to be moving upward at 90 m/s; the initial pressure of magma in the drift for the decompression analyses (Simulation A1) is also 12.5 MPa. This pressure, approximated from Figure 6-34 of DTN: MO0411EG831811.000 [DIRS 174959] (Disk 1), represents confining stresses on a magma-filled dike 1,000 years after waste emplacement. The value of velocity was selected to be "high," but the analyses are insensitive to these values over a considerable range. The velocity will quickly modify to a quasi steady-state consistent with the initial temperature and pressure of the magma.

The equations and algorithms employed by the software GMFIX V1.61 (BSC 2005 [DIRS 174137]) are derived from and discussed by Dartevelle (2004 [DIRS 174132]). Other input parameters from the same source include the molecular weight of air equal to 28.9644 kg/kmol, and the gas constant equal to 8,314.56 J kmol^{-1} K^{-1} (Dartevelle 2004 [DIRS 174132], Table A1). An inelastic collisional coefficient between grains and between grains and boundaries of 0.9 is defined by Dartevelle (2004 [DIRS 174132], Eq. 7 and Table A1). The minimum solid volumetric concentration of 50 vol % above which plastic bulk behavior of flow begins ($^{min}\varepsilon_s$) (Dartevelle 2004 [DIRS 174132], Equation T5.19) is found in Table 5, and its effect is illustrated in Figure 4, of Dartevelle (2004 [DIRS 174132]), as is the

maximum possible volumetric concentration of 64 vol % for a randomly packed grain structure. The angle of internal friction between grains of 30.25° is provided by Dartevelle (2004 [DIRS 174132], Table A2).

Overall Physical Representativeness of the Simulations–The geometry, and initial and boundary conditions, of Simulation A presented below represent two hypothetical scenarios, based upon understanding of magma-repository interactions. They do not represent the full range of scenarios, which could have different combinations of parameters such as: feeder dike width, volatile content, feeder dike pressure, pyroclast particle size, pyroclast concentration (for Simulation A1), magma velocity within the feeder dike, and location of the intersection of the feeder dike with respect to the length of a drift. In addition, the simulations are two-dimensional and do not account for details of flow around waste packages. The width of the secondary opening in Simulation B is intentionally set at a unrealistic value, primarily for computational convenience. Scaling of this feature down to more realistic widths developed in *Dike/Drift Interactions* (BSC 2004 [DIRS 170028]) is described in Section 6.4.2.2. Because the calculations do not account for the finite width of the drift (i.e., the calculations are two-dimensional) or components such as waste packages and drip shields–all features that would increase the drag on the flow–it is possible that velocities (particularly for flow along the drift floor) are overestimated in this report compared to a real situation. Nevertheless, the simulations provide a general picture of the phenomena that are expected to occur if a fragmental magmatic flow intersects an open drift.

6.4.2 Initial Interaction with Drifts

6.4.2.1 Simulation A–Initial Flow into a Closed Drift

Results of Simulation A (using configuration in Figure 6-16a) are shown in Figure 6-17, which shows the solid volumetric concentration of the gas–pyroclast mixture at selected times in the calculations. At very early time while most (see Figure 6-20) of the gas-pyroclast mixture flows vertically up the dike, rapid decompression of the mixture into the drift causes a gas shock that propagates into the drift ahead of the pyroclastic flow, with horizontal speed of ~210 m/s and dynamic pressure at the roof of ~9.4×10^4 Pa (at 0.06 s, 26 m into the drift; dynamic pressure is defined as $P_{dyn} = 1/2\rho v^2$, where ρ is the mixture density and v is the horizontal speed of the volume-fraction-weighted mixture). A hot, buoyant pyroclastic flow immediately follows and propagates along the roof with horizontal speed at the roof of ~131 m/s and dynamic pressure of ~1.4×10^7 Pa, while on the floor the dynamic pressure of ~1.8×10^5 Pa is only generated by the gas-phase momentum (e.g., 0.30 s, 22 m, Figure 6-17). At ~0.3 s, the initial gas shock has reached the end of the drift with horizontal speed of ~300 m/s and dynamic pressure of ~2.7×10^5 Pa, and is reflected backwards toward the feeder dike. This reflected gas shock creates a quasi "zero dynamic pressure front" moving upstream as pre- and post-shock-reflection gas velocities cancel each other out. When the reflected shock hits the buoyant pyroclastic flow (~0.5 s), it creates an instability on the pyroclastic flow front that enhances vorticity and definition of the flow "head" (as seen at t ~0.60 s in Figure 6-17). At 1.2 s, the pyroclastic flow has reached the 150-m end-wall with dynamic pressures ranging from ~1.0×10^4 (floor) to 2.2×10^6 Pa (roof). The pyroclastic flow turns downward and forms a dense flow on the drift floor that moves back toward the main dike (see 3.0 s in Figure 6-17). This concentrated

pyroclastic flow moves with typical horizontal speed of ~–62 m/s, dynamic pressure ~1.2×10^6 Pa, and concentration of ~12 vol % (e.g., at 3.0 s and 90 m in the drift). Eventually, at ~3.7 s, the flow has returned to the main dike, with some of the material potentially being vented toward the surface and some being recirculated back into the drift. The drift will eventually fill up through a process of recirculating flow with continuous introduction of new material until the concentration of pyroclasts becomes sufficiently high that flow is inhibited. Although Figure 6-20 indicates that the ratio of magma flow continuing up the upward extension of the dike to the influx from below increases to as much as 80 percent, this ratio is certainly exaggerated at later times by the boundary condition of constant, 10^5 Pa, pressure at the upper outlet only 7 m above the top of the drift. In reality, such low pressure would occur much higher in the crack tip, and pressures 7 m above the drift will be much higher due to the continuing flow of magma mixture.

6.4.2.2 Simulation B–Effect of Secondary Opening on Initial Interactions

Simulation B involves a hypothetical 1-m-wide opening extending upward from the crown of the drift. As suggested by Figure 6-17 and further shown in Figure 6-18, there are only minor differences in the dynamics of the multiphase flows of Simulations A and B. Some material (around 10 percent and 35 percent by volume, see Figure 6-20) is diverted into the secondary opening. As for Simulation A, the percentages at later times may be exaggerated by proximity to the low pressure boundary condition. Note also that the normalized mass flow at any time need not sum to 1.0 because the drift acts as a dynamic buffer with varying amounts of pyroclastic magma moving back and forth. The midway flow between roof and floor is more diluted than in Simulation A; yet, at the roof and on the floor, the concentrations, bulk horizontal speeds and dynamic pressures are nearly identical between the two simulations (see Figure 6-18a,b,c).

As mentioned in Section 6.4.1, the 1-m opening in this analysis is highly stylized and does not represent expected host rock conditions. Section 6.5.1.2 and Figure 6-62 of Dike/Drift Interactions (BSC 2004 [DIRS 170028]) illustrate that even under effusive magmatic conditions it can take several minutes or more to reach crack widths of 25 mm, even given a pre-existing crack of 1-mm aperture. Inspection of Figure 6-20 shows that the distribution of flow between the primary dike ~60 percent) and the secondary dike (~30 percent) is approximately given by their relative cross-sections (2 m in the primary versus 1 m in the secondary). Using that relation, one would expect that only approximately one percent of magma rising in a 2-m wide dike would be diverted into a 0.025-m wide secondary opening, even if that opening existed to the surface. When the effect of boundary conditions (see previous paragraph) is included, a better estimate of flow into a secondary opening would be less than one percent.

6.4.2.3 Simulation A1–Decompression after Vent Blockage

Simulation A1 explores sudden decompression of a pyroclast-filled dike-drift system as might occur following the failure of a magma plug in the overlying volcanic vent (e.g., Section 6.3.1). The geometry is the same as in Simulation A. Initially the drift is filled with pyroclastic materials with a silicate concentration of 40 vol % under a pressure of 12.5 MPa (Table 6-5). The decompression (the upper dike boundary is at a pressure of 0.1 MPa), creates a rarefaction wave that propagates into the pyroclastic material. Hence, the material progressively moves out from the drift into the dike but at the same time pyroclasts settle to the drift floor. For example,

in Figure 6-19a,b, at 2 s and 135 m down the drift, the concentration at the roof is ~7 vol % with horizontal speed of 7.75 m/s, while at the floor level, concentrations are ~52 vol %, comprising a dense pyroclastic flow (e.g., mixture density of 1,300 kg/m^3 at 2 s) with speed of 2.66 m/s. At 5 s and at the same location, there is a nearly static <1-m-thick granular deposit and the upper part of the drift is being cleared of any residual pyroclasts (Figure 6-19a). Over 5 s of simulation, the maximum dynamic pressure encountered at the floor of the drift is ~7×10^5 Pa.

6.4.3 Discussion

In Simulation A and B scenarios, while most (between 70 percent and 80 percent after 2.5 s) of the rising pyroclast-gas mixture simply continues up the feeder dike, some material is drawn into the drift. The drift experiences two dynamic pressure waves, one generated by the clean-gas shock (~10^5 Pa) due to the initial expansion of the magma-gas mixture, which is quickly followed by a stronger dynamic pressure wave of a maximum of ~10^7 Pa due to the higher bulk density of the subsequent pyroclastic flow. Because of the closed end of the drift, a backward-flowing, concentrated pyroclastic flow is formed with typical dynamic pressures on the order of ~10^6 Pa. If this dynamic pressure were applied on the end of a typical 1.5-m-diameter waste package it would result in a force on the order of ~180 kN if this canister were fully exposed end-on to the flow. BSC (2004 [DIRS 170028], Section 6.4.8.2) finds that such forces would not be sufficient to move waste packages. Since waste packages will generally have gaps only on the order of tens of centimeters between them, it is likely that there would be significant "shadowing" effects so that it is not expected that a package would experience this full force.

These simulations have significant differences from earlier simulations by Woods et al. (2002 [DIRS 163662]):

- The Woods analysis treats magma as a single compressible phase while the present analysis treats magma as two separate phases (vapor and incompressible droplets) with exchange of momentum and thermal energy between the phases. The two-phase analysis allows mixing of air into expanding magma, which is then heated. This results in lower densities and the early "roof-hugging" flow into the drift. Separation of phases also provides for greater energy dissipation than will occur in single phase flow.

- The Woods analysis is one-dimensional (but with variable cross-section, an approach sometimes referred to as "one-and-a-half dimensional), whereas the present analysis is two-dimensional. Because it is two-dimensional, the present analysis properly separates the buoyant flow into the drift along the roof from the denser return flow along the floor that develops after the pyroclastic magma reflects off the end of the drift.

- The Woods analysis does not include an open crack tip ahead of the magma, but the present analysis includes this feature. Analyses of dike propagation, summarized in BSC (2004 [DIRS 170028], Section 6.3), indicate that an open tip cavity is to be expected. The open cavity above the drift will capture most of the magma rising in the dike, with only a fraction of the original flow being diverted into the drift.

As a result of these differences, the flow into the drift in the present analysis is more realistically simulated, especially the vertical segregation of the flow into the drift and the return flow back toward the dike. The flow regime in the drift is also less intense (in terms of dynamic pressures and velocities) and more realistic in this analysis than in the analysis of Woods et al. (2002 [DIRS 163662]).

A second, hypothetical 1-m-wide opening to the surface does not significantly affect the dynamics of the multiphase flow within the drift. A much wider opening like that chosen by Woods et al. (2002 [DIRS 163662]) may affect the amount of pyroclastic material and pressure to such an extent that the flow dynamics may be notably modified. The last scenario involves a drift filled with 40 vol % pyroclasts initially pressurized to lithostatic pressure. The main dike is the pathway through which pyroclastic material flows out of the drift. In this scenario, typical dynamic pressures are on the order of ~10^5 Pa during decompression, leading to an applied force on a waste package (fully exposed end-on to the flow) on the order of ~17 kN.

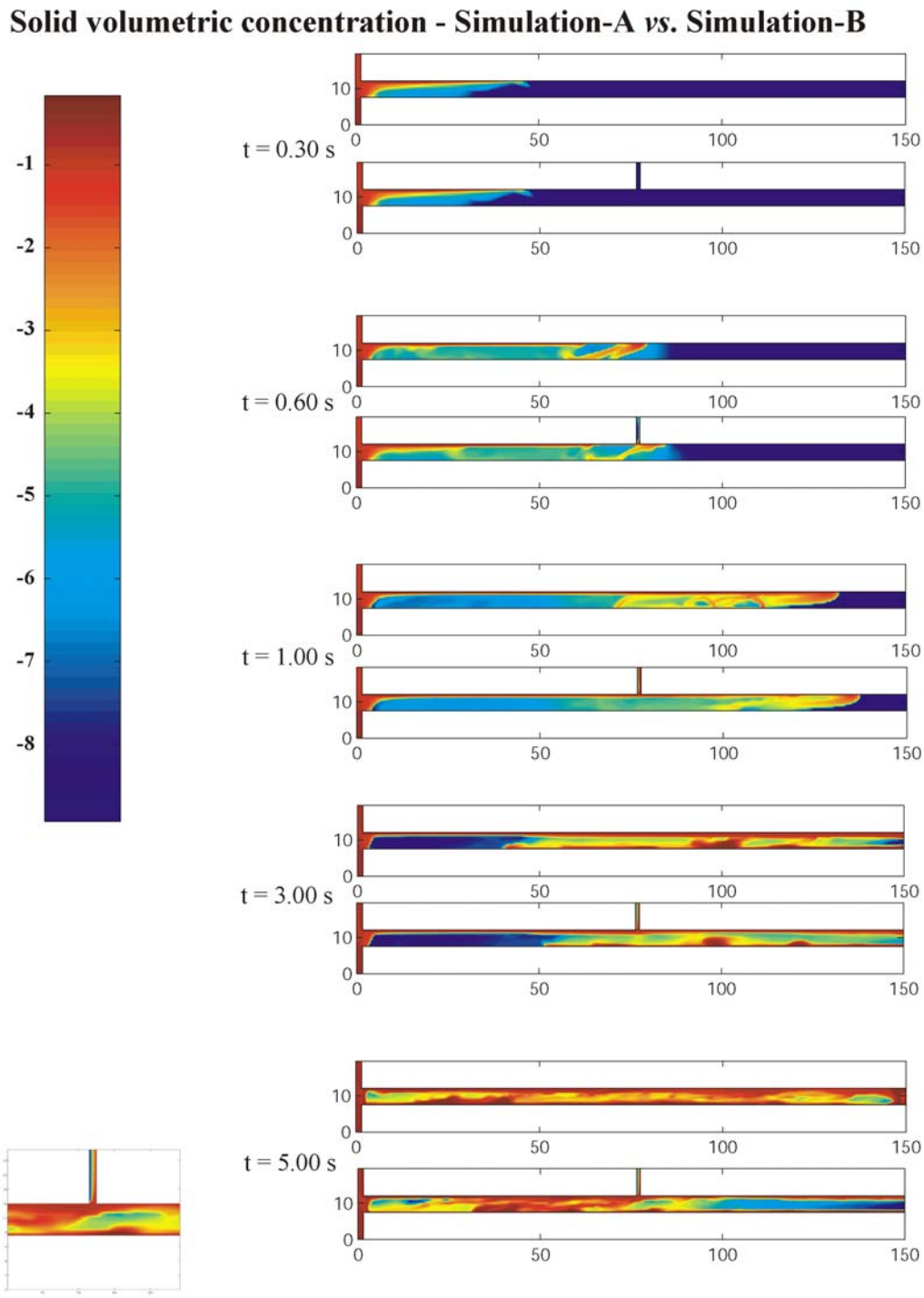

NOTE: The upper figure at each time is for Simulation A, the lower for Simulation B. The insert at the bottom represents Simulation B (5 s) zoomed in around the second opening. For illustration purposes only.

Figure 6-17. Color Plot of the Logarithm of Volumetric Solid Concentration at Different Times taken in the Drift for Two Simulations

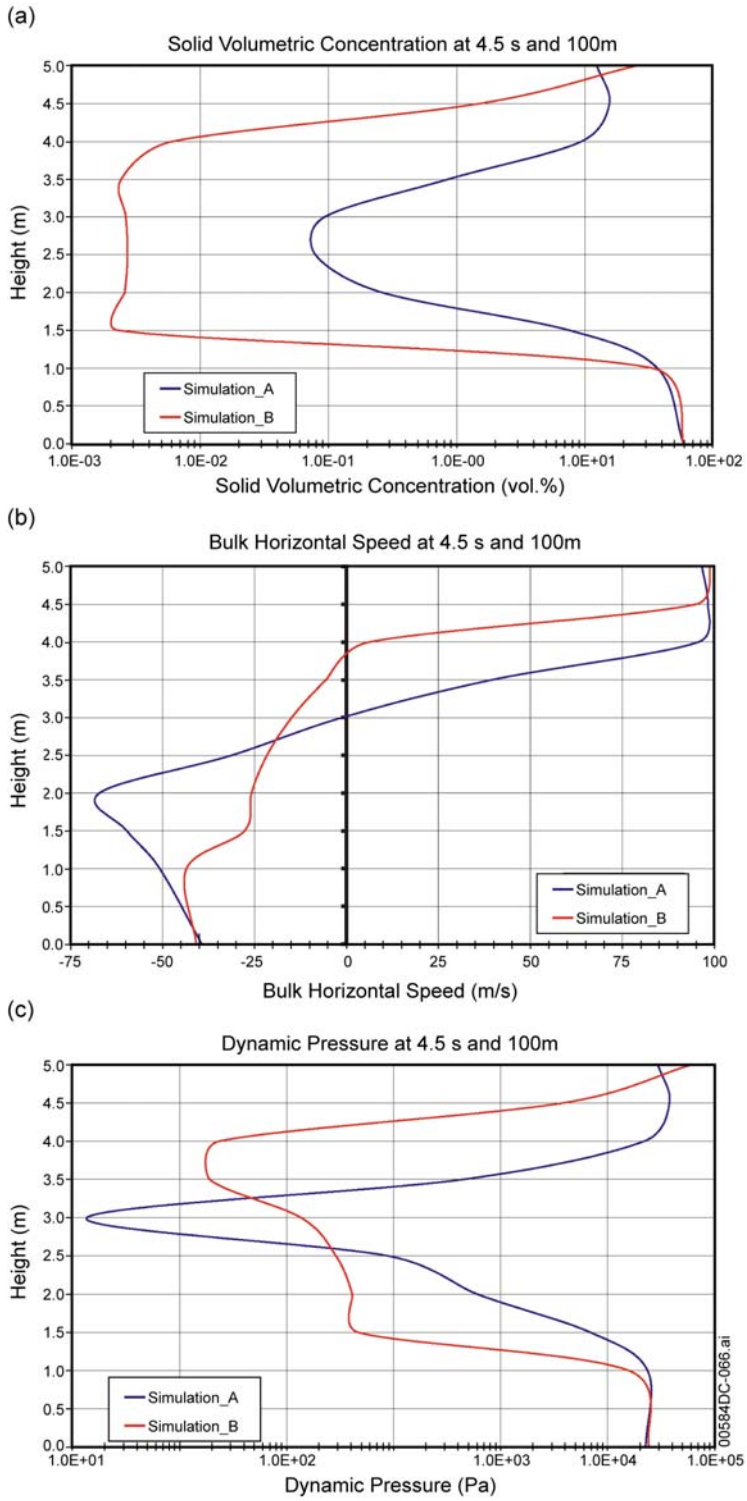

NOTE: (a) Volumetric solid concentration [vol %], (b) Horizontal speed [m/s], and (c) Dynamic pressure [Pa] versus height [m]. For illustration purposes only.

Figure 6-18. Vertical Profiles of Parameters Calculated at a Distance of 100 m away from the Dike (Blue Curve is Simulation A and Red Curve is Simulation B)

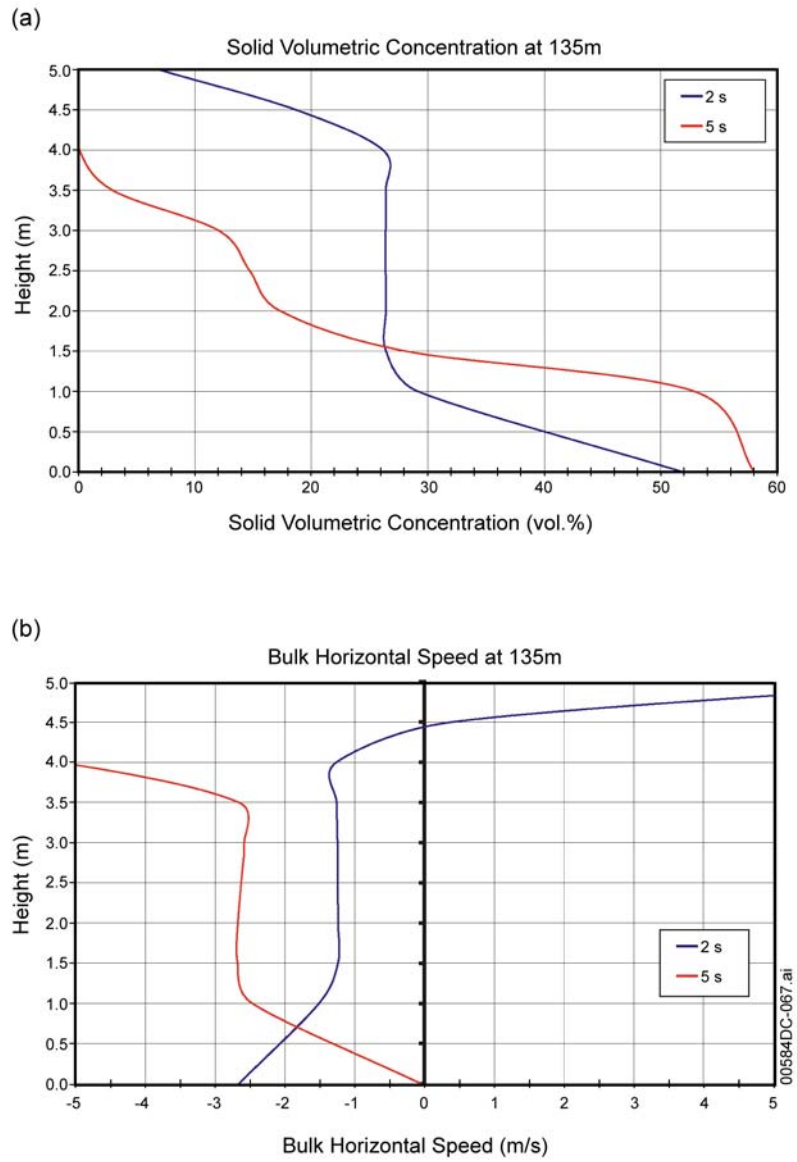

NOTE: (a) Volumetric concentration [vol %], (b) Bulk horizontal speed [m/s]. As the granular concentration gradually increases to 60 vol %, the horizontal speed of the granular flow dwindles to zero. For illustration purposes only.

Figure 6-19. Time Sequence at 2 s (Blue Curve) and 5 s (Red Curve) for Simulation A1, 135 m Down the Drift from the Dike

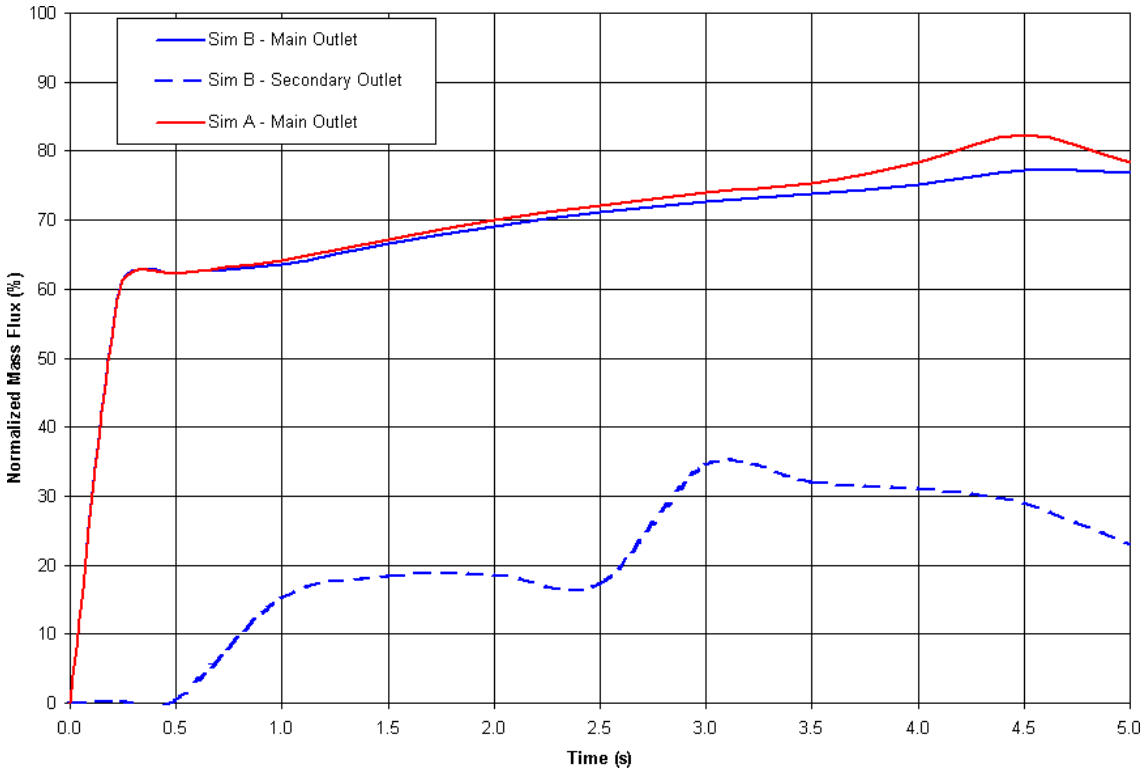

NOTE: Red curve for Simulation A; blue curves for Simulation B with plain curve at the main outlet and dashed curve at the secondary outlet. For illustration purposes only.

Figure 6-20. Outlet Mass Flux Normalized by the Constant Inlet Mass Flux (182,124 kg/s/m) versus Time

INTENTIONALLY LEFT BLANK

7. CONCLUSIONS

This report describes intrusive and eruptive volcanic features at four analogue sites in Nevada and New Mexico. The sites represent a limited set of small-volume eruptions of basaltic magma that range in age from ~9 Ma to ~2 Ma, but which are suitably eroded and incised to provide observations of their subvolcanic structures. The following broad conclusions, detailed in Section 6.2, derive from those observations:

- In some basaltic volcanic settings, the vent diameter (or width in the case of fissure eruptions) decreases with depth from many tens of meters down to the width of the deeper feeder dikes above a depth which would be comparable to repository depth.

- Analogue studies show that complexity of subvolcanic intrusive structures (number of dikes and dikelets, bifurcations, crosscutting dikes, sills, etc.) increases up-section toward the Earth's surface and may be limited to less than ~200-m to 250-m depth for small-volume systems.

- Orientations of multiple dike intrusions in an area with a pre-existing structural grain (faults) may tend to follow that grain but are not restricted in azimuth or width, particularly on a small scale.

- Thin dikes, which may generally be parallel to structural grain, can converge over short distances to intersect and supply a conduit for continued, focused magma transport to the surface.

- Measurements of analogue subsurface volcanic features (Section 6.2) corroborate the distributions given in *Characterize Eruptive Processes at Yucca Mountain, Nevada*, (BSC 2004 DIRS 169980]), including dike width, dike spacing, and number of dikes in a set. Conduit diameter is also corroborated, but the maximum diameter (150 m) may be exceeded at Paiute Ridge if the intruded, disturbed zone is included in the measurement (220 m × 110 m; Section 6.2.4).

This report also describes analyses of temporary blockages within subsurface magmatic pathways and the accompanying increases in magmatic pressures that might result in a secondary breakout of magma. Breakout is defined as initiating a crack or pathway within the surrounding host rock (either tuff, basalt, or scoria) as determined by magma pressures exceeding the tensile strength of basalt, under the conditions specified in Section 6.3. These analyses explore scenarios that could occur during the full duration of an igneous event. Conclusions derived from these analyses include:

- In the majority of cases analyzed for blockage caused by slumping of scoria into an active vent, breakout may occur by hydrofracture of the conduit walls at a magma pressure of approximately 10 MPa before a potentially more-explosive uplift of the scoria plug.

- If hydrofracture is inhibited (for example, by a zone of plastically deformable warm basalt), magma pressures may be considerably higher and catastrophic failure of the scoria cone may result in accelerations sufficient to initiate ballistic trajectories.

- Breakout from a blockage formed by solidification of magma in a conduit beneath a lava flow is also likely to occur by hydrofracture at similar pressures.

- If a dike is interrupted by an active fault, magma is likely to follow the fault plane toward the surface with magma pressures only a few tenths MPa above those pressures driving the original flow in the dike.

- Magma injected into a centimeter-scale crack to initiate a secondary path to the surface will freeze in the crack in less than 100 s, which precludes further propagation. Freezing within the crack occurs approximately 15 percent sooner if the surrounding rock is cold than if the rock has been preheated by intrusion to 300°C.

Also, this report describes calculations which explore the intersection of a pressurized volatile-rich magma with a drift at atmospheric pressure and the resulting pyroclastic expansion into the drift. Broad conclusions from these analyses include:

- For the abrupt initial conditions analyzed, initial intersection of a volatile-rich magma front with an open drift results in rapid expansion with a shock wave traveling down the drift ahead of a pyroclastic flow front.

- If the main dike continues to the Earth's surface, providing an open pathway above the drift, the majority of the pyroclastic material with flow up that path and the amount that flows into the drift is greatly reduced compared to a situation where the vertical dike pathway terminates at the drift.

- In a situation where the main dike provides a pathway above the drift, a secondary opening at some distance down-drift has negligible effect on the flow field; the opening is not very susceptible to becoming a secondary path for two-phase flow to the surface and the fraction of flow into a secondary opening of realistic width will be less than one percent.

- Decompression of a magma-filled dike-drift system by the removal of blockage above repository level is not strongly influenced by the presence of a secondary opening some distance down drift from the main dike.

The results above provide further insight for understanding other reports on the effects of potential igneous intrusion activity at Yucca Mountain.

- Calculated magma pressures necessary to initiate hydrofracture after scoria cone slumping or magma solidification, as defined in Section 6.3.1 and Section 6.3.1.3, are similar to pressures used in the analysis of secondary breakout pressures in *Dike/Drift Interactions* (BSC 2004 [DIRS 170028], Section 6.5.1). However, when the additional

hydrostatic head at repository depth is considered, the range of pressures addressed in BSC (2004 [DIRS 170028], Section 6.5.1) may be too small by a factor of two or three.

- When magma breakout is associated with deformation of the entire scoria plug, as defined in Section 6.3.1 and Section 6.3.1.3, magma pressures calculated here may be over three times those used in analysis of breakout pressures in *Dike/Drift Interactions* (BSC 2004 [DIRS 170028], Section 6.5.1).

- Blockage of magma flow caused by a fault cutting an active dike, also defined in Section 6.3.1 and Section 6.3.1.3, can result in diversion of magma flow upward along the fault plane. The rise in magma pressure beneath the fault necessary before flow is initiated is similar to that observed in *Dike Drift Interactions* (BSC 2004 [DIRS 170028], Section 6.5.1).

- Results of the Simulation A1 for drift decompression of pyroclastic flow show that the approach used in *Number of Waste Packages Hit by Igneous Intrusion* (BSC 2005 [DIRS 174066]) is viable for the conditions described here. Specifically, the number of waste packages erupted is probably not increased by a temporary blockage and sudden release in the magmatic path to the surface.

7.1 PRODUCT OUTPUT

There is no product output from this analysis report because of the descriptive nature of analogue studies and the specific focus of the numerical analyses. The analogues provide basis for potential scenarios of shallow magma emplacement and eruptive phenomena, while the analyses advance aspects of the numerical work reported in *Dike/Drift Interactions* (BSC 2004 [DIRS 170028]). As described in Section 1.2, this report is intended as an exploration of potential consequences that could occur during an igneous event. Limitations to the uses of the results of this analysis report are discussed in Section 1.4.

INTENTIONALLY LEFT BLANK

8. INPUTS AND REFERENCES

8.1 DOCUMENTS CITED

BSC (Bechtel SAIC Company) 2003. *Dike/Drift Interactions.* MDL-MGR-GS-000005 REV 00. Las Vegas, Nevada: Bechtel SAIC Company. ACC: DOC.20031022.0001. 165923

BSC 2004. *Characterize Eruptive Processes at Yucca Mountain, Nevada.* ANL-MGR-GS-000002 REV 02. Las Vegas, Nevada: Bechtel SAIC Company. ACC: DOC.20041004.0006; DOC.20050718.0005. 169980

BSC 2004. *Characterize Framework for Igneous Activity at Yucca Mountain, Nevada.* ANL-MGR-GS-000001 REV 02. Las Vegas, Nevada: Bechtel SAIC Company. ACC: DOC.20041015.0002. 169989

BSC 2004. *Dike/Drift Interactions.* MDL-MGR-GS-000005 REV 01. Las Vegas, Nevada: Bechtel SAIC Company. ACC: DOC.20041124.0002; DOC.20050622.0002. 170028

BSC 2004. *Drift Degradation Analysis.* ANL-EBS-MD-000027 REV 03. Las Vegas, Nevada: Bechtel SAIC Company. ACC: DOC.20040915.0010; DOC.20050419.0001. 166107

BSC 2004. *Heat Capacity Analysis Report.* ANL-NBS-GS-000013 REV 01. Las Vegas, Nevada: Bechtel SAIC Company. ACC: DOC.20041101.0003. 170003

BSC 2004. *Thermal Conductivity of the Potential Repository Horizon.* MDL-NBS-GS-000005 REV 01. Las Vegas, Nevada: Bechtel SAIC Company. ACC: DOC.20040928.0006. 169854

BSC 2004. *Yucca Mountain Site Description.* TDR-CRW-GS-000001 REV 02 ICN 01. Two volumes. Las Vegas, Nevada: Bechtel SAIC Company. ACC: DOC.20040504.0008. 169734

BSC 2005. *Number of Waste Packages Hit by Igneous Intrusion.* ANL-MGR-GS-000003 REV 02. Las Vegas, Nevada: Bechtel SAIC Company. 174066

BSC 2005. *Q-List.* 000-30R-MGR0-00500-000-002. Las Vegas, Nevada: Bechtel SAIC Company. ACC: ENG.20050805.0006. 174269

BSC 2005. *Technical Work Plan for: Igneous Activity Assessment for Disruptive Events.* TWP-WIS-MD-000007 REV 08. Las Vegas, Nevada: Bechtel SAIC Company. ACC: DOC.20050815.0001. 174773

Byers, F.M., Jr. and Barnes, H. 1967. *Geologic Map of the Paiute Ridge Quadrangle, Nye and Lincoln Counties, Nevada.* Map GQ-577. Washington, D.C.: U.S. Geological Survey. ACC: HQS.19880517.1104. 101859

Byers, F.M., Jr.; Carr, W.J.; Orkild, P.P.; Quinlivan, W.D.; and Sargent, K.A. 1976. *Volcanic Suites and Related Cauldrons of Timber Mountain-Oasis Valley Caldera Complex, Southern Nevada.* Professional Paper 919. Washington, D.C.: U.S. Geological Survey. TIC: 201146. 104639

Canori, G.F. and Leitner, M.M. 2003. *Project Requirements Document.* TER-MGR-MD-000001 REV 02. Las Vegas, Nevada: Bechtel SAIC Company. ACC: DOC.20031222.0006. 166275

Carter Krogh, K.E. and Valentine, G.A. 1996. *Structural Control on Basaltic Dike and Sill Emplacement, Paiute Ridge Mafic Intrusion Complex, Southern Nevada.* LA-13157-MS. Los Alamos, New Mexico: Los Alamos National Laboratories. ACC: MOL.20030828.0138. 160928

Christiansen, R.L.; Lipman, P.W.; Carr, W.J.; Byers, F.M., Jr.; Orkild, P.P.; and Sargent, K.A. 1977. "The Timber Mountain-Oasis Valley Caldera Complex of Southern Nevada." *Geological Society of America Bulletin, 88,* (7), 943-959. Boulder, Colorado: Geological Society of America. TIC: 201802. 157236

Crowe, B.; Self, S.; Vaniman, D.; Amos, R.; and Perry, F. 1983. "Aspects of Potential Magmatic Disruption of a High-Level Radioactive Waste Repository in Southern Nevada." *Journal of Geology, 91,* (3), 259-276. Chicago, Illinois: University of Chicago Press. TIC: 216959. 100972

Crumpler, L.S. 1980. "An Alkali-Basalt through Trachyte Suite, Mesa Chivato Mount Taylor Volcanic Field, New Mexico: Summary." *Geological Society of America Bulletin, Part I, 91,* (1), 253-255. Boulder, Colorado: Geological Society of America. TIC: 257320. 173900

Crumpler, L.S. 2003. "Natural Scoria Cone Half-Section, East Grants Ridge: A Test of Basalt Pyroclastic Eruption Models." *Geology of the Zuni Plateau, New Mexico Geological Society Fifty-Fourth Annual Field Conference, September 24-27, 2003.* Lucas, S.G., Semken, S.C., Berglof, W.R., and Ulmer-Scholle, D.S., eds. Pages 155-164. Socorro, New Mexico: New Mexico Geological Society. TIC: 257282. 174074

CRWMS M&O 1996. *Probabilistic Volcanic Hazard Analysis for Yucca Mountain, Nevada.* BA0000000-01717-2200-00082 REV 0. Las Vegas, Nevada: CRWMS M&O. ACC: MOL.19971201.0221. 100116

CRWMS M&O 1997. *Yucca Mountain Site Geotechnical Report.* B00000000-01717-5705-00043 REV 01. Two volumes. Las Vegas, Nevada: CRWMS M&O. ACC: MOL.19971017.0736; MOL.19971017.0737. 103564

CRWMS M&O 1999. *TBV-332/TBD-325 Resolution Analysis: Geotechnical Rock Properties.* B00000000-01717-5705-00134 REV 00. Las Vegas, Nevada: CRWMS M&O. ACC: MOL.19991005.0235. 126475

Dartevelle, S. 2004. "Numerical Modeling of Geophysical Granular Flows: 1. A Comprehensive Approach to Granular Rheologies and Geophysical Multiphase Flows." *Geochemistry Geophysics Geosystems, 5,* (8), 1-28. Washington, D.C.: American Geophysical Union. TIC: 257366. 174132

Dartevelle, S.; Rose, W.I.; Stix, J.; Kelfoun, K.; and Vallance, J.W. 2004. "Numerical Modeling of Geophysical Granular Flows: 2. Computer Simulations of Plinian Clouds and Pyroclastic Flows and Surges." *Geochemistry Geophysics Geosystems, 5,* (8), 1-36. Washington, D.C.: American Geophysical Union. TIC: 257405. 174139

Detournay, E.; Mastin, L.G.; Pearson, J.R.A.; Rubin, A.M.; and Spera, F.J. 2003. *Final Report of the Igneous Consequences Peer Review Panel, with Appendices.* Las Vegas, Nevada: Bechtel SAIC Company. ACC: MOL.20031014.0097; MOL.20030730.0163. 169660

DOE (U.S. Department of Energy) 2004. *Quality Assurance Requirements and Description.* DOE/RW-0333P, Rev. 16. Washington, D.C.: U.S. Department of Energy, Office of Civilian Radioactive Waste Management. ACC: DOC.20040907.0002. 171539

Duncan, J.M.; Byrne, P.; Wong, K.S.; and Mabry, P. 1980. *Strength, Stress-Strain and Bulk Modulus Parameters for Finite Element Analyses of Stresses and Movements in Soil Masses.* UCB/GT/80-01. Berkeley, California: University of California, College of Engineering, Office of Research Services. TIC: 253873. 161776

EPRI (Electric Power Research Institute) 2004. *Potential Igneous Processes Relevant to the Yucca Mountain Repository: Extrusive-Release Scenario.* EPRI TR-1008169. Palo Alto, California: Electric Power Research Institute. TIC: 256654. 171915

Gupta, A.S. and Rao, K.S. 2000. "Weathering Effects on the Strength and Deformational Behaviour of Crystalline Rocks under Uniaxial Compression State." *Engineering Geology, 56,* 257-274. New York, New York: Elsevier. TIC: 257315. 174063

Hoek, E. and Brown, E.T. 1997. "Practical Estimates of Rock Mass Strength." *International Journal of Rock Mechanics and Mining Science & Geomechanics Abstracts, 34,* (8), 1165-1186. Oxford, England: Pergamon. TIC: 256245. 170501

Incropera, F.P. and DeWitt, D.P. 2002. *Fundamentals of Heat and Mass Transfer.* 5th Edition. New York, New York: John Wiley & Sons. TIC: 254280. 163337

Keating, G. 2005. Volcanological Investigations. Scientific Notebook: SN-LANL-SCI-311-V1 [partial submittal]. Pages TOC - 5, 8-59 and 62-82. ACC: MOL.20050622.0222; MOL.20050810.0012; MOL.20050808.0238. 174988

Keating, G.N. and Valentine, G.A. 1998. "Proximal Stratigraphy and Syn-Eruptive Faulting in Rhyolitic Grants Ridge Tuff, New Mexico, USA." *Journal of Volcanology and Geothermal Research, 81,* 37-49. Amsterdam, The Netherlands: Elsevier. TIC: 246096. 111236

Keating, G.N.; Geissman, J.W.; and Zyvoloski, G.A. 2002. "Multiphase Modeling of Contact Metamorphic Systems and Application to Transitional Geomagnetic Fields." *Earth and Planetary Science Letters, 198,* 429-448. New York, New York: Elsevier. TIC: 257642. 174077

Kokajko, L.E. 2005. "Staff Review of U.S. Department of Energy Response to Igneous Activity Agreement Item IA.2.18." Letter from L.E. Kokajko (NRC) to J.D. Ziegler (DOE/ORD), January 10, 2005, 01108054475, with enclosure. ACC: MOL.20050211.0288. 174026

Krier, D.J. 2005. Ash Redistribution, Lava Morphology, and Igneous Processes Studies [final submittal]. Scientific Notebook SN-LANL-SCI-286-V2. Pages TOC-152. ACC: MOL.20050718.0148. 174079

Laughlin, A.W.; Perry, F.V.; Damon, P.E.; Shafiqullah, M.; WoldeGabriel, G.; McIntosh, W.; Harrington, C.D.; Wells, S.G.; and Drake, P.G. 1993. "Geochronology of Mount Taylor, Cebollita Mesa, and Zuni-Bandera Volcanic Fields, Cibola County, New Mexico." *New Mexico Geology, 15,* (4), 81-92. Socorro, New Mexico: New Mexico Bureau of Mines and Mineral Resources. TIC: 225061. 174240

Lipman, P.W.; Christiansen, R.L.; and O'Connor, J.T. 1966. *A Compositionally Zoned Ash-Flow Sheet in Southern Nevada.* Professional Paper 524-F. Washington, D.C.: U.S. Geological Survey. TIC: 219972. 100773

Marachi, N.D.; Chan, C.K.; and Seed, H.B. 1972. "Evaluation of Properties of Rockfill Materials." *Journal of the Soil Mechanics and Foundations Division, Proceedings of the American Society of Civil Engineers, 98,* (SM1), 95-114. New York, New York: American Society of Civil Engineers. TIC: 252235. 157883

Nicholis, M.G. and Rutherford, M.J. 2004. "Experimental Constraints on Magma Ascent Rate for the Crater Flat Volcanic Zone Hawaiite." *Geology, 32,* (6), 489-492. Boulder, Colorado: Geological Society of America. TIC: 256878. 173945

NRC (U.S. Nuclear Regulatory Commission) 1998. *Issue Resolution Status Report Key Technical Issue: Igneous Activity.* Rev. 0. Washington, D.C.: U.S. Nuclear Regulatory Commission. ACC: MOL.19980514.0576. 100297

NRC 2002. *Integrated Issue Resolution Status Report.* NUREG-1762. Washington, D.C.: U.S. Nuclear Regulatory Commission, Office of Nuclear Material Safety and Safeguards. TIC: 253064. 159538

NRC 2003. *Yucca Mountain Review Plan, Final Report.* NUREG-1804, Rev. 2. Washington, D.C.: U.S. Nuclear Regulatory Commission, Office of Nuclear Material Safety and Safeguards. TIC: 254568. 163274

Orkild, P.P.; Sargent, K.A.; and Snyder, R.P. 1969. *Geologic Map of Pahute Mesa, Nevada Test Site and Vicinity, Nye County, Nevada.* Miscellaneous Geologic Investigations Map I-567. Washington, D.C.: U.S. Geological Survey. TIC: 217639. 106460

Perry, F.V.; Baldridge, W.S.; DePaolo, D.J.; and Shafiqullah, M. 1990. "Evolution of a Magmatic System During Continental Extension: The Mount Taylor Volcanic Field, New Mexico." *Journal of Geophysical Research, 95,* (B12), 19,327-19,348. Washington, D.C.: American Geophysical Union. TIC: 257257. 173994

Perry, F.V.; Crowe, B.M.; Valentine, G.A.; and Bowker, L.M., eds. 1998. *Volcanism Studies: Final Report for the Yucca Mountain Project.* LA-13478. Los Alamos, New Mexico: Los Alamos National Laboratory. TIC: 247225. 144335

Ratcliff, C.D.; Geissman, J.W.; Perry, F.V.; Crowe, B.M.; and Zeitler, P.K. 1994. "Paleomagnetic Record of a Geomagnetic Field Reversal from Late Miocene Mafic Intrusions, Southern Nevada." *Science, 266,* 412-416. Washington, D.C.: American Association for the Advancement of Science. TIC: 234818. 106634

Reamer, C.W. 1999. "Issue Resolution Status Report (Key Technical Issue: Igneous Activity, Revision 2)." Letter from C.W. Reamer (NRC) to Dr. S. Brocoum (DOE/YMSCO), July 16, 1999, with enclosure. ACC: MOL.19990810.0639. 119693

Reamer, C.W. 2001. "U.S. Nuclear Regulatory Commission/U.S. Department of Energy Technical Exchange and Management Meeting on Igneous Activity (September 5, 2001)." Letter from C.W. Reamer (NRC) to S. Brocoum (DOE/YMSCO), September 12, 2001, with enclosure. ACC: MOL.20011114.0008. 159894

Rocchi, V.; Sammonds, P.R.; and Kilburn, C.R.J. 2004. "Fracturing of Etnean and Vesuvian Rocks at High Temperatures and Low Pressures." *Journal of Volcanology and Geothermal Research, 132,* 137-157. New York, New York: Elsevier. TIC: 257313. 173995

Sagar, B., ed. 1997. *NRC High-Level Radioactive Waste Program Annual Progress Report: Fiscal Year 1996.* NUREG/CR-6513, No. 1. Washington, D.C.: U.S. Nuclear Regulatory Commission. ACC: MOL.19970715.0066. 145235

Schlueter, J.R. 2003. "Igneous Activity Agreement 2.09, Additional Information Needed." Letter from J.R. Schlueter (NRC) to J.D. Ziegler (DOE/ORD), March 25, 2003, 0331036684, with enclosure. ACC: MOL.20031009.0249. 165740

Slate, J.L.; Berry, M.E.; Rowley, P.D.; Fridrich, C.J.; Morgan, K.S.; Workman, J.B.; Young, O.D.; Dixon, G.L.; Williams, V.S.; McKee, E.H.; Ponce, D.A.; Hildenbrand, T.G.; Swadley, W C; Lundstrom, S.C.; Ekren, E.B.; Warren, R.G.; Cole, J.C.; Fleck, R.J.; Lanphere, M.A.; Sawyer, D.A.; Minor, S.A.; Grunwald, D.J.; Laczniak, R.J.; Menges, C.M.; Yount, J.C.; Jayko, A.S.; Mankinen, E.A.; Davidson, J.G.; Morin, R.L.; and Blakely, R.J. 2000. *Digital Geologic Map of the Nevada Test Site and Vicinity, Nye, Lincoln and Clark Counties, Nevada, and Inyo County, California, Revision 4; Digital Aeromagnetic Map of the Nevada Test Site and Vicinity, Nye, Lincoln, and Clark Counties, Nevada, and Inyo County, California; and Digital Isostatic Gravity Map of the Nevada Test Site and Vicinity, Nye, Lincoln, and Clark Counties, Nevada, and Inyo County, California.* Open-File Report 99-554—A, —B, and —C. Denver, Colorado: U.S. Geological Survey. TIC: 248049; 251985; 251981. 150228

Thaden, R.E.; Santos, E.S.; and Raup, O.B. 1967. *Geologic Map of the Grants Quadrangle, Valencia County, New Mexico.* GQ-681. Washington, D.C.: U.S. Geological Survey. On Order 174076

Timoshenko, S.P. and Goodier, J.N. 1970. *Theory of Elasticity.* 3rd Edition. New York, New York: McGraw-Hill. TIC: 245469. 121096

Valentine, G.A.; WoldeGabriel, G.; Rosenberg, N.D.; Carter Krogh, K.E.; Crowe, B.M.; Stauffer, P.; Auer, L.H.; Gable, C.W.; Goff, F.; Warren, R.; and Perry, F.V. 1998. "Physical Processes of Magmatism and Effects on the Potential Repository: Synthesis of Technical Work Through Fiscal Year 1995." Chapter 5 of *Volcanism Studies: Final Report for the Yucca Mountain Project.* Perry, F.V.; Crowe, B.M.; Valentine, G.A.; and Bowker, L.M., eds. LA-13478. Los Alamos, New Mexico: Los Alamos National Laboratory. TIC: 247225. 119132

WoldeGabriel, G.; Keating, G.N.; and Valentine, G.A. 1999. "Effects of Shallow Basaltic Intrusion into Pyroclastic Deposits, Grants Ridge, New Mexico, USA." *Journal of Volcanology and Geothermal Research, 92,* (3), 389-411. New York, New York: Elsevier. TIC: 246037. 110071

Woods, A.W.; Sparks, S.; Bokhove, O.; LeJeune, A-M.; Conner, C.B.; and Hill, B.E. 2002. "Modeling Magma-Drift Interaction at the Proposed High-Level Radioactive Waste Repository at Yucca Mountain, Nevada, USA." *Geophysical Research Letters, 29,* (13), 19-1 through 19-4. Washington, D.C.: American Geophysical Union. TIC: 254467. 163662

8.2 CODES, STANDARDS, REGULATIONS, AND PROCEDURES

10 CFR 63. 2005 Energy: Disposal of High-Level Radioactive Wastes in a Geologic Repository at Yucca Mountain, Nevada. ACC: MOL.20050405.0118. 173273

40 CFR 197. 2004 Protection of Environment: Public Health and Environmental Radiation Protection Standards for Yucca Mountain, Nevada: ACC: MOL.20050324.0101. 173176

LP-2.12Q-BSC, Rev. 0, ICN 0. *Peer Review.* Washington, D.C.: U.S. Department of Energy, Office of Civilian Radioactive Waste Management. ACC: DOC.20050113.0008.

AP-2.22Q, Rev. 1, ICN 1. *Classification Analyses and Maintenance of the Q-List.* Washington, D.C.: U.S. Department of Energy, Office of Civilian Radioactive Waste Management. ACC: DOC.20040714.0002.

LP-SIII.9Q-BSC, Rev. 0, ICN 1. *Scientific Analyses.* Washington, D.C.: U.S. Department of Energy, Office of Civilian Radioactive Waste Management. ACC: DOC.20050622.0004.

LP-SI.11Q-BSC, Rev. 0, ICN 1. *Software Management.* Washington, D.C.: U.S. Department of Energy, Office of Civilian Radioactive Waste Management. ACC: DOC.20041005.0008.

8.3 SOURCE DATA, LISTED BY DATA TRACKING NUMBER

LA0407DK831811.001. Physical Parameters of Basaltic Magma and Eruption Phenomena. Submittal date: 07/15/2004. 170768

MO0403MWDRPNLR.000. Rock Properties for Nonlithophysal Rock. Submittal date: 03/31/2004. 168896

MO0411EG831811.000. Dike Propagation Model Results. Submittal date: 11/16/2004. 174959

MO0508SPAMAGMA.000. Magma Solidification Temperature. Submittal date: 08/16/2005. 175008

SNF37100195002.001. Hydraulic Fracturing Stress Measurements in Test Hole: ESF-AOD-HDFR1, Thermal Test Facility, Exploratory Studies Facility at Yucca Mountain. Submittal date: 12/18/1996. 131356

8.4 SOFTWARE CODES

BSC 2004. *Software Code: FLAC.* V4.04. PC, Windows 2000. STN: 10167-4.04-00. 172432

BSC 2004. *Software Code: UDEC.* V3.14. PC, WINDOWS 2000. STN: 10173-3.14-00. 172322

BSC 2005. *Software Code: GMFIX.* V1.61. PC, Windows XP. STN: 11192-1.61-00. 174137

APPENDIX A

YUCCA MOUNTAIN REVIEW PLAN ACCEPTANCE CRITERIA

APPENDIX A

YUCCA MOUNTAIN REVIEW PLAN ACCEPTANCE CRITERIA

A1. BACKGROUND

Early in 1995, the Nuclear Regulatory Commission (NRC) recognized the need to refocus its prelicensing repository program on resolving issues most significant to repository performance. In 1996, the NRC identified 10 key technical issues (Sagar 1997 [DIRS 145235]) intended to reflect the topics that the NRC considered most important to repository performance. Nine of the issues were technical, and the tenth concerned the development of the dose standard for a repository at Yucca Mountain (40 CFR Part 197 [DIRS 173176]). The technical issues included igneous activity, and the status of resolution of each issue and associated open items were described by the NRC in a series of issue resolution status reports (e.g., Reamer 1999 [DIRS 119693]). In 2002, the NRC consolidated the subissues into a series of integrated subissues and replaced the series of nine issue resolution status reports with *Integrated Issue Resolution Status Report* (NRC 2004 [DIRS 159538]). The integrated issue resolution status report was based on the realization that the issue resolution process was "mature enough to develop a single integrated issue resolution status report that would clearly and consistently reflect the interrelationships among the various key technical issue subissues and the overall resolution status" (NRC 2002 [DIRS 159538], pp. xviii and xix). *Integrated Issue Resolution Status Report* and periodic letters from the NRC (e.g., Schlueter 2003 [DIRS 165740]) provide information about the resolution status of the integrated subissues that are described in *Yucca Mountain Review Plan*, *Final Report* (NRC 2003 [DIRS 163274]).

A2. IGNEOUS ACTIVITY KEY TECHNICAL ISSUE

The key technical issue for igneous activity was defined by the NRC staff as "predicting the consequence and probability of igneous activity affecting the repository in relationship to the overall system performance objective" (NRC 1998 [DIRS 100297], p. 3). Hence, the NRC defined two subissues for the igneous activity key technical issue: probability and consequences (NRC 1998 [DIRS 100297], p. 3). The probability subissue addresses the likelihood that future igneous activity would disrupt a repository at Yucca Mountain. The DOE estimated the probability of future disruption of a repository at Yucca Mountain in *Probabilistic Volcanic Hazard Analysis for Yucca Mountain, Nevada* (CRWMS M&O 1996 [DIRS 100116]). For the TSPA for the license application, an analysis based on *Probabilistic Volcanic Hazard Analysis for Yucca Mountain, Nevada* (CRWMS M&O 1996 [DIRS 100116]) results and consideration of the repository LA design were both updated and documented in *Characterize Framework for Igneous Activity at Yucca Mountain, Nevada* (BSC 2004 [DIRS 169989], Section 6.3).

The consequences subissue examined the effects of igneous activity on various engineered and natural components of the repository system. The consequences subissue comprises four integrated subissues: mechanical disruption of engineered barriers (NRC 2003 [DIRS 163274] Section 2.2.1.3.2); volcanic disruption of waste packages (NRC 2003 [DIRS 163274] Section 2.2.1.3.10); airborne transport of radionuclides (NRC 2003 [DIRS 163274] Section 2.2.1.3.11); and redistribution of radionuclides in soil (NRC 2003 [DIRS 163274]

Section 2.2.1.3.13). This analysis report addresses selected aspects of the integrated subissues of mechanical disruption of engineered barriers (NRC 2003 [DIRS 163274], Section 2.3.1.3.2) that are concerned with multiphase magma flow. Also addressed are aspects of the integrated subissue of volcanic disruption of waste packages (NRC 2003 [DIRS 163274], Section 2.2.1.3.10) that are concerned with the potential for development of secondary conduits during the duration of an igneous event. The evaluation of the amount of damage to waste packages contacted by magma is addressed in *Dike/Drift Interactions* (BSC 2004 [DIRS 170028], Section 6.4.8), and *Number of Waste Packages Hit by Igneous Intrusion* (BSC 2004 [DIRS 174066], Sections 6.3 and 6.4).

A3. YUCCA MOUNTAIN REVIEW PLAN ACCEPTANCE CRITERIA

The YMRP (NRC 2003 [DIRS 163274]) specifies requirements for general information and for scenario analysis and event probability that are associated with regulatory requirements listed in 10 CFR 63.21(b)(5) and 10 CFR 63.114(d) [DIRS 173273]. The YMRP also associates the integrated subissues of mechanical disruption of engineered barriers and volcanic disruption of waste packages with the requirements listed in 10 CFR 63.114(a)-(c) and (e)-(g) [DIRS 173273]. The YMRP (NRC 2003 [DIRS 163274], Sections 2.2.1.3.2.3 and 2.2.1.3.10) describes the acceptance criteria that the NRC will use to evaluate the adequacy of information in the license application addressing the integrated subissues of mechanical disruption of engineered barriers and volcanic disruption of waste packages.

The information provided by this analysis report supplements the descriptions of eruptive volcanic processes that are described in *Characterize Eruptive Processes at Yucca Mountain, Nevada* (BSC 2004 [DIRS 169980]) and the potential interactions between a magmatic dike and various components of the engineered barrier system discussed in *Dike/Drift Interactions* (BSC 2004 [DIRS 170028], Sections 6.3 and 6.4). The analyses documented in this report describe the results of field analogue studies that have been undertaken to refine descriptions of volcanic processes, studies of the development of blockages in volcanic conduits and effects on the subsequent development of magma pathways, and evaluate the potential effects of multiphase magma flow.

Although not clearly described in the YMRP, the integrated issue resolution status report (NRC 2002 [DIRS 159538], Section 3.3.10.1, Paragraph 1) specifically notes, “Interactions between basaltic magma and waste packages not located along a subvolcanic conduit to the surface are evaluated in the Mechanical Disruption of Engineered Barriers Integrated Subissue” (Section 2.2.1.3.2).

A4. YUCCA MOUNTAIN REVIEW PLAN CRITERIA ASSESSMENT

The YMRP (NRC 2003 [DIRS 163274]) specifies requirements for general information and for scenario analysis and event probability that are at least partially addressed by information in this report. In addition, the NRC has identified two integrated subissues, mechanical disruption of engineered barriers and volcanic disruption of waste packages (NRC 2003 [DIRS 163274]) that are at least partially addressed by information in this report.

The YMRP (NRC 2003 [DIRS 163274]) provides the review methods and acceptance criteria that the NRC staff will use to evaluate the technical adequacy of the license application. The applicable acceptance criteria, which may also be addressed in other analysis and model reports, are fully addressed when this report is considered in conjunction with those reports.

A4.1 NUREG-1804, REV 2, SECTION 1.5.3: DESCRIPTION OF SITE CHARACTERIZATION WORK

Acceptance Criterion 2: The "General Information" Section of the License Application Contains an Adequate Description of Site Characterization Results

> *(2) Adequate information is provided for evolution of future events and processes likely to be present in the Yucca Mountain that could affect repository safety.*
>
> This report provides basic descriptive information about selected volcanic eruptive features and processes that are characteristic of the Yucca Mountain region, as exemplified by features observed at analogue sites including East Grants Ridge, New Mexico (Sections 6.2.1 and 6.2.2); and Paiute Ridge, Basalt Ridge, and Basalt Ridge East, Nevada (Sections 6.2.3 and 6.2.4). The analogue information provides the basis for comparisons of vent geometry and structure, and the potential for development of secondary vents (Section 6.2). The analyses documented in this report describe vent characteristics (Section 6.2), potential for blockage of vents, effects on development of magma pathways (Section 6.3), and potential for multiphase magma flow (Section 6.4). The analyses support the TSPA modeling of the direct-release and indirect-release volcanic scenarios for the duration of an igneous event.

A4.2 NUREG-1804, REV. 2, SECTION 2.2.1.2.1.3: SCENARIO ANALYSIS AND EVENT PROBABILITY

Acceptance Criterion 1: The Identification of a List of Features, Events, and Processes is Adequate

> *(1) The Safety Analysis Report contains a complete list of features, events, and processes, related to the geologic setting or the degradation, deterioration, or alteration of engineered barriers (including those processes that would affect the performance of natural barriers), that have the potential to influence repository performance. The list is consistent with the site characterization data. Moreover, the comprehensive features, events, and processes list includes, but is not limited to, potentially disruptive events related to igneous activity (extrusive and intrusive); seismic shaking (high-frequency-low magnitude, and rare large-magnitude events); tectonic evolution (slip on existing faults and formation of new faults); climatic change (change to pluvial conditions); and criticality.*
>
> Relevance of the analyses documented in this report to screening of features, events, and processes related to igneous activity at the site are described in Section 1.1. This analysis provides a summary of calculations developed to

quantify the response of emplacement drifts that have been filled with magma and repressurized.

Numerical analyses are presented that describe the possible pyroclastic flow of magma from a dike into an empty drift and determine the magma pressures needed for magma to break through or to go around a blockage in a dike or conduit above repository level. The pressure calculations provide input to a second series of numerical analyses conducted to estimate the flow fields of magma that might produce secondary dikes at distances removed from the initial intersection of a drift by a dike or conduit or that might draw magma from an emplacement drift into an erupting conduit, either of which could result in increased volumes of waste being released in a volcanic eruption.

This report provides information about specific features and processes that is used to develop parameters that support the TSPA model. Specific examples include vent geometry and structure and the potential for development of secondary vents (Section 6.2) that may be used in the analysis of the number of waste packages damaged in the eruption case. The report also describes the potential for blockage of a vent and the potential effects on the development of magma pathways (Section 6.3). This information is used to evaluate the potential for the development of a secondary pathway or dogleg in hot rock (Section 6.3). The analysis of multiphase magma flow provides basic information needed to evaluate the potential for a dike stopping once it has intersected a drift, continuing toward the surface along the original path (Sections 6.4.1 and 6.4.2), or developing a secondary dike following blockage of the pathway and subsequent disruption of the blockage or development of an alternate magma flow pathway (Section 6.4.2). All of these analyses contribute to the evaluation of the consequences of disruption of the repository by an igneous event for the duration of the event.

Acceptance Criterion 2: Screening of the List of Features, Events, and Processes is Appropriate

(1) The U.S. Department of Energy has provided justification for those features, events, and processes that have been excluded. An acceptable justification for excluding features, events, and processes is that either the feature, event and process is specifically excluded by regulation; probability of the feature, event, and process (generally an event) falls below the regulatory criterion; or omission of the feature, event, and process does not significantly change the magnitude and time of the resulting radiological exposures to the reasonably maximally exposed individual, or radionuclide releases to the accessible environment.

The magma dynamics analysis report provides inputs for other analyses, but does not provide the basis for any used to include or exclude features, events, and processes related to igneous activity at Yucca Mountain.

(2) The U.S. Department of Energy has provided an adequate technical basis for each feature, event, and process excluded from the performance assessment, to

support the conclusion that either the feature, event, or process is specifically excluded by regulation; the probability of the feature, event, and process falls below the regulatory criterion; or omission of the feature, event, and process does not significantly change the magnitude and time of the resulting radiological exposures to the reasonably maximally exposed individual, or radionuclide releases *to the accessible environment.*

The magma dynamics analysis report provides inputs for other analyses, but does not provide the basis for any used to include or exclude features, events, and processes related to igneous activity at Yucca Mountain.

A4.3 NUREG-1804, REV 2, SECTION 2.2.1.3.2.3: MECHANICAL DISRUPTION OF ENGINEERED BARRIERS

The following description identifies information from this report that addresses *Yucca Mountain Review Plan, Final Report* (NRC 2003 [DIRS 163274], Section 2.2.1.3.2.3) acceptance criteria and/or review methods related to the integrated subissue of mechanical disruption of engineered barriers.

Acceptance Criterion 1: System Description and Model Integration are Adequate

(1) Total system performance assessment adequately incorporates important design features, physical phenomena, and couplings, and uses consistent and appropriate assumptions throughout the mechanical disruption of engineered barrier abstraction process.

(2) The description of geological and engineering aspects of design features, physical phenomena, and couplings that may affect mechanical disruption of engineered barriers is adequate.

This report describes select physical phenomena and couplings that could occur if a potential future igneous event were to disrupt the repository. Analogue information provides a basis for constraints on vent geometry and structure and the potential for development of secondary vents (Section 6.2) that may be used in the analysis of the number of waste packages damaged in the eruption case. The report also describes the potential for blockage of a vent and the potential effects on the development of magma pathways (Section 6.3). This information is used to evaluate the potential for the development of a secondary pathway or dogleg in hot rock (Section 6.3). The analysis of multiphase magma flow provides basic information needed to evaluate the potential for a dike stopping once it has intersected a drift, continuing toward the surface along the original path (Section 6.4), or developing a secondary dike following blockage of the pathway and subsequent disruption of the blockage or development of an alternate magma flow pathway (Section 6.4). Characterization of these processes supports the evaluation of the potential for damaging waste packages in drifts that are not intersected by a dike (Zone 2). All of these analyses contribute to the evaluation

of the consequences of disruption of the repository by an igneous event for the duration of the event.

Acceptance Criterion 2: Data are Sufficient for Model Justification

(1) Geological and engineering values, used in the license application to evaluate mechanical disruption of engineered barriers, are adequately justified. Adequate descriptions of how the data were used and appropriately synthesized into the parameters are provided.

This report describes select physical phenomena and couplings that could occur if a potential future igneous event were to disrupt the repository. The report describes the potential for blockage of a vent and the potential effects on the development of magma pathways (Section 6.3). This information is used to evaluate the potential for the development of a secondary pathway or dogleg in hot rock (Section 6.3). The analysis of multiphase magma flow provides basic information needed to evaluate the potential for a dike stopping once it has intersected a drift, continuing toward the surface along the original path (Section 6.4), or developing a secondary dike following blockage of the pathway and subsequent disruption of the blockage or development of an alternate magma flow pathway (Section 6.4).

(2) Sufficient data have been collected on the geology of the natural system, engineering materials, and initial manufacturing defects to establish initial and boundary conditions for the total system performance abstraction of mechanical disruption of engineered barriers.

This report describes selected physical phenomena and couplings between processes that are characteristic of igneous events in the Yucca Mountain region and other analogue sites outside the region. The analogue information provides a basis for constraints on vent geometry and structure, and the potential for development of secondary vents (Section 6.2). Parameters describing vent characteristics (Section 6.2), analyses of potential blockage of vents and effects on development of magma pathways (Section 6.3), and multiphase magma flow potential (Section 6.4) are developed for use in analyses of igneous processes or as inputs to TSPA models that support the analysis of the direct-release and indirect-release volcanic scenarios. The report does not address characteristics of engineered materials and occurrence of initial manufacturing defects.

(3) Data on geology of the natural system, engineering materials, and initial manufacturing defects, used in the total system performance assessment abstraction, are based on appropriate techniques. These techniques may include laboratory experiments, site-specific field measurements, natural analog research, and process-level modeling studies. As appropriate, sensitivity or uncertainty analyses used to support the U.S. Department of Energy total system performance assessment abstraction are adequate to determine the possible need for additional data.

This report describes selected physical phenomena and couplings between processes that are characteristic of igneous events in the Yucca Mountain region and other analogue sites outside the region. The analogue information provides a basis for constraints on vent geometry and structure and the potential for development of secondary vents (Section 6.2.6). Parameters describing vent characteristics (Section 6.2.6), analyses of potential blockage of vents and effects on development of magma pathways (Section 6.3), and multiphase magma flow potential (Section 6.4) are developed for use in analyses of igneous processes or as inputs to TSPA models that support the analysis of the direct-release and indirect-release volcanic scenarios. The report does not address characteristics of engineered materials and occurrence of initial manufacturing defects.

Acceptance Criterion 3: Data Uncertainty is Characterized and Propagated Through the Model Abstraction

(1) Models use parameter values, assumed ranges, probability distributions, and bounding assumptions that are technically defensible, reasonably account for uncertainties, and variabilities, and do not result in an under-representation of risk.

This analysis report describes selected physical phenomena and couplings between processes that are characteristic of igneous events in the Yucca Mountain region and other analogue sites outside the region. The analogue information provides a basis for constraints on vent geometry and structure, and the potential for development of secondary vents (Section 6.2). Parameters describing vent characteristics (Section 6.2), analyses of potential blockage of vents and effects on development of magma pathways (Section 6.3), and multiphase magma flow potential (Section 6.4) are developed for use in analyses of igneous processes or as inputs to TSPA models that support the analysis of the direct-release and indirect-release volcanic scenarios for the duration of a potential future igneous event. The report does not discuss the specific uses of the parameters in the downstream models, nor does the report discuss potential effects of parameter variations on the representation of risk.

(2) Process-level models used to represent mechanically disruptive events within the emplacement drifts at the proposed Yucca Mountain repository are adequate. Parameter values are adequately constrained by Yucca Mountain site data, such that the estimates of mechanically disruptive events on engineered barrier integrity are not underestimated. Parameters within conceptual models for mechanically disruptive events are consistent with the range of characteristics observed at Yucca Mountain.

This report describes select physical phenomena and couplings that could occur if a potential future igneous event were to disrupt the repository. The report describes the potential for blockage of a vent and the potential effects on the development of magma pathways (Section 6.3). This information is used to evaluate the potential for the development of a secondary pathway or dogleg in

hot rock (Section 6.3). The analysis of multiphase magma flow provides basic information needed to evaluate the potential for a dike stopping once it has intersected a drift, continuing toward the surface along the original path (Section 6.4), or developing a secondary dike following blockage of the pathway and subsequent disruption of the blockage or development of an alternate magma flow pathway (Section 6.4).

(3) Uncertainty is adequately represented in parameter development for conceptual models, process-level models, and alternative conceptual models considered in developing the assessment abstraction of mechanical disruption of engineered barriers. This may be done either through sensitivity analyses or use of conservative limits.

Uncertainties in field analogue measurements are discussed in Section 6.2. Uncertainties related to the analyses documented in this report are described in Sections 6.3 and 6.4.

Acceptance Criterion 4: Model Uncertainty is Characterized and Propagated Through the Model Abstraction

Acceptance Criterion 4(1) and (3) are not applicable because no alternative modeling approaches are developed in this report and no model abstractions are developed. Acceptance Criterion 4(2) is applicable because this report describes information that has been collected through studies at analogue sites from the Yucca Mountain region and elsewhere, and investigated through numerical analysis of specific scenarios of volcanic phenomena that could occur during an igneous event. By comparing focused analogue data with existing data, and by examining parameter ranges in the numerical analyses (e.g., magma pressures, magma breakout, pyroclastic flow dynamics), this report addresses some model and parameter uncertainties of downstream models. The report identifies information that has been collected from the Yucca Mountain region as well as information that has been developed from studies at analogue sites. Data uncertainties for inputs to, and outputs from, this analysis and limitations on use of outputs are described in detail in Sections 4 and 6. However, this report does not discuss the specific uses of the parameters in the downstream models, nor does the report discuss potential effects of parameter variations on the representation of risk.

(1) Alternative modeling approaches of features, events, and processes are considered and are consistent with available data and current scientific understanding, and the results and limitations are appropriately considered in the abstraction.

(2) Consideration of conceptual model uncertainty is consistent with available site characterization data, laboratory experiments, field measurements, natural analog information and process-level modeling studies; and the treatment of conceptual model uncertainty does not result in an under-representation of the risk estimate.

Uncertainties in field analogue measurements are discussed in Section 6.2. Uncertainties related to the analyses documented in this report are described in Sections 6.3 and 6.4.

A4.4 NUREG-1804, REV 2, SECTION 2.2.1.3.10.3: VOLCANIC DISRUPTION OF WASTE PACKAGES

Acceptance Criterion 1: System Description and Model Integration Are Adequate

(1) Total system performance assessment adequately incorporates important design features, physical phenomena, and couplings, and uses consistent and appropriate assumptions throughout the volcanic disruption of waste package abstraction process.

This report describes selected physical phenomena and couplings between processes that are characteristic of igneous events in the Yucca Mountain region and other analogue sites outside the region. The analogue information provides the basis for comparisons of vent geometry and structure, and the potential for development of secondary vents (Section 6.2). Parameters describing vent characteristics (Section 6.2), analyses of potential blockage of vents and effects on development of magma pathways (Section 6.3), and multiphase magma flow potential (Section 6.4) are developed and could be used in analyses of igneous processes or as inputs to TSPA models that support the analysis of the direct-release and indirect-release volcanic scenarios for the duration of a potential future igneous event.

(2) Models used to assess volcanic disruption of waste packages are consistent with physical processes generally interpreted from igneous features in the Yucca Mountain region and/or observed in active igneous systems.

This report provides basic descriptive information about selected volcanic eruptive features and processes that are characteristic of the repository, as exemplified by features observed at analogue sites including East Grants Ridge, New Mexico (Section 6.2); Paiute Ridge and Basalt Ridge, Nevada (Section 6.2). The analogue information provides the basis for comparisons of vent geometry and structure, and the potential for development of secondary vents (Section 6.2). The report describes the potential for blockage of a vent and the potential effects on the development of magma pathways (Section 6.3). This information is used to evaluate the potential for the development of a secondary pathway or dogleg in hot rock (Section 6.3). The analysis of multiphase magma flow provides basic information needed to evaluate the potential for a dike stopping once it has intersected a drift, continuing toward the surface along the original path (Section 6.4), or developing a secondary dike following blockage of the pathway and subsequent disruption of the blockage or development of an alternate magma flow pathway (Section 6.4).

(3) Models account for changes in igneous processes that may occur from interaction with engineered repository systems.

The report describes the potential for blockage of a vent and the potential effects on the development of magma pathways (Section 6.4). This information is used to evaluate the potential for the development of a secondary pathway or dogleg in hot rock (Section 6.3). The analysis of multiphase magma flow provides basic information needed to evaluate the potential for a dike stopping once it has intersected a drift, continuing toward the surface along the original path (Section 6.4), or developing a secondary dike following blockage of the pathway and disruption of the blockage or development of an alternate magma flow pathway (Section 6.4).

Acceptance Criterion 2: Data Are Sufficient For Model Justification

(1) Parameter values used in the license application to evaluate volcanic disruption of waste packages are sufficient and adequately justified. Adequate descriptions of how the data were used, interpreted, and appropriately synthesized into the parameters are provided.

This report provides basic descriptive information about selected volcanic eruptive features and processes that are characteristic of the repository, as exemplified by features observed at analogue sites including East Grants Ridge, New Mexico (Section 6.2); Paiute Ridge and Basalt Ridge, Nevada (Section 6.2). The analogue information provides the basis for comparisons of vent geometry and structure, and the potential for development of secondary vents (Section 6.2). The report describes the potential for blockage of a vent and the potential effects on the development of magma pathways (Section 6.3). This information is used to evaluate the potential for the development of a secondary pathway or dogleg in hot rock (Section 6.3). The analysis of multiphase magma flow provides basic information needed to evaluate the potential for a dike stopping once it has intersected a drift, continuing toward the surface along the original path (Section 6.4), or developing a secondary dike following blockage of the pathway and subsequent disruption of the blockage or development of an alternate magma flow pathway (Section 6.4).

(2) Data used to model processes affecting volcanic disruption of waste packages are derived from appropriate techniques. These techniques may include site-specific field measurements, natural analog investigations, and laboratory experiments.

This report provides basic descriptive information about selected volcanic eruptive features and processes that are characteristic of the repository, as exemplified by features observed at analogue sites including East Grants Ridge, New Mexico (Section 6.4); and Paiute Ridge and Basalt Ridge, Nevada (Section 6.2). The analogue information provides the basis for comparisons of

vent geometry and structure, and the potential for development of secondary vents (Section 6.2.6).

Acceptance Criterion 3: Data Uncertainty Is Characterized and Propagated Through the Model Abstraction

(1) Models use parameter values, assumed ranges, probability distributions, and bounding assumptions that are technically defensible, and reasonably account for uncertainties and variabilities, and do not result in an under-representation of the risk estimate.

This report provides basic descriptive information about selected volcanic eruptive features and processes that are characteristic of the repository, as exemplified by features observed at analogue sites including East Grants Ridge, New Mexico (Section 6.2); and Paiute Ridge and Basalt Ridge, Nevada (Section 6.2). The analogue information provides the basis for comparisons of vent geometry and structure, and the potential for development of secondary vents (Section 6.2). This report also describes selected physical phenomena and couplings between processes that are characteristic of igneous events in the Yucca Mountain region and other analogue sites outside the region. Parameters describing vent characteristics (Section 6.2), analyses of potential blockage of vents and effects on development of magma pathways (Section 6.3), and multiphase magma flow potential (Section 6.4) are developed for use in analyses of igneous processes or as inputs to TSPA models that support the analysis of the direct-release and indirect-release volcanic scenarios for the duration of a potential future igneous event. However, the report does not discuss the specific uses of the parameters in the downstream models, nor does the report discuss potential effects of parameter variations on the representation of risk.

(2) Parameter uncertainty accounts quantitatively for the uncertainty in parameter values observed in site data and the available literature (i.e., data precision), and the uncertainty in abstracting parameter values to process-level models (i.e., data accuracy).

This report describes selected physical phenomena and couplings between processes that are characteristic of igneous events in the Yucca Mountain region and other analogue sites outside the region. The analogue information provides the basis for comparisons of vent geometry and structure, and the potential for development of secondary vents (Section 6.2). Parameters describing vent characteristics (Section 6.2), analyses of the potential for blockage of vents and effects on development of magma pathways (Section 6.3), and multiphase magma flow potential (Section 6.4) are developed for use in analyses of igneous processes or as inputs to TSPA models that support the analysis of the direct-release and indirect-release volcanic scenarios for the duration of a potential future igneous event.

INTENTIONALLY LEFT BLANK

APPENDIX B
DATA QUALIFICATION REPORT

APPENDIX B
DATA QUALIFICATION REPORT

B1. ROCK MASS PROPERTIES OF THERMAL/MECHANICAL UNIT TCW

B1.2 DATA SET FOR QUALIFICATION

Mechanical properties for the thermal mechanical unit, TCw, are to be qualified for intended use in ANL-MGR-GS-000005. The intended use is for analysis of stresses and deformations in and surrounding a potential basalt conduit or dike. Specific data are found in *TBV-332/TBD-325, Resolution Analysis: Geotechnical Rock Properties* (CRWMS M&O 1999 [DIRS 126475]).

The data that are being qualified are for rock-mass quality category 5 only. Specific data are:

Rock mass modulus of elasticity = 29.39 GPa from Table 10,
Rock mass Poisson's ratio = 0.21 from Table 11,
Rock mass cohesion = 3.9 MPa from Table 12,
Rock mass friction angle = 57° from Table 13, and
Rock mass tensile strength = 2.35 MPa from Table 15.

NOTE: The terms "modulus of elasticity" and "Young's modulus" are equivalent.

B1.3 METHOD OF QUALIFICATION SELECTED AND RATIONALE

Corroborating Data–Corroborating data include mechanical properties data for subunit Tptpmn of the TSw2 thermal mechanical unit from DTN: MO0403MWDRPNLR.000 [DIRS 168896], which are qualified but are intact properties for a different stratigraphic horizon with generally similar properties (see Section 4).

Young's modulus, in file: *intact strength nonlith v2.xls* [Elastic Properties worksheet],
Summary statistics for Tptpmn
Poisson's ratio, in file: *intact strength nonlith v2.xls* [Elastic Properties worksheet],
Summary statistics for Tptpmn
Cohesion, in file: *intact strength nonlith v2.xls* [Cohesion and Friction Angle worksheet],
Summary statistics for Tptpmn
Friction angle, in file: *intact strength nonlith v2.xls* [Cohesion and Friction Angle worksheet],
Summary statistics for Tptpmn
Tensile strength, in file: *intact strength nonlith v2.xls* [Tensile Strength worksheet],
Summary statistics for Tptpmn

FLAC V4.04 (BSC 2004 [DIRS 172432]) is used to calculate the tensile stress in a cylindrical sleeve of basalt pressurized internally and surrounded by tuff with the properties to be qualified or tuff with the properties in the corroborating data.

A total of eight calculations were done to corroborate the data, as indicated in Table B-1. The calculations facilitate the corroboration by allowing a quantitative evaluation of the effect of the input rock mass properties on parameters of interest to the analysis in Section 6.3.1 of this report.

In addition to considering rock mass properties for the data to be qualified and for qualified data from the TSw2 unit, calculations include variations of the far-field pressure applied to the outer diameter of the tuff cylinder and use either a coarse or fine mesh.

Table B-1. Configurations for Corroboration Calculations

Properties Source	Confining Pressure	2.3 MPa	2.3 MPa	2.9 MPa	2.9 MPa
	Mesh Size	Fine	Coarse	Fine	Coarse
TSw2		X	X	X	X
TCw		X	X	X	X

The axial portions of the mesh for the FLAC V4.04 calculations are illustrated in Figure B-1. For the fine mesh, the grid spacing at the magma/basalt interface (radial distance of 7.5 m) is 0.5 m; for the coarse mesh, the grid spacing is 2.5 m. Both meshes increase radially by 1 percent per zone. The material properties for basalt, as listed in Table 6-1 of this report, are used for zones between 7.5 m and 25 m; properties for tuff, from either Table 6-1 or from DTN: MO0403MWDRPNLR.000 [DIRS 168896], are used from 25 m to the outer edge of the mesh at 240 m radius. Roller boundaries are used on the top and bottom sides of the mesh. A confining stress of either 2.3 MPa or 2.9 MPa is applied to the outer edge of the mesh. Pressures are applied to the interior edge, increasing from the value of the confining stress in 1-MPa steps, and tensile stress at a point near 1.25-m from the inner edge is recorded until the tensile stress exceeds 6.4 MPa. The location of the tensile stress is similar to that used in Section 6.3.1 to estimate if hydrofracture would occur at a stress of 6.4 MPa. Thus the corroborative calculations cover the conditions analyzed in Section 6.3.1.

B1.4 EVALUATION CRITERIA

The evaluation criteria stated in the Data Qualification Plan (attached below) are that, based on comparison of tabulated values, tangential stresses in basalt adjacent to the magma/basalt interface, calculated with the data to be qualified, be within 1 MPa or 5 percent of those calculated with corroborating inputs.

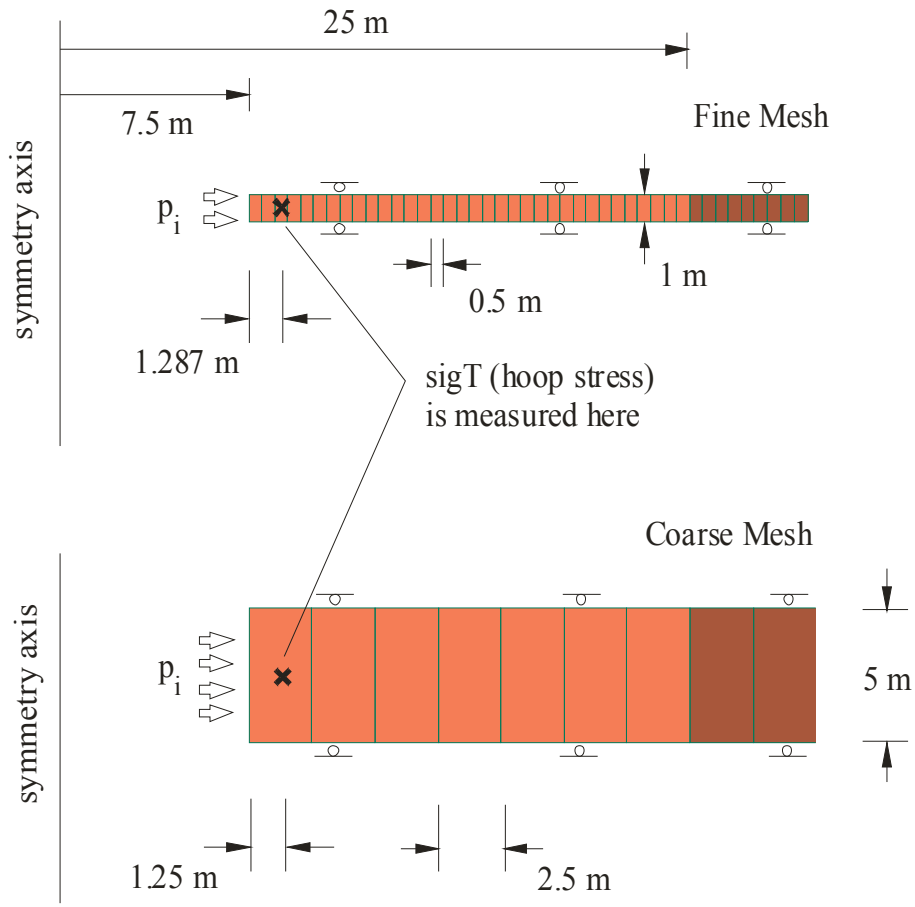

Figure B-1. Central Portion of Computational Grid for Corroborative Calculations

B1.5 EVALUATION OF THE TECHNICAL CORRECTNESS OF THE DATA

The Paintbrush Group at Yucca Mountain is part of a large ash-flow field and includes a sequence of four flow units: the Tiva Canyon, Yucca Mountain, Pah Canyon, and Topopah Spring tuffs. The Tiva Canyon and Topopah Spring tuffs are very similar and can be difficult to distinguish in the field (Lipman et al. 1966 [DIRS 100773], p. F-3). The Topopah Spring and Tiva Canyon tuffs are voluminous, mostly densely welded, compositionally zoned, outflow sheet, pyroclastic-flow deposits that grade upward from rhyolite composition to quartz latite composition (BSC 2004 [DIRS 166107], Section 6.1.1). These tuffs have similar fracture and mechanical characteristics, as seen in the following observations (CRWMS M&O 1997 [DIRS 103564], Section 4.2.1):

- Observations of the fracture network at Pavement P2001 at Fran Ridge by the U.S. Geological Survey showed that the Tptpmn zone within the Topopah Spring Tuff contained large and continuous fractures similar to those recognized in the ESF North Ramp in the Tpc zone within the Tiva Canyon Tuff.

- The joint sets observed in the Tpc of the ESF North Ramp are similar to fracture patterns in existing oriented-core data from the Tptpmn.
- The Tpc and Tptpmn have been subjected to the same post emplacement tectonic stresses.

Based on these observations, it is anticipated that the mechanical behavior of the Tiva Canyon and Topopah Spring tuffs will be similar.

B1.6) DATA GENERATED BY THE EVALUATION

The calculations described in Section 2 generated the data summarized in Table 2.

B1.7 EVALUATION RESULTS

The tensile stresses generated by the evaluations differ by no more than 0.15 MPa when qualified properties for unit TSw2 are used relative to the tensile stresses generated when the properties being evaluated are used. Percentage differences exceed 5 percent only when the absolute values of the stresses are small.

B1.8 CONCLUSION

The results reported in Section 6 support changing the qualification status of the data because they meet the evaluation criteria described in Section B1.4 of this report and in the Data Qualification Plan (attached below).

Table B-2. Data from Evaluations

P_{int} (MPa)	Far-field pressure = 2.9 MPa				P_{int} (MPa)	Far-field pressure = 2.3 MPa			
	Fine Mesh		Coarse Mesh			Fine Mesh		Coarse Mesh	
	tensile stress @ 1.25 m		tensile stress @ 1.287 m			tensile stress @ 1.25 m		tensile stress @ 1.287 m	
	TCw	TSw2	TCw	TSw2		TCw	TSw2	TCw	TSw2
2.9	2.9 MPa	2.9 MPa	2.9 MPa	2.9 MPa	2.3	2.3 MPa	2.3 MPa	2.3 MPa	2.3 MPa
3.9	2.18	2.19	2.16	2.18	3.3	1.58	1.59	1.56	1.59
4.9	1.42	1.44	1.40	1.41	4.3	0.82	0.85	0.79	0.82
5.9	0.65	0.69	0.61	0.65	5.3	0.05	0.09	0.01	0.05
6.9	-0.12	-0.07	-0.18	-0.12	6.3	-0.72	-0.67	-0.78	-0.73
7.9	-0.89	-0.82	-0.97	-0.91	7.3	-1.49	-1.43	-1.57	-1.50
8.9	-1.65	-1.59	-1.77	-1.67	8.3	-2.26	-2.19	-2.37	-2.29
9.9	-2.43	-2.35	-2.53	-2.46	9.3	-3.03	-2.95	-3.16	-3.07
10.9	-3.21	-3.11	-3.33	-3.25	10.3	-3.81	-3.71	-3.95	-3.85
11.9	-3.97	-3.87	-4.15	-4.02	11.3	-4.58	-4.47	-4.75	-4.64
12.9	-4.74	-4.63	-4.93	-4.81	12.3	-5.35	-5.22	-5.53	-5.42
13.9	-5.52	-5.38	-5.72	-5.60	13.3	-6.13	-5.99	-6.33	-6.21
14.9	-6.30	-6.15	-6.52	-6.37	14.3	-6.90	-6.75	-7.12	-6.98
15.9	-7.07	-6.91		-7.16					

B1.9 RATIONALE FOR ABANDONING QUALIFICATION METHODS

No methods were abandoned.

B1.10 LIMITATIONS OR CAVEATS

Neither the calculations of this evaluation nor the calculations in the analyses of Section 6.3.1 of this report generate states at or outside the failure envelopes of the tuff. Therefore, the failure criteria of the data evaluated (cohesion, tensile strength, and friction angle) have not really been evaluated. The data qualified should only be considered qualified for cases where failure does not occur and behavior is fully elastic.

B1.11 SUPPORTING DOCUMENTS

CRWMS M&O 1999. *TBV-332/TBD-325 Resolution Analysis: Geotechnical Rock Properties.* B00000000-01717-5705-00134 REV 00. Las Vegas, Nevada: CRWMS M&O. ACC: MOL.19991005.0235. [DIRS 126475]

MO0403MWDRPNLR.000. Rock Properties for Nonlithophysal Rock. Submittal date: 03/31/2004. [DIRS 168896]

BSC 2004. *Software Code: FLAC* V4.04. PC, Windows 2000. STN: 10167-4.04-00. [DIRS 172432]

CRWMS M&O 1997. *Yucca Mountain Site Geotechnical Report.* B00000000-01717-5705-00043 REV 01. Two volumes. Las Vegas, Nevada: CRWMS M&O. ACC: MOL.11971017.0736; MOL.19971017.0737. [DIRS 103564]

Lipman, P.W.; Christiansen, R.L.; and O'Connor, J.T. 1966. *A Compositionally Zoned Ash-Flow Sheet in Southern Nevada.* Professional Paper 524-F. Washington, D.C.: U.S. Geological Survey. TIC: 219972. [DIRS 100773]

BSC 2004. *Drift Degradation Analysis.* ANL-EBS-MD-000027 REV 03. Las Vegas, Nevada: Bechtel SAIC Company. ACC: DOC.20040915.0010; DOC.20050419.0001. [DIRS 166107]

B1.13) OTHER REFERENCES

The Data Qualification Plan for this effort is presented below.

DATA QUALIFICATION PLAN

BSC	Data Qualification Plan *Complete only applicable items.*	QA: QA Page 1 of 1

Section I. Organizational Information

Qualification Title

Qualification of mechanical properties for TCw unit for magma breakout calculations

Requesting Organization

PCA-Igneous Activity

Section II. Process Planning Requirements

1. List of Unqualified Data to be Evaluated

Mechanical properties for the thermal mechanical unit, TCw, will be qualified for intended use in ANL-MGR-GS-000005 and subsequent related scientific activities performed by the Igneous Activity team. Specific data are found in *TBV-332/TBD-325, Resolution Analysis: Geotechnical Rock Properties* (CRWMS M&O 1999 [DIRS 126475]). The data that are being qualified are for rock-mass quality category 5 only. Specific data are:

Rock mass modulus of elasticity = 29.39 GPa from Table 10,
Rock mass Poisson's ratio = 0.21 from Table 11,
Rock mass cohesion = 3.9 MPa from Table 12,
Rock mass friction angle = 57° from Table 13, and
Rock mass tensile strength = 2.35 MPa from Table 15.

NOTE: the terms "modulus of elasticity" and "Young's modulus" are equivalent.

2. Type of Data Qualification Method(s) [Including rationale for selection of method(s) (Attachment 3) and qualification attributes (Attachment 4)]

Corroborating Data: Corroborating data will include:
mechanical properties data for subunit Tptpmn of the TSw2 thermal mechanical unit from DTN MO0403MWDRPNLR.000 [DIRS 168896], which are qualified but are intact properties for a different horizon with generally similar properties.

Tensile strength: intact strength nonlith v2.xls [Tensile Strength], *Summary statistics for Tptpmn*
Young's modulus: intact strength nonlith v2.xls [Elastic Properties], *Summary statistics for Tptpmn*
Poisson's ratio: intact strength nonlith v2.xls [Elastic Properties], *Summary statistics for Tptpmn*
Cohesion: intact strength nonlith v2.xls [Cohesion and Friction Angle], *Summary statistics for Tptpmn*
Friction angle: intact strength nonlith v2.xls [Cohesion and Friction Angle], *Summary statistics for Tptpmn*.

FLAC v4.04 (STN: 10167-4.04-00) [DIRS 172432] will be used to calculate the tensile stress in a cylindrical sleeve of basalt pressurized internally and surrounded by tuff with the properties to be qualified or tuff with the properties in the corroborating data. This approach is selected because it applies the corroborative data in a manner analogous to the intended application in Section 6.3.1 of this report. The use of these calculations is strictly a means to corroborate the data sets and the results are not to be used beyond this report.

3. Data Qualification Team and Additional Support Staff Required

Chairperson: Don Krier
Team members: Carlos Carranza-Torres (or Terje Branshaug)

4. Data Evaluation Criteria

Based on comparison of tabulated values, are tangential stresses in basalt adjacent to the magma/basalt interface, calculated with the data to be qualified, within 1 MPa or 5% of those calculated with corroborating inputs?

5. Identification of Procedures Used

LP-SIII.9Q-BSC and LP-SIII.2Q-BSC

Section III. Approval

Qualification Chairperson Printed Name	Qualification Chairperson Signature	Date
Don Krier	Donald Krier	8/28/05
Responsible Manager Printed Name	**Responsible Manager Signature**	**Date**
Mike Cline	Mike Cline	8/28/05

LP-SIII.2Q-BSC FORM NO. LSIII2-1 (Rev. 01/19/2005)